

BRACHYPODIUM DISTACHYON SEEDLING GROWTH VISUALIZATION
UNDER OSMOTIC STRESS AND OVEREXPRESSION OF MIR7757 TO
INCREASE DROUGHT TOLERANCE.

By
Zaeema Khan

Submitted to the graduate school of Engineering and Natural Sciences in partial
fulfilment of the requirements for the degree of Doctor of Philosophy in Molecular
Biology, Genetics and Bioengineering

Sabancı University

July 2018

TITLE OF THE THESIS/DISSERTATION

Brachypodium distachyon seedling growth visualization under osmotic stress
and overexpression of miR7757 to increase drought tolerance

APPROVED BY:

Prof. Dr. Hikmet Budak.....
(Thesis Supervisor)



Prof. Dr. Ali Koşar.....



Assoc. Prof. Dr. Levent Ozturk.



Asst. Prof. Dr. Emrah Nikerel



Asst. Prof. Dr. Bahar Soğutalmaz Ozdemir



DATE OF APPROVAL: 09/07/2018

© ZAEEMA KHAN, JULY 2018

ALL RIGHTS RESERVED

ABSTRACT

BRACHYPODIUM DISTACHYON SEEDLING GROWTH VISUALIZATION UNDER OSMOTIC STRESS AND OVEREXPRESSION OF MIR7757 TO INCREASE DROUGHT TOLERANCE.

Zaeema Khan

Molecular Biology, Genetics and Bioengineering, PhD dissertation, July 2018

Supervised by: Prof. Dr. Hikmet Budak

Keywords: microRNA, *Brachypodium*, overexpression, drought, microscopy, root,

Brachypodium distachyon a monocot model plant has facilitated the downscaling for studying the most important cereal crops of the world both genetically and phenetically. This owes to its dwarf stature, small genome size and rapid life cycle which was utilized in our research for analysing its morphological features under osmotic stress. The purpose of this study was to visualize *Brachypodium* seedlings under osmotic pressure to observe morphological adaptation under drought-like conditions. It was found that *Brachypodium* displays the typical adaptive mechanisms of cereal plants mainly root apical meristem showing lateral hair growth and stunted growth. The root cells also displayed change in single cell morphology by swelling into compartment like structures as compared to non-stressed cells. This observation was made in the elongation and maturation zones of the root. Lateral hair growth was observed from the root apical meristem after 18 hours of PEG-mediated osmotic stress. *Brachypodium* not only manifests physiological adaptations to drought stress but also elicits molecular adaptation to counter it. To explore the genetic basis of drought tolerance the microRNAs involved in water deficit were traced out through a reverse genetics approach. The T-DNA mutant library of *Brachypodium distachyon* allowed for the investigation of a newly discovered microRNA miR7757 involved in water deficit to be overexpressed in *Brachypodium* to rapidly produce drought tolerant varieties bypassing conventional breeding techniques.

ÖZET

OSMOTİK STRES KARŞISINDA *BRACHYPODIUM DISTACHYON* BITKİLERİNİN BÜYÜMELERİNİN GÖZLEMLENMESİ VE MIR7757 AŞIRI İFADELEYEN BITKİLERDE KURAKLIĞA KARŞI DIRENCİN İNCELENMESİ.

Zaeema Khan

Moleküler Biyoloji, Genetik ve Biyomühendislik, Doktora Tezi, Temmuz 2018

Tez Danışmanı: Prof. Dr. Hikmet Budak

Anahtar kelimeler: mikroRNA, *Brachypodium*, aşırı ifalenme, kuraklık, mikroskop, kök *Brachypodium distachyon*, genetik veya fenotipik araştırmaların yürütüleceği tahıl çalışmalarını kolaylaştırmak adına kullanılan monocot bir bitki türüdür. Küçük yapısı, kısa genetik bilgisi ve hızlı yaşam döngüsüyle çalışmamızda osmotik strese yanıtın morfolojik olarak araştırılması için avantaj sağlamaktadır. Çalışmamızın iki temel amacı vardır. Öncelikli olarak *Brachypodium distachyon* bitkisinin osmatik strese yanıtlarını inceleyerek kuraklık benzeri koşullarda morfolojik değişimlerinin araştırılması hedeflenmiştir. *Brachypodium distachyon* 18 saat boyunca PEG koşulunda tutularak osmotik strese maruz bırakılmıştır. Strese maruz kalan bitkiler kontrol grubuna göre daha kısa boylu olmakla birlikte diğer tahıllarda da görülen tipik kuraklığa karşı apoptasyonlardan biri olan kök apikal meristeminde yanal kök tüylerinin artışı izlenmiştir. Bununla birlikte, kök hücreleri tek başına incelendiğinde kompartmanlar halinde şiştiği izlenmiştir. Diğer amacımız ise stress yanıtı olarak moleküler değişimlerin incelenmesidir. Kuraklık benzeri bu durum karşısında moleküler değişikliklerin irdelenmesi için hedef olarak kuraklık ile ilişkili miRNA'lar taranmıştır. T-DNA mutant kütüphaneler yardımıyla *Brachypodium distachyon* bitkisinde mir7757'in kuraklık direnci ile ilişkili olduğu bulunmuştur. *Brachypodium*de mir7757'nin aşırı ifadelenildiği bitkilerde kuraklık direnci ile ilişkisi irdelenmiştir. Çalışma geleneksel yöntemlerle yürütülen tahıl araştırmalarına bir alternatif sunmaktadır.

This work is dedicated to my family, foremost to my beautiful mother, my father, my lovely sister, my brothers, my sister-in-law, my sweet nephews and my dear uncle who left us just before I accomplished this feat. We miss you dearly Uncle.

I also dedicate this work to my doctors, my surgeon Op. Dr. Tolgay Şatana, and Uz. Dr. Cavit Meclisi without whom I would have never regained the ability to walk and be able to complete this document.

ACKNOWLEDGMENTS

I would like to express my gratitude to my thesis advisor Prof. Dr. Hikmet Budak for teaching me his skill, sharpness and charismatic approach towards research studies and scientific writing. I was always readily provided with everything I needed in the laboratory thanks to his rapid approach towards “getting the job done”.

I would like to thank Doç. Dr. Stuart Lucas for his precious guidance, mentoring and his invaluable advice and suggestions about my experiments and all kinds of support throughout the course of my doctorate. I thank Doç. Dr. Meral Yuce for her relentless support and express my deepest gratitude to her for her time and effort for helping me in challenging situations. I would like to thank Dr. VRSS Mokapatti for helping me to expand my horizon and explore boundaries where I had to go out of my comfort zone and think. I would also like to express my thanks to Dr. Meltem Elitaş for introducing me to a new world of interdisciplinary research. I would like to thank my jury members Prof. Dr. Ali Koşar, Assoc. Prof. Levent Öztürk, Asst. Prof. Emrah Nikerel, Asst. Prof. Bahar Soğutalmaz Özdemir for their valuable critical review of my work without which my academic development and success in doctorate would not be possible.

I would like to thank my lab fellows Sezgi Biyiklioğlu and Tuğdem Muslu for their presence and comradery. I offer many thanks to Dr. Mustafa Atilla Yazici and Yusuf Tutuş for their support and help. I want to offer eternal thanks Mariam Kassim Pili who helped me settle in Turkey. I want to thank my awesome friends and brilliant colleagues Dr. Yelda Birinci, Dr. Ghazaleh Gharib, Merve Zuvin, Melike Gezen, Rafaela Alenbrant Migliavacca, Hossein Alijani Alijanvand, Öznur Bayraktar, Yunus Akkoç, my country fellows Mahmuna Ifat, Muhammad Ayat, Fiaz Ahmad, Mansoor Ahmed for making my time here so comfortable and rememberable.

The most special recognition of never-ending gratitude goes to my highly talented gorgeous and accomplished mother who made me recognize how much more potential I had than I thought. She reminded me that she named me after a doctor Zaeema and I have now become that too.

I would like to acknowledge the Higher Education Commission of Pakistan for granting me this wonderful opportunity to pursue a doctorate abroad.

TABLE OF CONTENTS

A. INTRODUCTION TO THE THESIS	
A.2 Drought an Important Abiotic Stress.....	1
A.2.1 Drought Symptoms on a Plant.....	2
A.2.2 Physiological Stress Responses.....	2
A.2.3 Molecular Response and Abscisic Acid.....	3
A.2.4 Genetics of Drought Tolerance.....	4
A.2.4.1 Rice Gene NAC1 in Wheat.....	5
A.2.4.2 <i>Brachypodium</i>	5
A.2.4.3 Combined Molecular Response.....	5
A.2.4.4 Potential Role of Transcription Factors.....	6
A.2.4.5 General Molecular Response Pattern.....	6
B MATERIALS AND METHODS USED IN THE THESIS	
B.2 Plant Materials.....	8
B.3 Chemicals, Growth Media, Plant Growth Regulators, Antibiotics.....	8
B.4 Buffer and Solutions.....	8
B.5 Molecular Biology Kits.....	8
B.6 Equipment	8
B.7 Growth Conditions and Handling Techniques of <i>Brachypodium</i> Plants.....	9
B.7.1 Seed Surface Sterilization	9
B.8 Microscopy.....	9
CHAPTER 1 VISUALIZING MORPHOLOGICAL FEATURES OF YOUNG BRACHYPODIUM SEEDLINGS UNDER OSMOTIC STRESS	
1.1. Introduction.....	11
1.2. Materials and Methods.....	13
1.2.1. Device Fabrication.....	13
1.2.2. Preparation of Seeds and Measurement of Growth.....	14
1.2.3. Osmotic Stress Application.....	14
1.2.4. Imaging Studies.....	14
1.2.5. Imaging for Osmotic Stress.....	15
1.3. Results.....	17
1.4. Discussion.....	28
CHAPTER 2 OVEREXPRESSION OF A NEWLY DISCOVERED MICRORNA MIR7757 IN THE WHEAT WILD RELATIVE <i>BRACHYPODIUM DISTACHYON</i> T-DNA MUTANT FOR INVESTIGATING THE ROLE OF MIR7757 IN ABIOTIC STRESS	
1. Introduction.....	32
1.1. Reverse Genetics.....	33
1.2. Overexpression Advantages.....	33
1.3. <i>Arabidopsis</i> T-DNA Mutant Collection.....	34
1.3.1. T-DNA Insertional Mutagenesis.....	34
1.4. <i>Brachypodium</i> as a Model Organism.....	35
1.4.1. <i>Brachypodium</i> T-DNA Mutant Collection.....	35
1.5. microRNAs.....	38

1.5.1. microRNA Biogenesis and Gene Mediated Regulation.....	39
1.5.2. Role of microRNAs in stress responses.....	41
1.6. miRNA studies in <i>Brachypodium</i>	41
1.7. miR7757.....	43
1.8. microRNA overexpression and studies.....	43
1.9. Overexpression in Drought Studies.....	45
2 Materials and Methods.....	46
2.1 Production of Immature Embryos from Bd21-3 Wildtype and miR7757 T-DNA Mutant Plants.....	46
2.2 RNA Isolation, DNase Treatment and Gel Electrophoresis.....	46
2.3 Native Page Gel Electrophoresis.....	47
2.4 cDNA Synthesis by Reverse Transcription.....	47
2.5 Semiquantitative and Quantitative qRT-PCR for miR7757	48
2.6 Bioinformatic Analysis of T-DNA Insertion Sites with <i>Brachypodium</i> miRNA Database.....	49
2.6.1 Selection of miRNA Hits.....	49
2.7 T-DNA Genotyping with Multiplexed and Non-multiplexed Screening.....	50
2.7.1 DNA Isolation from <i>Brachypodium</i> Mutant Lines.....	50
2.7.2 Amplification of T-DNA Sequence by Multiplex PCR.....	51
2.8 Amplification of T-DNA Sequence by Non-Multiplexed PCR.....	51
2.9 Gel Electrophoresis and Gel Extraction.....	52
2.10 PCR Product Purification and Sequencing.....	52
2.11 Target Analysis of miR7757.....	52
2.12 Gateway BP-LR Cloning.....	53
2.12.1 Design of Gateway Cloning Primers for miR7757	53
2.12.2 Amplification of miR7757 Sequence from Wildtype <i>Brachypodium</i> with Attachment Sites.....	54
2.12.3 Gel Electrophoresis and Purification of att PCR Products.....	54
2.12.4 Preparation of Competent Cells.....	54
2.12.5 BP Reaction.....	55
2.12.5.1 DH5 α chemical transformation protocol.....	55
2.12.5.2 M13 primers colony PCR.....	55
2.12.5.3 miR gene specific colony PCR.....	56
2.12.5.4 Plasmid DNA isolation from transformed <i>Escherichia coli</i> cells.....	56
2.12.5.5 Transformation of Plasmids from LR reaction into <i>Escherichia coli</i>	57
2.13 SEM analysis of leaf blades.....	57
2.14 <i>Agrobacterium tumefaciens</i> Transformation into <i>Brachypodium</i> Compact Embryonic Callus.....	58
2.14.1 Transformation of Destination Clones into <i>Agrobacterium tumefaciens</i> cells..	58
2.14.2 Plasmid DNA Isolation from <i>Agrobacterium tumefaciens</i> Cells.....	58
2.14.3 Preparation of <i>Agrobacterium tumefaciens</i> Infection Inoculum.....	58
2.14.4 Transformation of <i>Brachypodium</i> by Callous Embryonic Culture.....	58
2.14.5 Selection of Transformed Calli with GFP and PPT.....	59
2.15 Regeneration of Transgenic MIR7757 Overexpressing Plants.....	59
3 Results.....	60
3.1 Bioinformatic Screening of <i>Brachypodium</i> miRNAs from T-DNA lines.....	60

3.2	Multiplex and Nonmultiplex screening of T-DNA mutants.....	61
3.3	Gel Extraction of T-DNA Genotyping for Selection of T-DNA Mutants.....	62
3.4	Sequencing Results.....	62
3.5	Target Analysis of the Selected Screened miR7757.....	65
3.6	Gel Electrophoresis of Wildtype miR7757 with Attachment att Sites	65
3.7	Transformation of BP Cloning Products into Competent Cells.....	67
3.7.1	Colony PCR of BP Reaction Transformants.....	69
3.8	Transformation of LR Reaction Products into Competent Cells.....	70
3.8.1	Colony PCR of LR Reaction Transformants.....	71
3.9	Transformation of LR Reaction Products into <i>Agrobacterium tumefaciens</i> cells...	71
3.10	<i>Brachypodium</i> Wildtype and T-DNA Mutant Growth and Phenotype.....	72
3.10.1	Microscopic Analysis of Mutant and Wildtype Leaf Blades.....	73
3.11	RNA Gel of Leaf and Root Samples and Semiquantitative qPCR.....	74
3.12	Growth Stages of <i>Brachypodium</i> Plants used in Transformation Studies.....	75
3.12.1	Compact Embryonic Callus Generation.....	75
3.12.2	<i>Agrobacterium tumefaciens</i> Infection of <i>Brachypodium</i> Immature Embryo.....	77
3.12.3	Co-cultivation of Infected Embryonic Callus Culture.....	77
3.12.4	Screening of transformed calli with BASTA and GFP.....	79
3.12.5	Regeneration of transgenic plants.....	80
4	Discussion.....	82
	C. CONCLUSION TO THE THESIS.....	84
	APPENDIX A.....	86
	APPENDIX B.....	87
	APPENDIX C.....	89
	APPENDIX D.....	92
	APPENDIX E.....	93
	APPENDIX F.....	94
	APPENDIX G.....	96
	APPENDIX H.....	98
	APPENDIX I.....	99
	D. REFERENCES.....	101

LIST OF TABLES

Table 1. Examples of microfluidic devices developed for plant biotechnology research.....	94
Table 2 psRNATarget hits from the <i>Brachypodium</i> coding sequence for bdi-miR7757-5p.1.....	96
Table 3 Predicted target gene hits in relative monocot species.....	96
Table 4 Predicted target genes of miR7757 in <i>Brachypodium distachyon</i>	97
Table 5 Comparison of average height between mutant and normal plants.....	98
Table 6 Sorted out <i>Brachypodium</i> T-DNA mutant lines having mutations in miRNAs.....	98

LIST OF FIGURES

Figure 1.1 Testing <i>Brachypodium</i> seedlings for orientation, compatibility and growth.....	17
Figure 1.2 The PDMS mold prepared for growth and visualization analysis.....	18
Figure 1.3 Growth curve of <i>Brachypodium</i> seedlings in 24 hours.....	19
Figure 1.4. Root growth trend of two seedlings under PEG stress for 12h.....	20
Figure 1.5 Experimental setups for imaging.....	21
Figure 1.6 Fluorescent microscopic observations of normal and osmotic stressed roots....	22
Figure 1.7 Cross section comparison of normal and drought stressed root samples.....	23
Figure 1.8 Comparison of root tip and maturation zone under osmotic stress.....	24
Figure 1.9 Cross section fluorescent visualization of transport tissue under normal and osmotic stress.....	25
Figure 1.10 Neutral Red stained stressed samples under fluorescence and brightfield microscopy.....	26
Figure 1.11. Confocal microscopy images under drought.....	27
Figure 1.12 showing possibility of an array platform.....	27
Figure 2.1 Promoters used for creating T-DNA mutations.....	37
Figure 2.2 miRNA biogenesis and mechanism of action pathway.....	40
Figure 2.3 miRNA overexpression overview as depicted in Approaches to microRNA discovery, Nature Genetics (Berezikov, Cuppen, and Plasterk 2006).....	44
Figure 2.4 miR7757 screening by T-DNA genotyping.....	61
Figure 2.5 Gel extracted PCR products of amplified T-DNA regions.....	62
Figure 2.6 Sequencing results from SeqTrace showing alignments of the T-DNA amplified PCR product with the wildtype MIR7757 gene.....	62
Figure 2.7 Working sequence generated from sequencing results of T-DNA insertion in MIR7757.....	63
Figure 2.8 Nucleotide BLAST results of the T-DNA working sequence with pre-miRNA sequence showing only 598 nucleotides.....	64
Figure 2.9 Alignment of the T-DNA+miR7757 PCR product with wildtype MIR7757 gene.....	64
Figure 2.10 The amplified att:MIR7757 PCR product at 850bp.....	65
Figure 2.11 Percentage identity and sequence alignment of miR7757 sequence with overhangs. This shows the working sequence generated from the att forward primer.....	66

Figure 2.12 Working sequence generated from the att reverse primer aligned to the <i>Brachypodium distachyon</i> nucleotide database shows alignment and 99% identity to miR7757.....	67
Figure 2.13 Transformation of BP reaction att:MIR7757 into pDONR and transformants on selective media containing antibiotics tetracycline and kanamycin.....	68
Figure 2.14 Colony PCR amplification of att:MIR7757 transformant colonies with M13 primers. 1,2,3,4,5 represent bacterial colonies.....	69
Figure 2.15 Colony PCR amplification of att:MIR7757 transformant colonies with MIR7757 forward and reverse primers.....	69
Figure 2.16 LR reaction and the transformants plated on the selective antibiotic plates containing kanamycin, and chloramphenicol and kanamycin.....	70
Figure 2.17 Colony PCR of LR reaction transformant colonies 5,6,7 and 8 with miR specific primers and CaMV promoter primers.....	71
Figure 2.18 <i>Agrobacterium</i> transformed with LR reaction product and spread on plates for use for transformation.....	72
Figure 2.19 Comparison of plant height between mutant line JJ15278 and wildtype Bd21-3.....	72
Figure 1.20 Light microscopic analysis of hair cuticle density of mutant and wildtype..	73
Figure 2.21 Scanning electron micrographs of mutant and normal <i>Brachypodium distachyon</i> mature leaf blades.....	73
Figure 2.22 Native page gel of RNA samples from drought root, drought leaf, normal root and normal leaf of Bd21 wildtype.....	74
Figure 2.23 qRT-PCR of miR7757 of normal and drought stressed leaves and roots of wildtype <i>Brachypodium</i>	75
Figure 2.24 Swollen but green immature seed used for immature embryo dissection....	76
Figure 2.25. 6 weeks growth of the immature embryo into the opaque callus ready for splitting.....	76
Figure 2.26 Flooding of the 6 week calli with <i>Agrobacterium</i> culture.....	77
Figure 2.27 Initial incubation for 2 days on MSB3+AS60 media.....	78
Figure 2.28 Growth on MSB+Cu0.6+H40+T225 showing growth of the calli after 3 weeks.....	78
Figure 2.29 Selected calli which grew under PPI for 6 weeks and were subsequently analyzed under GFP.....	79
Figure 2.30 Transformed calli displaying clear GFP fluorescence.....	80
Figure 2.31 Regeneration of the GFP calli on selective media to promote shoot growth.....	80

LIST OF SYMBOLS AND ABBREVIATIONS

°C	degree Celsius
μ	micro
2, 4-D	2, 4-Dichlorophenoxyacetic acid
ARS	Agricultural Research Service
BAP	6-benzylamino-purine
BLAST	Basic Local Alignment Search Tool
CaMV	Cauliflower mosaic virus
CEC	Compact Embryonic Callus
CER	controlled environment room
DCL1	Dicer-Like 1 Protein
DNA	deoxyribonucleic acid
dNTP	deoxynucleotide
EDTA	Ethylenediaminetetraacetic acid
GUS	β-glucuronidase
HEN1	HUA ENHANCER1
hpt	hygromycin resistance gene
HST	HASTY
MES	2-(N-morpholino) ethanesulfonic acid
miRNA	microRNA
mRNA	messenger RNA
MS	Murashige-Skoog basal salt medium
NCBI	National Centre for Biotechnology Information
PDMS	polydimethylsiloxane
PPT	phosphinothricin
pre-miRNA	Preliminary microRNA
pri-miRNA	Primary microRNA
psi	per square inch
qRT-PCR	quantitative-Real Time Polymerase Chain Reaction
RISC	RNA-induced silencing complex
RNA	Ribonucleic Acid
RNase	Ribonuclease
Taq	Thermus aquaticus

T-DNA

Transfer DNA

USDA

United States Department of Agriculture

WRRC

Western Regional Research Centre

A INTRODUCTION TO THE THESIS

A.2 Drought an Important Abiotic Stress

Drought stress can be defined as soil water deficit and is the most common environmental stresses affecting agricultural yield worldwide (H. Chen, Li, and Xiong 2012). The development of drought is complex and slow and involves multiple variables and factors. Drought is often classified into four different categories being a deficit in precipitation (meteorological), deficit in ground water, surface water and reservoir storage (hydrological drought), unequal water demand and supply (socioeconomic drought), but the one referred to throughout this review is agricultural drought being the water deficit in soil moisture severely affecting crops (Wilhite and Glantz 1985). Drought is a natural environmental stress factor and displays the highest percentage 26% when viewed in all stress factors affecting usable areas of the earth (Kalefetoğlu and Ekmekci 2010). According to current climate change prediction models the average surface temperature are predicted to rise by 3-5°C in the coming 50 -100 years, which will drastically affect agriculture (The Physical Science Basis: Working Group 2007). This will concurrently result in increased episodes of flood, drought and heat waves (Bates et al. 2008; Mittler and Blumwald 2010). In a report (Mittler 2006), between 1980 and 2004 in the US the total agricultural losses amounted to US \$20 billion. These losses combined with both heat stress and drought totalled US\$120 billion, pointing that the presence of another stress can intensify the devastating effects of the prior one. In recent years drought has taken its toll on North America destroying the corn fields and severely damaging the corn produce. Due to drought the plants face premature death and due to the drought the plants are vulnerable to stalk rot (Wu and Chen 2013). In China also the drought has been associated with cold stress and affected farmer livelihood, agricultural produce and landscape (Barriopedro et al. 2012).

A.2.1 Drought Symptoms on a Plant

The signs of drought in a plant are the leaf area decreases, the leaf drops, root growth is affected, stomata close, leaves start yellowing and overall the plant wilts and if the drought continues the plant eventually dies. Plant physiological responses to the stress are to limit the expansion of leaf so that less water is lost through transpiration; the size of each leaf could decrease as well as the leaf number. As the stress persists the plant responds by dropping its leaves. Underground the plant grows longer and dissects out more roots to reach out to deeper pockets and sources of water. The plant closes its stomata to decrease respiration this also decreasing the amount of photosynthesis which results in the yellowing of leaves. The continuation of stress results in wilting of the leaves, droop in broadleaved plants and inward curling of leaf blades in grasses e.g. corn. This activity reduces the total leaf surface area in contact with the sun and air. If the water deficit continues then the plant turns brown and dies. In arid conditions a plant may experience drought cycles twice or thrice a season (Bhargava and Sawant 2013). Drought stress when combined with other stresses such as heat has devastating effects, causing heavy damage to the crops than any of the stress alone. Under heat stress the plants usually open their stomata to cool the leaves but along with drought stress this would prove very devastating as the water loss would be harmful (Rizhsky 2004).

A.2.2 Physiological Stress Responses

Survival of a plant in stress conditions influences the physiology and productivity of the plant. The growth of the plant is most sensitive to drought followed by photosynthesis and respiration. The duration and magnitude of these slumps are governed by changes and adaptive methods for water balance between water supply and use, carbon balance and actions to even out water loss in the form of transpiration with carbon gain i.e. biomass production (Duque et al. n.d.; Lipiec et al. 2013). The ATP and NADPH produced from photochemical reactions are used in all processes except for supplying CO₂ to the chloroplast in the C₃ pathway plants, thus any retardation in photosynthesis such as those brought about by drought can affect the plant bioenergetics' status. When plants are subjected to drought the decrease in photosynthesis and thus photorespiration is

due to the reduction in the availability of O₂ and CO₂ in the chloroplast (Duque et al. n.d.). In drought plants usually no reduction or change in respiration is seen in leaves and the variations are always small as compared to photosynthesis despite both being interdependent through photorespiration (Duttilleul et al. 2003). But at the whole plant level the share of respiration to plant bioenergetics is relevant as it accounts for a release of 30-70% of the daily carbon fixed in normal watered plants but in drought stressed plants the proportion of lost carbon accelerated mostly due to the decrease in photosynthesis (Duque et al. n.d.). The photosynthesis quantum yields of C₃ plants under drought stress or heat stress in high temperatures results in less efficient light usage for fixing CO₂ (Nunes et al. 2009){39}. Like rice, wheat, and barley, *Brachypodium* also uses the C₃ photosynthetic pathway. In C₄ plants however this is not observed. Under water deficit in both C₃ and C₄ plants the decrease in the relative water content leaf and water potential coincides with a decrease in photosynthetic rate. Whether photosynthesis is restricted by stomatal limitation i.e. water deficit through restricted CO₂ supply to metabolism or through destruction of other processes involved in decreasing the photosynthesis rate, i.e. nonstomatal limitation (Duque et al. n.d.). Indeterminate plants such as peanut and cotton possess the ability to benefit from inconsistent water cycle in such that they do not have a strict fruiting pattern, thus growing vegetatively and reproductively simultaneously. On the other hand determinate crops must set fruit as a very specific time and in the case of water deficit at that time the yield will be severely affected as in the case of corn (Anon n.d.).

A.2.3 Molecular Response and Abscisic Acid

Under drought stress conditions the plants synthesize the regulatory hormone abscisic acid. This hormone induces changes at all levels and in the entire plant from the leaves, root tips and even flowers. Plants begin to conserve water under the influence of this hormone, seeds maintain dormancy, leaves close their stomata, plants slow down growth and reprogram themselves at the genetic level to strive towards survival (Lipiec et al. 2013). Generally, plant molecular responses are linked through crosstalk between numerous signalling and stress response networks e.g. the dehydration response elements DRE proteins, redox controls and the downstream processes regulated by them are crucial in drought and freeze stress response. Important signalling molecules

in drought response are MAPKinases, SNF1-like kinases, phosphatases, phospholipids, salicylic acid, nitric oxide and calcium(Melda Kantar, Lucas, and Budak 2011). The antagonism between abscisic acid and auxin restricts the horizontal growth and proliferation of root in response to drought e.g. it was recently discovered that the stress regulated noncoding regulatory microRNA miR393 targets the auxin receptors mRNA AFB2 and TIRI in order to inhibit lateral root growth (H. Chen et al. 2012) Plant hormones such as abscisic acid regulate the interaction between both abiotic and biotic stresses which involves an extensive crosstalk amongst transcription factors, other hormones, and regulatory components if biotic and abiotic stress occurs simultaneously such as ROS, jasmonic acid, salicylic acid, pathogenesis relates proteins, systemic acquired resistance and heat shock factors, as well as regulatory microRNAs. This makes a complex interaction network allowing the plant to respond very specifically to the stress encountered or to the combination of stresses. This involves induction, positive regulation or inhibition or repression. (Atkinson and Urwin 2012)

A.2.4 Genetics of Drought Tolerance

Much effort has been made in the empirical breeding of drought tolerance in wheat focusing on increasing yield and yield components. But drought resistance traits are complex genetically, difficult to manipulate and subtle hence there has been little success to breed drought tolerant varieties in wheat in the past 50 years (Khan et al. 2011). However in recent years the drought tolerant extremophiles *Populus euphratica* (Brinker et al. 2010; Qiu et al. 2011) whole transcriptome has been discovered and *P. euphratica* microRNAs have been extensively analyzed in stress conditions (Li, Yin, and Xia 2009).

Analysis of drought tolerance strategies of plants reveals that the tolerance to environmental abiotic stress is multigenic in nature, inherent, and thus it's difficult to manipulate genetically a multigene characteristic through classic breeding. Thus molecular markers such as Randomly Amplified Polymorphic DNA (RAPD) are preferable used for polymorphism detection of genetic traits important in drought tolerant varieties (Shah et al. 2009).

A.2.4.1 Rice Gene NAC1 in Wheat

In rice (*Oryza sativa*) a drought stress responsive transcription factor encoded by NAC1 gene in rice (SNAC1) has an important function in stress tolerance. This SNAC1 gene was introduced in an elite wheat variety Chinese Yangmai12 under a maize ubiquitin promoter. The plants expressing this SNAC1 gene showed higher tolerance to drought as well as salinity in multiple generations, the plants contained a much higher level of water and chlorophyll in their leaves in comparison with the wild type. Furthermore there was also an increase in the fresh and dry weights of the roots and leaves of the transgenic plants as well as higher sensitivity to abscisic acid thus leading to the inhibition of shoot and root growth (Saad et al. 2013).

A.2.4.2 *Brachypodium*

Plant drought stress response has been extensively studied in *Arabidopsis* and a few other grass species. Amongst a wheat wild relative *Brachypodium* has many characteristics to tolerate and adapt to drought due to its geographical location and many efforts are being done to translate these desirable traits in related crops such as barley and wheat. Different developmental leaf zones in *Brachypodium* showed differing responses to *Brachypodium* when the transcriptomic profile was analyzed using Affymetrix GeneChip (Verelst et al. 2013).

A.2.4.3 Combined Molecular Response

In combined stresses such as heat and drought it has been recently shown in transcriptome analysis in *Arabidopsis* as well as tobacco that the molecular stress response to simultaneous drought and heat stress is not additive. It instead triggers a new blueprint of gene expression and induction of specially regulated genes, that cannot be studied in either stress alone (Rizhsky 2004). Among these genes regulated under both abiotic stresses in *Arabidopsis* are those encoding HSPs (heat shock proteins) lipid biosynthesis enzymes, proteases, and starch degrading enzymes. Others include protein kinases, MYB TFs, and defence proteins functioning in oxidative stress protection (Nishiyama et al. 2011; Rizhsky 2004)

A.2.4.4 Potential Role of Transcription Factors

From amongst transcription factors involved in drought stress response and induced through abscisic acid are the MYB type of genes in wheat and Arabidopsis e.g. MYB2 and MYB96, PIMP1. RD26 is an important NAC type gene, other genes are the ERF gene family including BIERF1-4 and ERF3 and ABF gene family of which AREB1 transcription factor has an important function. Interestingly these genes are not only involved in stress tolerance but also other stresses such as salinity, pathogen attack cold and wounding and may also be induced by other phytohormones such as jasmonic acid. Most of the action of these transcription factors is to regulate ABA or stress inducible genes.

A.2.4.5 General Molecular Response Pattern

The general molecular response to stress involves perception of the signal whether it is abiotic or biotic and then the signal transduction cascade either MAP kinase cascades, hormone signalling or ROS accumulation. These then further induce multiple and individual stress induced transcription factors such as the one mentioned above AP2/ERF, WRKY, NAC, MYB, DREB/CBF etc. The post transcriptional regulation of these TFs leads to the expression of functional downstream genes e.g. those involving ion channels, lignin and secondary metabolite biosynthesis, stomatal closure and growth regulation which hence elicit the stress response (Ren et al. 2010; Rushton et al. 2012; Seo et al. 2009; Wasilewska et al. 2008; Zou et al. 2010).

Drought is a difficult and significant issue to deal with and can have a devastating impact on crop yields; however, the plant responses to drought have been studied in great depth and even more advanced studies are ongoing. Incorporating drought tolerant genes from wild relatives or other crops or extremophiles shows a possible solution and provides hope against a highly complex multigenic abiotic stress such as drought.

Studies on abiotic stress in cereal crop plants focus on their genetic manipulation and the corresponding genotypic variations arising from stressed conditions. The visual changes occurring with stress conditions are also a salient feature of cereal crop plants in adjusting to stress. These

changes can be observed directly either as wilting and drooping of leaves on a macro scale or shrinkage of cells at microscopic scale. *Brachypodium* seedlings were observed for onsite investigation of seed growth and root development under normal and osmotic stress conditions. The effects of osmotic stress on the seed growth and root development was observed through various microscopic studies at the cellular level where the cells manifested difference in physical morphology as compared to the non-stressed control. This study presents a rudimentary analysis of the growth of *Brachypodium* seedlings in normal conditions and under osmotic stress at a relatively early stage of development and thus reveals important details regarding the osmotic stress adaptation of this model plant. The method reported in this study can easily be adapted for further refined, comprehensive and in-depth physical and physiological analyses under diverse stress conditions, and it can be further developed into automated and high-throughput quantitative analyses systems for plant molecular dynamic studies at single cell level. Furthermore, study of mechanical and physical parameters of *Brachypodium* seed growth can also be elucidated in more advanced microfluidic systems.

B MATERIALS AND METHODS USED IN THE THESIS

B.2 Plant Materials

In this study *Brachypodium distachyon* wild type cultivar Bd21-3 was used. Fourteen T-DNA mutant lines JJ13854, JJ3177, JJ12516, JJ2088, JJ5868, JJ3284, JJ54, JJ15278, JJ5803, JJ5856, JJ5899, JJ5912, JJ5843, JJ5820 from T-DNA blast hits and bioinformatic analysis were selected out. Plant seeds for these mutant lines were obtained from The WRRC *Brachypodium* T-DNA group collection DOE Joint Genome Institute

B.3 Chemicals, Growth Media, Plant Growth Regulators, Antibiotics and Enzymes

The list of all the chemicals used for growth media, hormones and enzymes and antibiotics are listed in Appendix A.

B.4 Buffer and Solutions

The buffers and solutions were prepared according to the protocols given in Sambrook et al 2001.

B.5 Molecular Biology Kits

Molecular Biology kits are listed in Appendix B

B.6 Equipment

Equipment utilized in this study are listed in Appendix C

B.7 Growth Conditions and Handling Techniques of *Brachypodium distachyon* Plants.

Brachypodium seeds were placed in between wet filter papers in petri plates and vernalized for 5-7 days at 4°C in the dark. After stratification they were kept under light in the laboratory at room temperature for 4-5 days. After germination they were transferred to high nutrition peat in small soil pots. After establishment of seedlings, they were put into size 6 plastic pots containing 2kg of soil (from Sultanonu Eskisehir) and grown under controlled conditions in the greenhouse 16/8 light/dark period, temperature 25/22°C, relative humidity 60-70% and a photosynthetic photon flux of 320 $\mu\text{mol m}^{-2}\text{s}^{-1}$ at canopy height provided by fluorescent lamps. For basal fertilization the growth media was treated with 200mg kg⁻¹ N (Ca(NO₃)₂), 100mg kg⁻¹ P (KH₂PO₄), 20mg kg⁻¹ S (K₂SO₄), 5mg kg⁻¹ Fe (Fe-EDTA), and 2.5mg kg⁻¹ Zn (ZnSO₄).

B.7.1 Seed Surface Sterilization

Brachypodium seeds mature and immature for both studies were dehusked and subjected to surface sterilization by immersing in 10% bleach and a few drops Tween-20 for 15 minutes and then rinsed 4 times. The immature seeds were used for immature embryo dissection. The mature seeds were placed in between two layers of sterile filter paper soaked with deionized water inside a petri dish. The plates were sealed with parafilm and covered with aluminum foil and left at 4°C in the dark for 5 days. After vernalization they were left for a 2 days at 25°C with a 16hr photoperiod. (Alves et al. 2009). Media prepared was Murashige and Skoog 4.43 g, MES monohydrate 0.5 g, sucrose 30 g, and plant hormone 6-benzylaminopurine (BAP) 2.5 mg/L. The germinated seedlings subsequently used for imaging were loaded onto the PDMS chip filled with MS broth.

B.8 Microscopy

For light microscopy stereomicroscopes Nikon SMZ 1500, Olympus SZ61 stereo microscopes and illuminator lamp Olympus LG-PS2 from Japan. Fluorescence imaging for both experiments was

performed with Axio Vert.A1 inverted microscope by Carl Zeiss (Germany) using different wavelength and filters for neutral red stain and for GFP fluorescence.

CHAPTER 1

VISUALIZING MORPHOLOGICAL FEATURES OF YOUNG *BRACHYPODIUM* SEEDLINGS UNDER OSMOTIC STRESS

1.1. Introduction

Abiotic stress related research in plants has considerably increased in recent years as a result of constant change in the global climate conditions (Frazier et al. 2011; Kumar et al. 2015). Plant growth under stress conditions is generally phenotyped and visualized by macroscale parameters (Verelst et al. 2013), which requires dedicated greenhouse space, labour, a great deal of test sample and consumables. These requirements thus limit the number of parallel experiments. Moreover, conventional plant growth techniques are not always compatible with state-of-the-art characterization tools. Such imaging tools prevent microscopic analyses at high-resolution due to optical transparency issues of the soil pots. Furthermore, the out of plane growth on agar plates hinders imaging on a single plane of focus. Engagement of microfabricated fluidic systems with plant biology research has paved the way for precise morphological and physiological analyses at microscale with reduced cost and labour (Elitaş, Yüce, and Budak 2017). Some examples of plant fluidic systems developed so far are presented in Table 1. Those pioneering devices have allowed miniaturisation of individual experiments and related costs while providing automated parallel assays to achieve accurate as well as high-throughput quantitative data (Elitaş et al. 2017; Sanati Nezhad 2014). *Arabidopsis thaliana* (Gooh et al. 2015; Massalha et al. 2017), *Camellia japonica* (Agudelo, Packirisamy, and Geitmann 2014), *Oryza sativa* (Iyer-Pascuzzi et al. 2010), *Nicotiana tabacum* (Ko et al. 2006; Wu et al. 2011), *Phalaenopsis chiada pioneer* (Hung and Chang 2012),

and *Physcomitrella patens* (Bascom et al. 2016) plant species have been employed in various microfluidic platforms for in-depth analyses of dicot seed germination, leaf development, cell phenotypes, protoplasts, pollen tube development and dynamics, shoot and root growth. These studies have largely been carried out in dicot plants and studies on monocot plants are still to be explored.

Roots are responsible for water and mineral nutrient uptake from soil. They offer structural stability to the plant and affect the growth and development of plant organs above the soil. Characterization of root behaviour at different developmental stages and under various environmental conditions is of great importance to reveal the plant tolerance mechanisms and dynamic changes. This is particularly essential for food cereal crops such as wheat, rice, maize, and barley. However, conventional techniques for root investigations are usually conducted at macro scale and do require relocation of the plants for microscopic analyses, which could cause dehydration, physical damage and lead to data shortage. In addition, other conventional tools including hydroponics, do not allow real-time observation of the changes in the root systems that are exposed to different stress conditions such as drought, salt, growth factors, drug or nanomaterials.

A number of chip platforms (Ghanbari et al. 2014; Nezhad et al. 2013; Parashar and Pandey 2011) and software (Galkovskyi et al. 2012) for microenvironment investigation have been reported for tip-growing cells such as root and pollen tube mostly in ornamental dicotyledonous plants. Although all these systems attempt to mimic the physical microenvironment and provide appropriate designs for analysing spherical seeds or pollen tube elongation, there exists a need for a platform capable of measuring the elongation and growth dynamics of larger monocot seeds which differ considerably in its seed architecture. Monocot seeds are usually elliptical, slender long grains, with embryo polarity which makes the germination behaviour at the tissue and cellular level distinct from dicots. The application of abiotic stress conditions at the microscale to monocot seeds may allow phenotyping of the most important staple food crops and offer a valuable resource for a better understanding of crop adaptation mechanisms with high precision.

In this study we will explore how monocot seedlings with polarity grow when inserted into a PDMS channel. A rudimentary plant chip will be designed to monitor real time changes under PEG-mediated osmotic stress in seedlings.

1.2 Materials and Methods

1.2.1 Device Fabrication

Rectangular PDMS pieces with a scale of 65x20x10 mm single, double and triple punched with 5 mm diameter punchers were initial seed growing reservoirs at different volumes to check biocompatibility. Acetone cleaned glass slides and PDMS pieces were plasma treated and bonded to get the final devices, which were used to test the compatibility of *Brachypodium* seeds with PDMS. A mold for the plant chip was designed with SOLIDWORKS Software, reproduced onto ABS 3D material, and 3D printed. The mold dimensions were 10mm height, 9.5mm channel length, 1mm outlet diameter, and each seed channel 4 mm in diameter. The channel height was fixed at 1 mm to ensure the growth of the root to remain in one plane and not be out of focus in the Z-axis under microscopy as was earlier observed for 2mm channel width and height in Fig. 1.12. For the construction of the device, PDMS and curing agent were mixed in 10:1 ratio and poured into the mold in a 100-mm diameter Petri dish, degassed in a desecrator, and cured at 75 °C for 60 min in an oven. The PDMS pieces were cut and gently peeled off from the mold on the Petri dish. The constructed device was submerged in Murashige and Skoog media overnight to ensure the hardening of the device. 0.17 mm coverslips and the PDMS pieces were plasma treated and bonded to get the final devices. Coverslips were used instead of the glass slides to facilitate fluorescent imaging. This setup was fixed with an adhesive to the Petri plate cover. Each channel was filled with MS media. Following 4-7 days of vernalization and two days post-germination —when the seedling stage was well established- the synchronously growing *Brachypodium* seedlings were inserted into the wells vertically at around 75-55° angle, with the scutellum facing slightly upwards and radicle facing downward. The anterior end was immersed in the well, and the posterior end was entirely out of the well, with the emerging leaf facing outwards. Two different designs were developed for top and bottom imaging studies. The top imaging setup consisted of the same PDMS mold with the cover glass covering only the outlet channel, and the root channel, the seed channel was kept empty. This setup was then sealed with a double-sided adhesive tape to a carved-out Petri plate cover. The plate was filled with media. The wells were supplied with a constant supply of

the media. The bottom setup consisted of the glass cover slip bonded to the entire device base to cover all the channels and the samples. Seeds were inserted anteriorly from the top.

1.2.2 Preparation of Seeds and Measurement of Growth

Brachypodium wild-type seed line Bd21-3 was used in this study. The seeds were dehusked then soaked in water for 10 minutes. They were sterilized for 1 minute with 70% ethanol in a sterile Petri dish. Ethanol was drained, and the seeds were rinsed with sterile deionized water. 20 ml of 1.3% NaOCl solution was poured into the Petri dish and rotated for 5 minutes. The seeds were then rinsed thrice with sterile deionized water. Ten seeds were placed in between two layers of sterile filter papers soaked in sterile water. After 7 day vernalization, the seeds were transferred to agar media and allowed to grow for 48h at 22°C with a 16h photoperiod and high relative humidity at 57%. Finally, the seedlings were transferred to the device. Epson perfection v700 photo scanner was used to visualise the full length of the seedlings grown in the microfluidic device and standard agar environment. WinRHIZO software (Regent Instruments, QC, Canada) was used to analyse the shoot and the root scan images (Fig. 1.12).

1.2.3 Osmotic Stress Application

To give osmotic stress 20% PEG 6000 was dissolved into the MS agar media and filled in the seed and root channel to three week plantlets at the 3-leaf stage. For 6h and 24h osmotic stress analyses, the seedlings were first stained with neutral red for 20 minutes and then transferred to the microchannel device containing 20% PEG-MS and visualised under fluorescence microscope.

1.2.4 Imaging Studies

The seedlings were selected at 2 days after germination (DAG) for microscopy studies. For standard visualisation of the control and stress samples, the device setup for top imaging was used. PEG-supplemented MS media was used for osmotic stress. The top imaging was performed using Nikon SMZ 1500, Olympus SZ61 stereo microscopes and illuminator lamp Olympus LG-PS2 from Japan. For bottom imaging of the samples with fluorescence, a stock solution of 4 μ M neutral red stain was prepared with 0.2X MS medium supplemented with 20mM potassium phosphate

buffer at 8.0 pH, according to the procedure reported earlier (Dubrovsky et al. 2006). The control and stressed plantlet roots were stained for 15-20 minutes following the removal of PEG-supplemented MS media. The staining procedure made the cells stained under brightfield and enabled fluorescent visualisation of the seedling roots. Cross section samples were prepared according to the protocol described online (Schiefelbein Lab. 2017). Fluorescence imaging was performed with Axio Vert.A1 inverted microscope by Carl Zeiss (Germany), using the bottom imaging setup. Confocal microscopy was performed with Carl Zeiss LSM 710, Germany and images recorded with Zen software (Carl Zeiss, Germany). Neutral red dye was used to visualize the live/dead parts of the roots of the young seedlings both for normal growth and for osmotic stress conditions. A single channel was used for visualisation with neutral red. Images were taken in 20X objective lens. Three-week old seedlings pre-stained with neutral red at the 2-DAG (days after germination) seedling stage (stained as mentioned previously) were selected. These seedlings were given osmotic stress for 6 hours in Murashige and Skoog (full strength) media with 20% polyethylene glycol 6000. Stressed and normal seedlings were embedded in agarose (as described for the fluorescence microscope staining) to enable section slicing as thin as possible. Cut sections ~ 0.5-0.9mm were achieved from the maturation zone of the plant. Transverse sections were removed from the agarose molds and placed separately on acetone-ethanol cleansed cover slips and glass slides. The cover slips were sealed securely with clear nail polish.

1.2.5 Imaging for Osmotic Stress

For visualisation of growth, the model PDMS device was used in both dorsal and ventral positions. Top imaging was achieved by plasma bonding the glass to the dorsal side, but only covering the root channel and the outlet channel, leaving the seed channel open for insertion, as can be seen in Fig. 1.4 A. Petri plate was used for maintaining humidity and growth in which the radicle was inserted into the channel, with the coleoptile facing upwards and outwards and a gap created in the lid to ensure growth for the shoot. The coverslip was attached to the lid with a strong double-sided adhesive. The objective was positioned to focus directly on the cover glass and gap. Two holes were bored inside the lid to insert the valves for constant media flow. This entire setup was prepared aseptically under laminar flow hood. However, the seed part for shoot growth was kept uncovered during the length of the experiment. Media was inserted into the dish and into the device

wells with the metal heads bored into the seed channel to ensure full media flow. The Petri plate lid and the bottom part was covered with paraffin film to ensure high humidity. The device could be maintained in this manner for 48h. The fluorescent bottom imaging was done with the entire ventral side of the device oxygen plasma bound to a glass coverslip. Seeds were inserted into the device with the coleoptile and radicula facing outwards and the bottom objective directly visualised the roots. The roots were separately stained with Neutral Red dye according to the protocol by Dubrovsky et al. (Dubrovsky et al. 2006) and rinsed in MS media and the channels filled with non-stained full strength MS media to avoid background. For fluorescence imaging 0.4 μ M neutral red solution and a 15-20 min incubation stained the roots sufficiently. 20% PEG was applied to full strength MS media for microscopic visualization of stress response morphological change of 2 DAG *Brachypodium* seedlings for 6, 18 and 24 hours.

1.3 Results

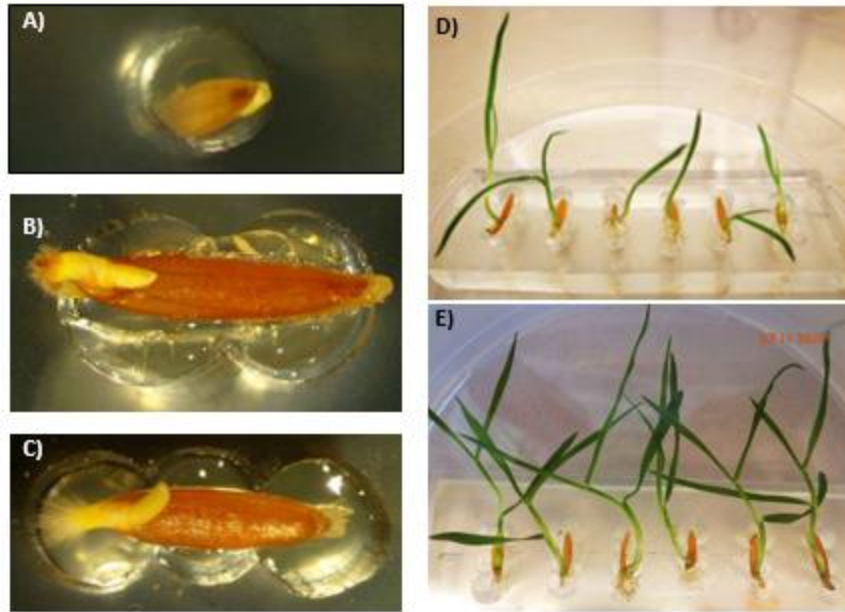


Figure 1.1 Testing *Brachypodium* seedlings for orientation, compatibility and growth. The growth of monocot seedlings from *Brachypodium distachyon* in (A) single, (B) double and (C) triple punched PDMS channel, (D) growth of six samples in parallel after 7 days in the triple punched PDMS channel e) growth of six samples in parallel after 21 days in the triple-punched PDMS channel. The images a, b and c were taken with Olympus SZ61 stereomicroscope, Japan.

PDMS with single, double and triple punches was tested for compatibility with *Brachypodium* seedling growth presented in Fig. 1.1 A, B and C. The single, double and triple punch microchannels had volume capacities of 130, 280 and 385 μl , respectively. Growth, directionality and compatibility was observed for *Brachypodium* seeds on all three PDMS punched molds and the results were in line with the previous reports conducted with *Nicotiana* and *Arabidopsis* (Ko et al. 2006; Lei et al. 2015; Meier et al. 2010). In the 3-punch preliminary device with the 385 μl MS media capacity, the five weeks of growth inside the Petri plate was achieved by refilling the wells with unsolidified agar with a micropipette every week. Growth was observed until formation of a small adult plant (6 leaf stage) and this observation was comparable to the plant-on-a-chip setup, reported previously for *Arabidopsis* (Jiang et al. 2014).

The monocot seedling growth in the final fabricated PDMS device in solid and liquid media after vernalization and synchronous growth was presented in Fig. 1.2 C. Two to three leaf stage of the

seedlings on plant microfluidic chip (on the 13th day) showed a standard growth trend in the device channels filled with 385 μ l of MS media.

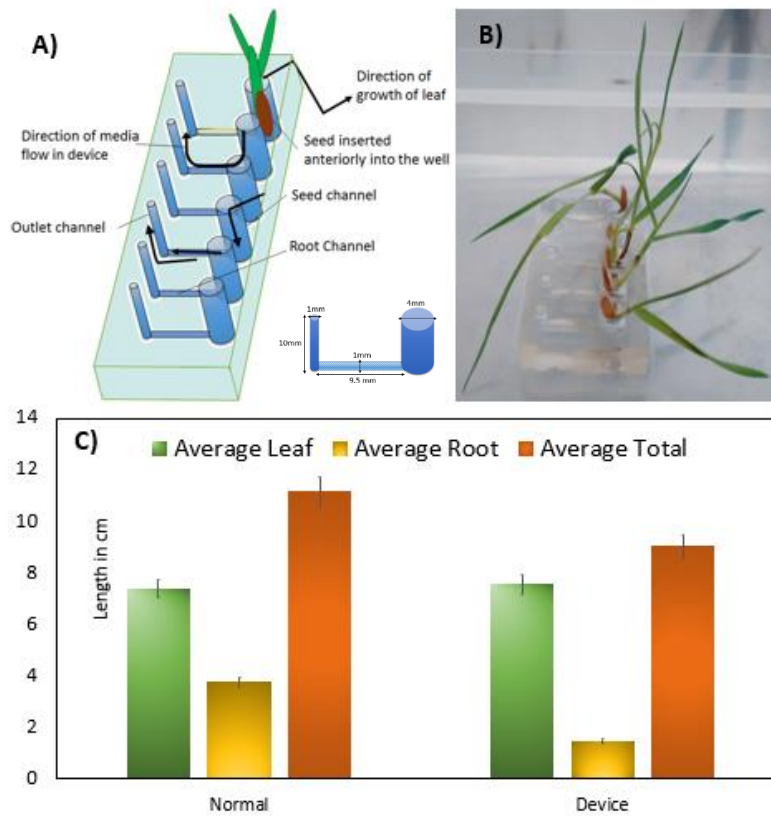


Figure 1.2 The PDMS mold prepared for growth and visualization analysis. The mold (A) used to construct the PDMS plant chip device (B) and comparison of the leaf and root growth in solid MS media plates and the plant chip device (C).

All stress analyses were performed with a control seedling in the same device, thus, under equal experimental conditions. The growth per minute of the root in the channel was compared with the growth per minute in standard MS agar plates in Fig. 1.2 C. The average height of the leaf was 13cm and average root length 1.63cm and maximum shoot length of 22.5cm and root length of 2.6cm was obtained after 3 weeks growth, which we propose as the maximum period to maintain the *Brachypodium* seedlings in the device (Fig. 1.12).

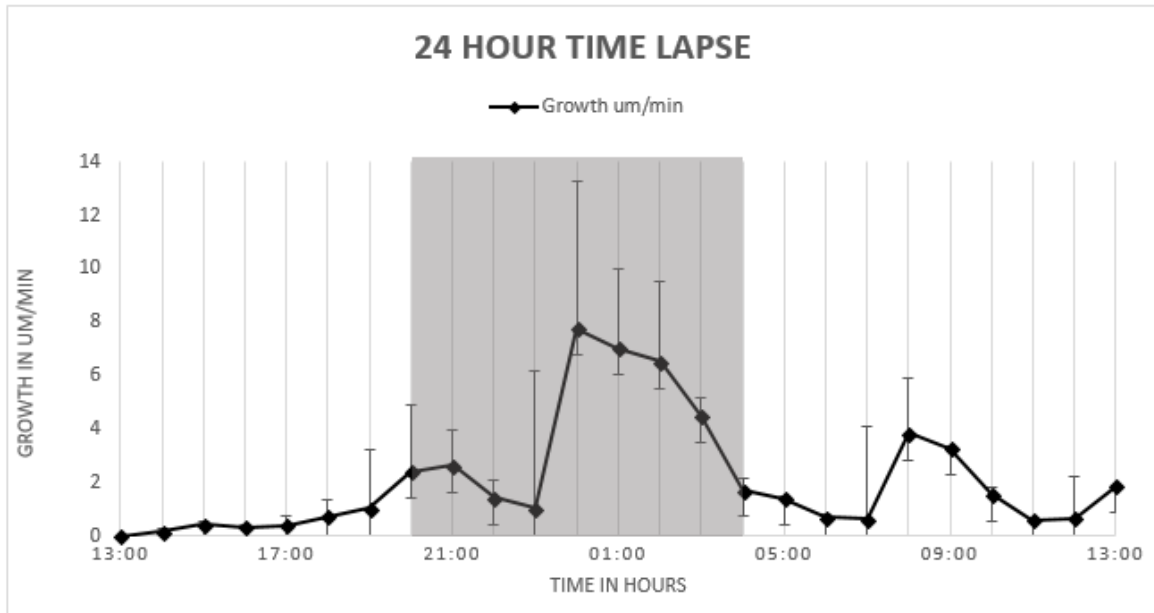


Figure 1.3 Growth curve of Brachypodium seedlings in 24 hours. The growth rate of three independent monocot seedlings in the plant chip device under 16h day and 8h night conditions. The 24h time lapse of Brachypodium seedlings was performed at 24oC with a relative humidity of 37.5%.

After several experiments, we concluded that after 4-7 days of vernalization and 2 DAG seedling stage, the seedling had to be inserted in the correct orientation in the chip to make it grow along the length of the narrow 1mm channel. Growth was observed with the root penetrating the length of the microchannel with slight curvature and bending. With time lapse recording, per minute and per hour growth was recorded and the growth over 24 hours was also monitored. In the plant chip device, the growth per minute was $4.3 \mu\text{m min}^{-1}$.

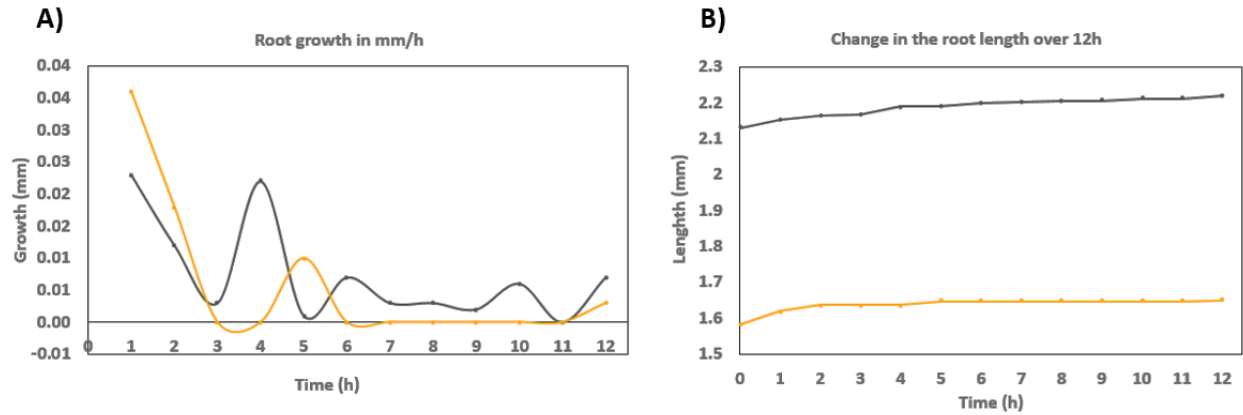


Figure 1.4. Root growth trend of two seedlings under PEG stress for 12h. The coloured lines show two seedling roots observed over a 12hour period.

The growth rates of three independent *Brachypodium* seeds were observed for 24h in the microfluidic device and presented in Fig. 1.3. The rate of growth under the dark conditions was high and in agreement with the results from previous reports (Grossmann et al. 2011, Yazdanbakhsh et al., 2011) in which a sudden increase in the growth rate was also noticed in the night for *Arabidopsis thaliana*.

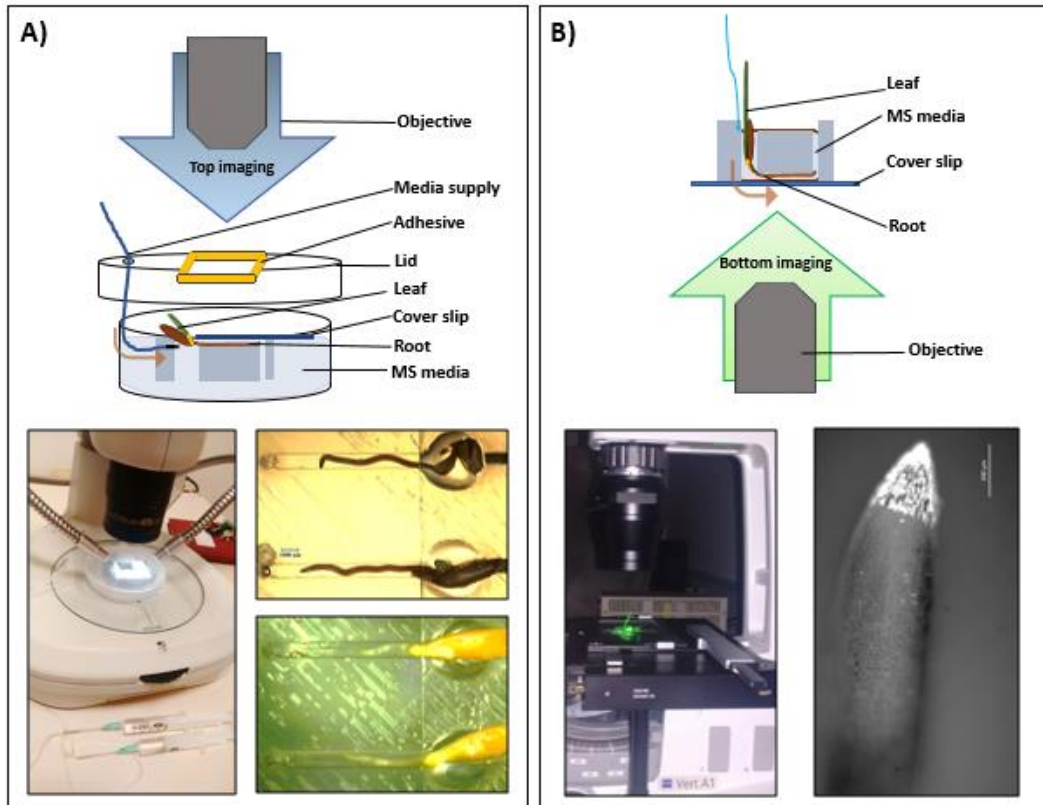


Figure 1.5 Experimental setups for imaging. Top imaging (A) and fluorescent bottom imaging (B). Three days-old seedlings having roots were mounted into wells for the top and bottom imaging. Top imaging studies were conducted with a Nikon SMZ 1500 stereomicroscope (Japan) while the fluorescent imaging studies were conducted with a Zeiss Axio Vert.A1 inverted microscope (Germany).

Fig. 1.5 shows the images obtained from both the top and bottom imaging arrangements. Fig. 1.5 B shows the direct focus of the fluorescence microscope on the cover glass with 0.17mm thickness to enable fluorescence. As mentioned before due to the size of the monocot seed more than 2 parallel experiments could not be observed. However, the synchronous growth of 2 channels was analysed. The bottom imaging setting allowed the imaging of a single channel at a time but nevertheless provided accurate fluorescent signal for comparison of stress and control samples. Fig. 1.6 shows the maturation (differentiation) zone that turned to be square-like large compartments following 6h osmotic stress by 20% PEG in comparison to the longitudinal cells observed during the normal growth. Also, the growth of several lateral roots was observed in the stressed samples, indicating an adaptive behaviour of the cells to expand the space and surface area for further water uptake (Paez-Garcia et al. 2015).

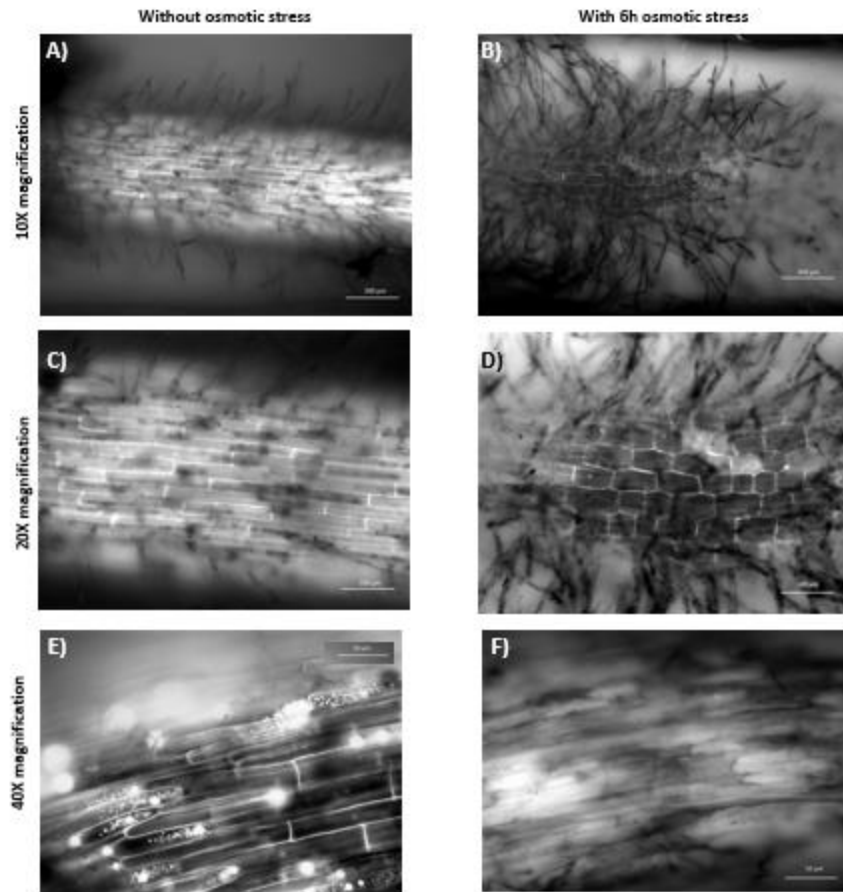


Figure 1.6 Fluorescent microscopic observations of normal and osmotic stressed roots. Growth in the plant chip device after 72h, maturation zone cells under normal conditions (A and C) and after 6h osmotic stress by 20% PEG (B and D). The images were taken with an Axio Vert.A1 inverted microscope by Carl Zeiss (Germany). (E) and (F) show the maturation zone with 40X magnification.

This behaviour of root hairs showing extensive growth was also observed after 18hour osmotic stress on the root tips (Fig. 1.8 A and B). Similar results were also achieved by cross-section analysis of the maturation zone and confocal microscopy experiments, as presented in, Fig. 1.7 and 1.11, respectively.

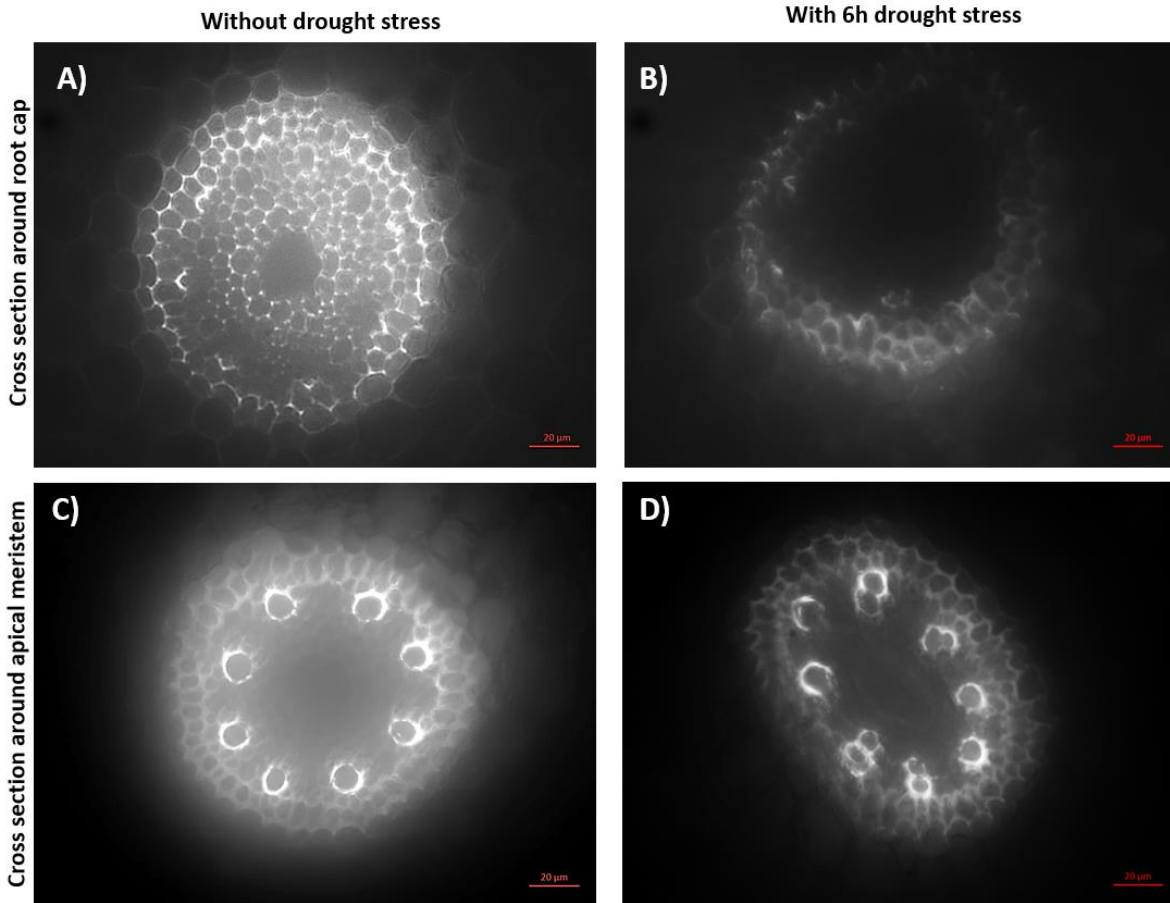


Figure 1.7. Cross section comparison of normal and drought stressed root samples. Cross-section images of maturation zone cells obtained from the plant samples under normal (A and C) and 24h osmotic stress conditions (B and D). The images were taken with an Axio Vert.A1 inverted microscope Carl Zeiss (Germany).

A study on young wheat seedlings also confirms such cell wall expansion in the maturation zone upon a low water potential around the roots and the authors suggest the accumulation of some solutes within the elongation and maturation zones in order to maintain the turgor pressure, resulting in an increase in the root diameter (Akmal and Hirasawa 2004). Although not seen in maturation zone cells, but a similar swelling behaviour of cells at the root apical meristem zone upon treatment with 5% PEG was previously reported for *Brachypodium* as well as wheat, rice, soybean, and maize (Ji et al. 2014), suggesting a collective response by root tissues of different plants to surmount the osmotic stress.

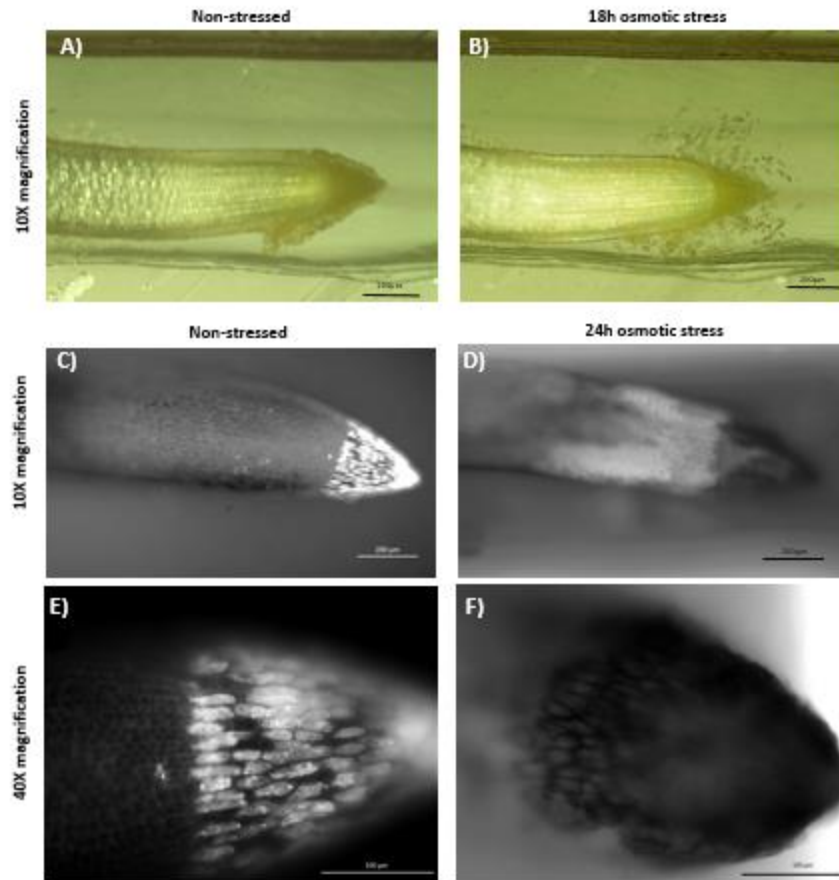


Figure 1.8 Comparison of root tip and maturation zone under osmotic stress. Brightfield visualization of the apical meristem without stress (A) and appearance of root hair after 18 hours (B). Root apical meristem in the root channel after 72h growth, under standard and 24h stress conditions by 20% PEG; (C) and (D) show the root cap samples with 10X magnification; (E) and (F) show the root cap samples with 40X magnification; The images were taken with an Axio Vert.A1 inverted microscope by Carl Zeiss (Germany).

In accordance with these results, Fig. 1.8 shows images of maturation zone cells obtained from plants under normal (C and E) and 24h osmotic stress conditions (D and F), which indicates abnormal differentiation within the stele region of the sample under 24h osmotic stress induced by PEG. On the other hand, high fluorescent signal with bright and distinctly visible organelles appears to be higher in the root cap cells under standard growth conditions. Under osmotic stress no fluorescence was observed in the root cap cells —which are the first sites of the plant in direct contact with the osmotic stress induced by the PEG molecules— as can be seen in Fig. 1.6 E and F.

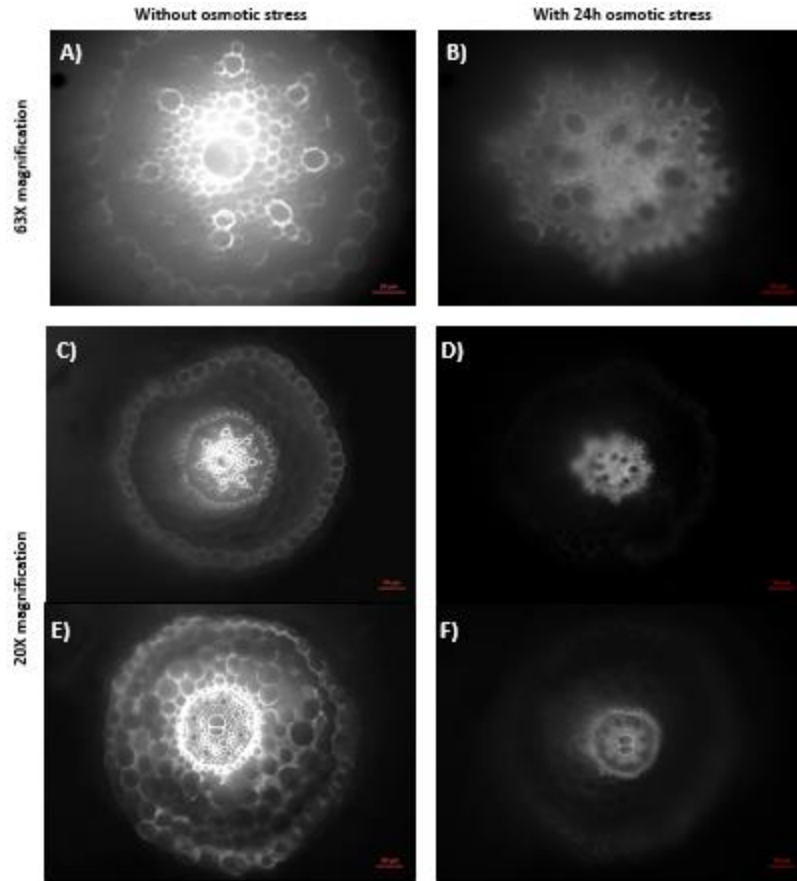


Figure 1.9 Cross section fluorescent visualization of transport tissue under normal and osmotic stress

In Fig. 1.9, cross section images taken 1.5 mm (around the tip) and 3 mm beneath (around the apical meristem) the root tips of the normal (A and C) and the stressed samples (B and D) additionally confirmed reducing fluorescent signals as well as deformation of the cells in the sample under 24h osmotic stress, as presented. Cross-section images of the elongation zones from standard and stressed plant samples also confirmed the decreased fluorescent signals around the peripheries of the plant under 24h osmotic stress, as shown in Fig. 1.9 E-F.

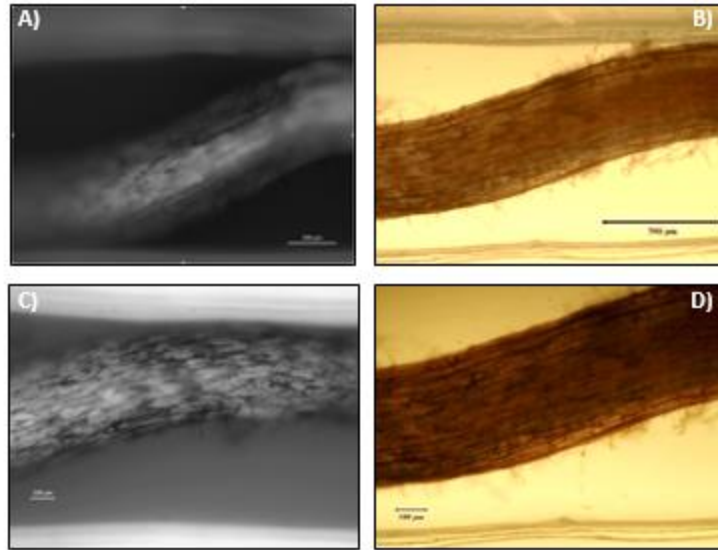


Figure 1.10 Neutral Red stained stressed samples under fluorescence and brightfield microscopy. Neutral Red staining of the root with (A and C) and without (B and D) fluorescence visualization was seen after 24hr, osmotic stress mostly concentrated in the internal vascular tissue. However, a reduction in the fluorescence was observed after 24hr stress in all samples.

The morphology of the midsection of the root was also analyzed with and without fluorescence as seen in Fig. 1.10 A-D. The striations of live and dead cells can be differentiated by the fluorescence of neutral red, which looks concentrated around the vascular cylinder rather than the peripheral cells. Staining appeared intense within the internal cells around stele zone and not on the peripheries which were in direct contact with PEG, indicating a hindered growth which was confirmed by fluorescence microscopy after 24h.

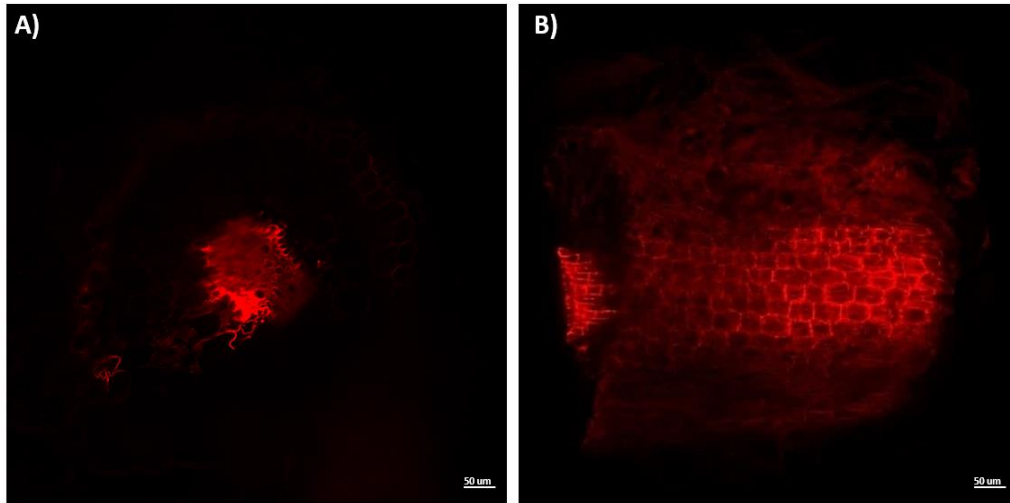


Figure 1.11. Confocal microscopy images under drought. Confocal microscopy shows the maturation zone cells after 6h osmotic stress by 20% PEG (B). The cross-section image (A) corresponds to Figure 1.6 D and the sideview confocal image (B) corresponds to the maturation zone images presented in the Figure 1.6 B in the manuscript.

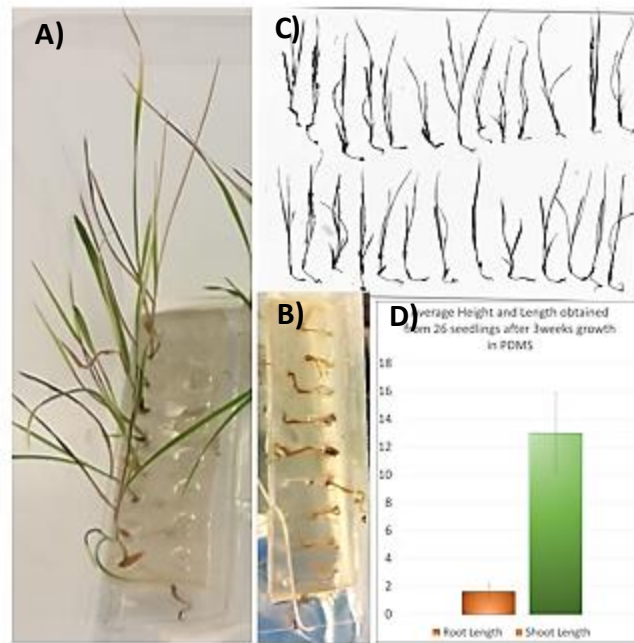


Figure 1.12 A) Growth at >3 weeks, B) showing the root growth in a single plane but hindered due to the channel. C) The maximum growth obtained after 3 weeks showing potential for a root array arrangement and maintenance for a month. D) The average growth of the plants roots and shoots obtained from the array.

1.4 Discussion

The behaviour of seedlings from *Brachypodium* in polydimethylsiloxane (PDMS) channels was explored in this study. Due to the large size (8mm x 2mm) and elliptical polarity of the root and shoot growth i.e. the differences between the anterior and posterior of monocot seeds with the embryonal axis from where the seed germinates, the horizontal 3-punch device proved to be well suited for the adequate development of the shoot and roots in agar media as compared to liquid media, as presented in Fig. 1.1 D and E. Multiple serial channels were prepared to imply the array utilization of this setup. Growth was observed for the *Brachypodium* seedlings inserted into narrow channels. Root growth in the microfluidic device was limited due to the space in the PDMS microchannel (Fig. 1.2 B and Fig. 1.12 B). The narrow 1mm long channel though restricted the normal growth but this facilitated the observation of the real time growth of the root and provided live analysis for root elongation along a single plane.

However, the multiple channels could not be simultaneously visualized under the microscope due to the macroscopic nature of the seed and PDMS platform size (Fig. 1.12). Studies were thus limited to analyzing single or double channels under low magnification (0.75x and 1X). With the facilitation of a single plane for of provided by a narrow 1mm Z axis PDMS channel the effects of osmotic stress on root development were investigated in real time with various microscopy studies. The microfluidic channel system allowed the positioning of monocot *Brachypodium* seeds at serially arranged microchannels where the root-cell microenvironment can be precisely controlled, watered, visualised in real-time, and desired stress conditions can be established. Earlier microscopic studies have been done on the morphology (Filiz et al. 2009; Oliveira et al. 2017), growth (Barrero et al. 2012) and development (Guillon et al. 2012) of *Brachypodium* and our study focuses on real time growth dynamics and osmotic stress conditions in young seedlings.

Abiotic stress studies have been under considerable scrutiny particularly in crop plants because of the loss in crop yield caused by the climate change (Akpınar, Lucas, and Budak 2013; Budak et al. 2015; M Kantar, Lucas, and Budak 2011). The plant *Brachypodium distachyon* is a model for monocotyledonous plants which constitute the major cereal and food crops of the world. *Brachypodium* has been used extensively in gene expression studies previously (Hong et al. 2008; Priest et al. 2014), because it is an ideal grass model regarding its sequenced genome, small stature, rapid growth time and evolutionary relation to the valuable crop species such as wheat (Bevan, Garvin, and Vogel 2010; Brkljacic et al. 2011; Budak and Akpınar 2011). Amongst wheat wild relatives *Brachypodium* also has many characteristics to tolerate and adapt to drought due to its geographical location and many efforts are being done to translate these desirable traits in related crops barley and wheat (Verelst et al. 2013). Studies on the genotypic manipulation of *Brachypodium* for drought tolerance are numerous but for phenotypic manipulation of *Brachypodium* for drought analysis including osmotic analysis have not been observed previously at early seedling level.

Arabidopsis thaliana is an important model plant due to its simple structure and small adult size, small seed size and has been used in microfluidic platforms to create an entire Plant on a chip array amongst many other PDMS devices and microfluidic designs (Jiang et al. 2014). However *Arabidopsis* in recent years has been reserved as a model for dicotyledonous plants. The small annual species *Brachypodium distachyon*, is a suitable framework for the investigation of particular developmental processes which include dissecting the cell wall biology, the development of the endosperm, the controls of flowering, and the development of the inflorescence (Fitzgerald et al. 2015; Girin et al. 2014; Kellogg 2015; Opanowicz et al. 2008; Vain 2011). In addition to ease of analysis of the physical structure development *Brachypodium* fit well into the framework of a model plant for phenotypic and growth dynamics analyses because of its small size and small seed size compared to other monocots, rapid cycling and the simplicity of its development furthermore making it a suitable candidate for microfluidic analyses. With the manipulation of solely dicot species in microfluidic platforms, the gaining importance of monocot model species as well as the ease of analysis of developmental structures of *Brachypodium* it was all the more appropriate to introduce the model monocot species into the novel technology of plant microfluidic analysis. In the current study, *Brachypodium* was selected to investigate the effects of osmotic stress on monocot plants in a microfluidic channel system. *Brachypodium* seeds (8mm

x 2mm) despite being considerably larger than *Arabidopsis* seeds (<500µm) (M. Chen et al. 2012) and having seed polarity, has the potential to be used in microfluidic systems. **Table 1** shows that major analyses of plant tissues done in microfluidics have majorly been pollen tubes, fungal spores and *Arabidopsis* seeds all of which are considerably smaller in size and less complex than *Brachypodium* seeds. We imply that a microfluidic platform can be utilized for analyzing the physical parameters of early seed growth in real time and osmotic stress analysis. Studies of the root elasticity, Young's modulus, physical tension, and root and root hair dynamics in PEG supplemented growth media are further areas of research which can be pursued. The aim of our study was to downsize the abiotic stress analysis on monocots and observe the effects of stress in real time by detailed microscopy analyses, which was achieved using a modified microchannel growth system.

The results obtained directly point towards the high resilience of *Brachypodium* roots under osmotic stress even at three days after germination. *Brachypodium* proved to be well adapted to the microfluidic system in contrast to other non-model monocot seeds such as wheat (Brkljacic et al. 2011) that has multiple roots, large seeds, and bending shoots and thus, hard to manipulate in a microfluidic platform. In the initial experiments, *Brachypodium* was able to survive in a minimal volume of agar media, and in the microchannels, it was able to reach a leaf height and root length to allow for microfluidic chip manipulation microscopic analysis. We successfully observed the effects of osmotic stress at microscale with for model *Brachypodium* seed. Our study provided a valuable modification to the standard Petri plate systems to minimise resources, apparatus, labour and time for the analysis. This multiplexed microchannel technology has the potential to interrogate a diverse range of abiotic stress microenvironments, both for functional phenotyping of the root cells and the comparison with normal growth cells. Such experiments can be performed with salt stress, nutrient deficiency and hormone (ABA) stress simultaneously, observing the real-time changes in the plant during the stress, similar to the macro-scale studies (Akpinar et al. 2012).

The living and dead parts of the *Brachypodium* root were shown using the differential stain neutral red. A prominent observation was the *Brachypodium* root dynamics under the osmotic stress. Growth of the root from the embryonic axis was physically stressed whilst growing the length of

the microchannel in a single plane Z axis but nevertheless necessary to ensure real time visualization. The large root size of the *Brachypodium* seed in comparison to *Arabidopsis* makes it difficult to manipulate for imaging in a microfluidic system, nevertheless by maintaining the *Brachypodium* root inside the microchannel in a single plane the imaging of the root cap, root cap hairs and elongation zone of the root was possible. Fluorescence imaging further facilitated the analyses of root zones inside the PDMS channels. The adaptive characteristics to the osmotic stress showed that the root cells tend to stop their growth (Fig. 1.11) and slow down their metabolism which was observed as a weak fluorescent signal after 24h of osmotic stress. The root tip showing vivid fluorescence under the standard conditions completely blurred out after 24h 20% PEG application. Striations were observed on the surface of the root length because of a diagonal pattern of the live and dead cells. No explicit observation was obtained in terms of root hair elongation such as in *Arabidopsis* (Grossmann et al. 2011), although at 18h in the osmotic stress, the root tip showed fanning out of root hairs (as shown in Fig. 1.6 A, B) comparable to that observed for the root hairs in Fig. 1.5. It was interesting to note that the protrusion of root hair under osmotic stress was only observed with unstained samples. This phenomenon was not observed when the samples were stained with neutral red neither under fluorescence nor under brightfield.

CHAPTER 2

OVEREXPRESSION OF A NEWLY DISCOVERED MICRORNA MIR7757 IN THE WHEAT WILD RELATIVE *BRACHYPODIUM DISTACHYON* T-DNA MUTANT FOR INVESTIGATING THE ROLE OF MIR7757 IN ABIOTIC STRESS

1. Introduction

The role of insertional mutagenesis by *Agrobacterium*-mediated transformation has resulted in extensive genomics and transcriptomics studies in various plants species by validating the function of a microRNA. The complete genome sequence availability of model plants such as *Brachypodium distachyon* has catapulted the amount of research regarding the role of a myriad of developmental and stress related genes and their confirmation and establishment of their role in different growth/stress conditions. MicroRNAs are important transcriptional and post transcriptional regulators of gene expression in eukaryotes such as plants. They play a crucial role in their development, and biotic and abiotic stress responses. miR7757 is a newly discovered microRNA with few studies on it. Most recent studies have shown its role in biotic and fewer reports in abiotic stress suggesting its role in development, cold/salt/water stress and pathogen stress. miR7757 has been shown to have a role in wheat leaf rust, fungal and bacterial disease, in dicot plantlets and wheat plantlet during water deficit, as well as in developing embryo. Since it is not well characterized and recently observed to be involved in wheat we selected this microRNA to study in the wheat wild relative monocot model plant *Brachypodium distachyon*. With the availability of the T-DNA mutant resources for *Brachypodium distachyon* we traced a seed line mutant for miR7757. Overexpression of miR7757 into T-DNA mutant line of *B. distachyon* via *Agrobacterium* transformation by compact embryogenic callus co-culture will generate overexpressing miR7757 plants which will subsequently be characterized for several biotic and abiotic stresses.

1.1 Reverse Genetics

The classical genetic approach for investigating biological pathways characteristically starts with identifying mutations that cause a phenotype of interest (Prelich 2012). This is the approach used in “forward genetics” to first analyze the genotype of a mutation and link it to an altered phenotype (Krysan 1999). However, a fundamentally different approach used to address the phenotype caused by a mutant gene sequence takes the tactic of first dealing with the mutant sequence or creating one and questioning what phenotypic change has been caused by the certain mutation. This modus operandi is called reverse genetics and is now being heavily pursued due to the recent and rapidly increasing availability of complete genome sequences and similar genetic and genomic resources. Reverse genetics studies involve gene knockout and null mutations which facilitate and comment directly on the function of the gene expression product in situ. As already implied above the altered genetic mutation, knockout or null mutation allows the monitoring of the gene mutation or deficiency to check its effect on the organism’s ability to function.

1.2 Overexpression Advantages

A massive variety of molecular mechanisms occurring in nature regulate the expression of genes at the appropriate level in the appropriate conditions. Certainly, a reduction in expression below the required threshold for normal functioning can be due to a partial or complete loss of function of the gene and can cause a mutant phenotype. Parallel to this the increased expression of normal wildtype gene should also be disruptive to the organism. However, overexpression phenotypes abound naturally, with gene amplification resulting in insecticide, drug, and heavy metal resistance. (Stark and Wahl 1984). Since the overexpression of wildtype genes can cause mutant phenotypes, this has been exploited by scientists working in controlled genetic environment setups as a similar approach to loss of function screens (Prelich 2012). Overexpression developed as a genetic tool before molecular cloning with studies in *Arabidopsis* showing a viral enhancer causing overexpression of the JAW miRNA affecting leaf development and resulting in a more distinctly prominent leaf phenotype (Palatnik et al 2003). Further studies showed that overexpression libraries could be used not for cloning genes by complementation as functional probes, but also could independently identify phenotypes in wildtype cells. Therefore, overexpression screens were established as a feasible research option in several organisms. However a main hindrance for the

widescale application was the lack of genetic resources to facilitate routine application (Prelich 2012). Thus, the need for a development for plant genetic mutant lines was imperative. The approach taken for *Arabidopsis* was the insertional mutagenesis by transfer DNA of *Agrobacterium tumefaciens* (Krysan 1999).

1.3 *Arabidopsis* T-DNA Mutant Collection

To reap the benefits of reverse genetics approach for genotype-phenotype analysis it is essential to apply targeted mutagenesis to create a pool of compromised genes and analyze their phenotypic effects. In mice knockout mutations were done by homologous recombination of murine embryonic stem cells, provided the mutation achieved was not embryonic lethal, the “knockout mice” could be developed in utero. Previously yeast and *E. coli* were also used for reverse genetics by targeted mutation by homologous recombination. Intact *Arabidopsis* plants were also initially tried for homologous recombination, but the frequency obtained was possibly too low to encompass the ~125000 genes of the 120MB genome.

1.3.1 T-DNA Insertional Mutagenesis

The role of insertional mutagenesis by *Agrobacterium* mediated transformation has resulted insertion mutant library development thereby facilitating the reverse genetics analysis. This has resulted in extensive genomics and transcriptomics studies in various plants species by validating the function of a gene, transcription factor and a microRNA. The complete genome sequence availability of model plants such as *Arabidopsis thaliana* and relatively recently monocot model plant *Brachypodium distachyon* has catapulted the amount of research regarding the role of a myriad of developmental and stress related genes and their confirmation and establishment of their role in different growth/stress conditions. In this aspect the T-DNA mutant database of *Arabidopsis* (Krysan et al 1999, <http://www.gabi-kat.de/>) has provided a crucial role in elucidating gene function in mutant lines. Likewise, with the recent availability of the *Brachypodium distachyon* WRRRC T-DNA database (Bragg et al 2012, <http://brachypodium.pw.usda.gov/TDNA/>) gene functional studies have greatly increased.

1.4 *Brachypodium* as a Model Organism

Arabidopsis is a dicotyledonous crucifer that is not only physiologically and morphologically different but also developmentally all in all different from the cereal grasses which are staple food for most of the world's population. Various parts of the biology of these cereal crops necessitate a model plant that closely resembles their features. Despite cereal crops being excellent models for certain purpose, most of them are inappropriate to work with because of special growth requirements as in rice, large size as of maize, or genetic characteristics such as their genome. Undoubtedly the most problematic for genetic studies are wheat, rye and barley and their related 375 wild species, which have some of the largest genomes of grasses. *Hordeum vulgare* haploid (1C) genome size is 5.1Gp and that of *Secale cereale* is 8.1Gp which are both much larger than that of maize. Barley and rye are both diploids and the large genomic size is attributed to accumulation of transposons. *Triticum aestivum* on the other hand is a hexaploid with a genome size of around at ~17 Gb. With such huge and difficult to manipulate genomes and growth conditions of most cereals. *Brachypodium*, in particular *Brachypodium distachyon* has become a suitable framework for investigation of biological processes such as dismembering the cell wall biology, the development of the endosperm, the controls of flowering, and the development of inflorescence. *Brachypodium* was initially chosen as a model due to the phylogenetic proximity to the *Triticeae* clan wheat and barley than to maize or rice. In addition it has the typical qualities of a model plant a small size both genetically and morphologically, rapid life cycle and simple development. (Fitzgerald et al. 2015; Girin et al. 2014; Kellogg 2015; Opanowicz et al. 2008; Vain 2011)

1.4.1 *Brachypodium* T-DNA mutant collection

The need for creating the *Brachypodium* T-DNA mutant line collection stemmed from the fact that this small grass species *Brachypodium distachyon* contains the many desirable characteristics of a genetic model organism harboring traits of scientific interest for the improvement and development of its relative grasses serving as cereal food, feed and fuel namely wheat, barely, switchgrass and *Miscanthus giganteus*. With the recognition of these advantages the Department of Energy Joint Genome Institute (DOE JGI) proposed the development of *Brachypodium* as a model species for cereal plants for use in the domestication of energy crops in the report "Breaking the Biological Barriers to Cellulosic Ethanol: A Joint Research Agenda" in 2005. This marked the

beginning of a comprehensive organization of the genomic resources of *Brachypodium* and to date this genomic resource has expanded vastly. This funded DOE Feedstock Genomics Program project aimed to add a huge collection of T-DNA mutants to the increasing *Brachypodium* genomic resources. These T-DNA lines were indexed through flanking sequence tags FSTs which facilitated the mapping of the T-DNA insertions in the *Brachypodium* genome. This collection hence serves to identify mutations in genes which putatively affect biomass quality and agronomic characteristics of cereal and energy crops. These T-DNA mutants lines were publicly available through the site <https://jgi.doe.gov/our-science/science-programs/plant-genomics/brachypodium/brachypodium-t-dna-collection/> which allows any interested scientist to identify knockouts in their genes of interest.

The creation and sequencing of the first 8,491 T-DNA lines was done by *Agrobacterium tumefaciens* mediated high efficiency transformation method. The collection contains the plants produced by various constructs made for different purposes. T-DNA constructs namely pOL001, pJJB/pJJ, pJJB2LB/pJJ2LB, pJJ2LBA, pJJ2LBP2, pJJ2LBP were used to generate most of the population of the USDA-ARS-WRRC T-DNA collection. All the plant lines in the collection are T-DNA insertional mutants and can create gene knockouts and it was the purpose of the plant lines created by using the pOL001, pJJH, pJJ2LB, pJJB, and pJJB2LB vectors. Most of the constructs also contained the β -glucuronidase reporter genes (GUS and GUSPlus) with a rice tubulin intron having splice donor and acceptor sites. The cauliflower mosaic virus 35S promoter (CaMV 35S) and transcriptional enhancer sequences (4x CaMV35S enhancer) was used for some of the insertional mutagenesis vectors including pJJ2LBA. The constructs also contained phosphinothricin acetyl transferase selection (*BAR*) gene and others contained hygromycin phosphotransferase selection marker (*HptII*) under the control of maize ubiquitin promoter. The *Zea Mays* ubiquitin promoter with intron (ZmUbi) was also present in almost all constructs. Inverse PCR was used to sequence the DNA flanking the insertion sites in the mutants (Bragg et al. 2012). Additionally, the T-DNA regions of pJJ2LBP and pJJ2LBP2 vectors encompass “gene trap” sequences and adjacent to the left border these contain a promoter-less GUS gene and a promoter-less GFP gene is placed adjacent to the right border. If the T-DNA inserts downstream of the promoter on either side of the promoter genes will show expression pattern of the disrupted gene. The constructs also contain several splice sites adjacent to the reporter genes for allowing efficient splicing in case the T-DNA inserts into an

intron. This the T-DNA lines can potentially provide hints regarding the role of the disrupted gene to understand its function and identify promoters having useful expression patterns.

The pJJ2LBA and pJJ2LBA2 vectors harbour transcriptional enhancers inside the T-DNA sequence. These are “activation tagging” constructs and are designed to enhance the nearby genes transcription. Significantly, the transcriptional enhancers were constructed to give overexpression with the same expression pattern, instead of constitutive expression, of affected genes. Activation tagging was particularly well suited to allocate function to genes with redundant functions where knockouts do not produce a phenotype in an individual family member.

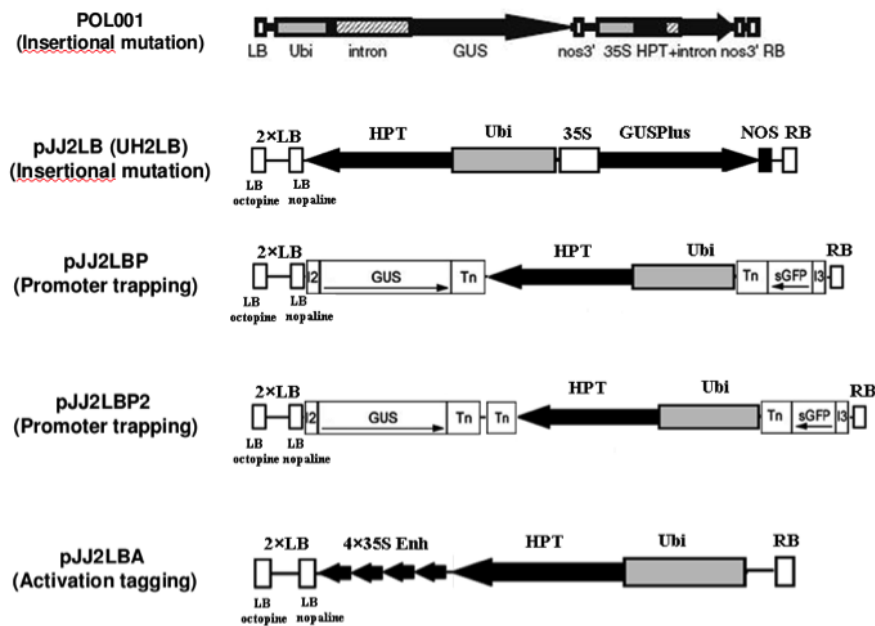


Figure 2.1 Promoters used for creating T-DNA mutations

To optimize transformation efficiency an extensive evaluation of vectors made with various promoters, selectable markers and reporter genes was done. Considerable variation in the plant fertility, survival and efficiency of transformation depended on the construct used. Transformations using hygromycin selection produced constantly higher efficiency and survival as compared to those using BASTA. The promoter driving the selectable marker greatly affected the transformation efficiency showing the highest efficiency of the maize promoter (maize ubiquitin > CaMV 35S with a 5' intron > CaMV 35S without a 5' intron >> rice tubulin) as compared to the lowest efficiency of the rice promoter. Keeping in view time and ease of

evaluation, screening transformed tissue for GUS staining was rapid and more efficient than for GFP or RFP fluorescence. T-DNA vectors having two left border sequences produced transformants that yielded a higher rate of positively recovering sequence flanking the T-DNA insertion sites. Ac/Ds and En/Spm transposons showed function in *Brachypodium*, but were lethal, conceivably because they are too active.

The current collection of the WRRC USDA updated on 11-2-2017 shows that the present lines in the T-DNA collection are 23,649 and the identified unique insertion sites stand at 25,977 (Hsia et al. 2017). The T-DNA insertions assembly version V3.0 updated 3-18-2016 is available on the *Brachypodium* T-DNA website. For searching for insertions in specific genes on interest JBrowse can be used in Phytozome (https://phytozome.jgi.doe.gov/pz/portal.html#!info?alias=Org_BdistachyonBd21_3_er)

1.5 microRNAs

MicroRNAs or miRNAs are small regulatory RNAs usually 20-24 nucleotide in length and are involved in the post transcriptional regulation of gene expression (Sunkar, Chinnusamy, and Zhu 2007). miRNAs act in two ways to downregulate the expression of their target genes either by cleavage or by translational repression (Khraiwesh, Zhu, and Zhu 2012). miRNAs are involved in regulating gene expression both in animals and in plants (Guleria et al. 2011). To date a substantial number of miRNAs have been discovered and reported both in animals and in plants and are available in the online miRNA database (www.mirbase.org). miRNAs have been shown to be extensively involved in a large range of plant stress responses either pathogen or abiotic (Budak and Akpinar 2011), developmental conditions (Wu et al. 2009) a few being flowering (anther production) (Aukerman 2003), and in signal transduction (Sun 2012).

1.5.1 microRNA Biogenesis and Gene Mediated Regulation

Primary transcripts of plant miRNAs are encoded by *MIR* loci that mostly reside in intergenic regions. Few plant miRNAs originating from intronic or exonic sequences of protein coding genes have also been reported (Colaiacovo et al. 2012; Liu 2012; Meng and Shao 2012; Rajagopalan et al. 2006), in addition to *MIR* loci located within Transposable Elements (TEs) (Kurtoglu, Kantar, and Budak 2014; Y. Li et al. 2011). Transcription from these *MIR* loci through the action of RNA polymerase II generates a primary transcript (pri-miRNA) that folds back into an imperfect hairpin structure (Voinnet 2009). The transcribed pri-miRNAs is stabilized by the addition of 5' 7-methylguanosine cap and 3' polyA tail, and by the help of additional proteins, such as DDL (DDL) that interacts with DCL1 (Xie, Zhang, and Yu 2015); in the absence of DDL activity, both pri-miRNA and mature miRNA levels drop (Yu et al. 2008). DDL protein likely has additional roles as *Arabidopsis ddl* mutants exhibited many developmental and reproductive defects (Morris, Chevalier, and Walker 2006). The fold-back structure of pri-miRNA is recognized by the members of the DCL family of ribonucleases. In the canonical route, DCL1 processes the pri-miRNA transcripts into stem-loop structures, called precursor miRNAs (pre-miRNAs), and subsequently catalyzes the release of the mature miRNA duplexes with 2-nt 3'overhangs from these pre-miRNAs (Axtell, Westholm, and Lai 2011; Xie et al. 2015). The DCL1-mediated cleavage of the pri-miRNA is assisted by DCL1 interacting proteins, Hyponastic Leaves 1 (HYL1), Serrate (SE) and nuclear Cap-Binding Complex (CBC). While DCL1 and HYL1 are specific to the miRNA biogenesis machinery, SE and CBC have broader functions in mRNA metabolism (Voinnet 2009). The 3'overhangs of the mature miRNA duplex, or the miRNA/miRNA* duplex, are prone to uridylation by uridyl-transferases, marking the duplex for degradation by Small RNA Degrading Nuclease (SDN) proteins. The miRNA/miRNA* duplex is protected through 2'-O-methylation at the 3' termini by Hua Enhancer 1 (HEN1) that prevents the action of exonucleases (Ramachandran and Chen 2008; Ren, Chen, and Yu 2015; Yu et al. 2005). The presence of HEN1 both inside the nucleus and in the cytoplasm suggests that methylation of the miRNA/miRNA* duplex can precede or follow the export of the duplex into the cytoplasm, which involves the mammalian Exportin-5 homolog HASTY (Axtell et al. 2011). However, *Arabidopsis hst* mutants did not accumulate miRNA duplexes inside the nucleus, raising the mammalian Exportin-5 homolog HASTY (Axtell et al. 2011).

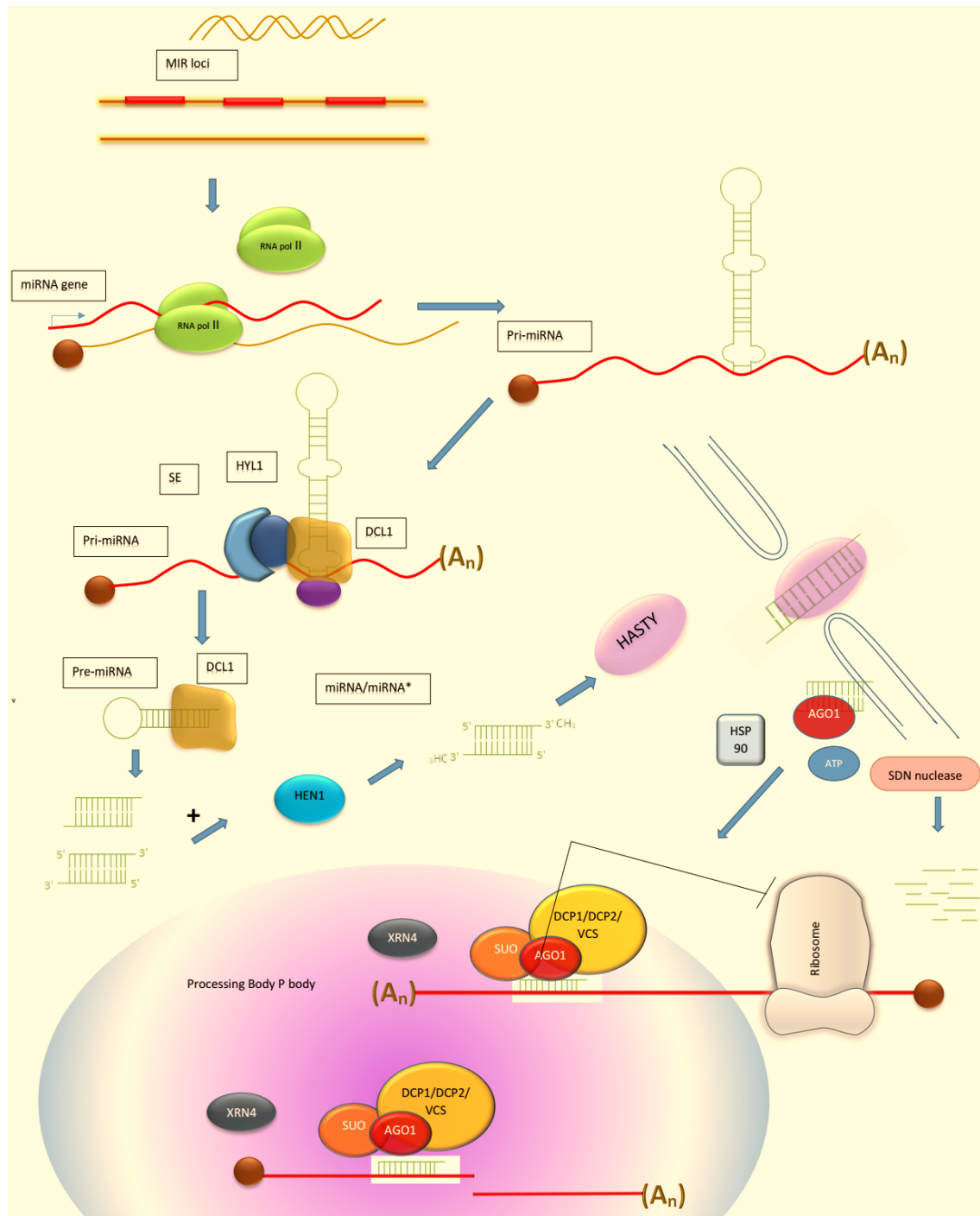


Figure 2.2 miRNA biogenesis and mechanism of action pathway

However, *Arabidopsis hst* mutants did not accumulate miRNA duplexes inside the nucleus, raising the possibility of novel export mechanisms that do not involve HASTY (Park et al. 2005). One of the strands, called the guide strand, of the mature miRNA duplex exported into the cytoplasm is

recruited to the members of the Argonaute (AGO) proteins, which contain an sRNA binding PAZ domain and an PIWI domain that carry out the endonucleolytic cleavage of the target gene. The thermodynamic stability of the 5' of each strand partially determines the selection of the guide strand, which is also assisted by accessory proteins such as HYL1 (Rogers and Chen 2013). While AGO1 exhibit a preference for 5'uridine residue, AGO2 and AGO4 mostly associate with 5'adenosine residues (Voinnet 2009). The guide strand bound by AGO proteins are then assembled into a functional RNA-Induced Silencing Complex (RISC) that drives the mRNA cleavage or translational repression of the target transcripts.

1.5.2 Role of microRNAs in Stress Responses

Plants being sessile organisms are under the full impact of environmental hazards and have thus evolved highly complex yet sophisticated responses to them in the form of molecular, physiological and even anatomical adaptations (Zhu, Ding, and Liu 2011). Amongst abiotic stresses drought salinity and heat have been widely studied and have been shown to be extensively involved in the transcriptional and post transcriptional regulation of an enormous number of genes in plants. From amongst this regulation of gene expression recent evidence has shed light on the regulatory role of plant miRNAs to abiotic stresses. The initial evidence for the association of miRNAs with plant stress came from a study on *Arabidopsis thaliana* under stress, showing the presence of miRNAs not identified previously in normal growth conditions (Jones-Rhoades and Bartel 2004). Currently thousands of plant miRNAs have been predicted and many of them have been experimentally verified as having roles in numerous plant abiotic stress responses.

1.6 miRNA Studies in *Brachypodium*

Sequencing analysis has been used recently in study of drought stress miRNA upregulation affecting leaves of *Brachypodium distachyon*. In the most recent study (Bertolini et al. 2013a) a drought assay was performed and the 3rd leaf of *Brachypodium* was grown in control and stress conditions and then generated small RNA libraries and subjected them to Illumina GAIIx deep sequencing. Extensive analysis of the reads revealed higher representation of 21nt molecules in the libraries, and ad hoc bioinformatic analysis revealed 66 of *Brachypodium* miRNA loci present in the miRBase directory (www.mirbase.org) as well as identification of 28 new miRNA genes which belong to previously identified miRNA gene families. The study identified varying

members of *miR167*, *miR5163*, *miR5167*, *miR5181*, *miR166*, *miR395*, *miR5174*, *miR156* and *miR5185* families. Interestingly *miR162*, *miR394*, *miR398*, *miR399* could not be predicted. These miRNA families belong to highly conserved families from which miR398 has been previously reported to be involved in ABA and salt stress in *Arabidopsis* and *Populus tremula* (Jia et al. 2009). More importantly they found 94 new novel *Brachypodium* specific miRNAs which were previously unidentified, and their precursors bore little similarity to miRBase precursor sequences. Upregulation of miR156 was observed in expanding cells depicting that the normal balance between cell number and size and being consistent with the miR156 SPL dependent drought response pathway. miR528 monocot specific miRNA was upregulated in expanding cells in drought. The miRCB167e locus may be significant. Among the miR167 family the 3' star is unique and is expressed at levels similar to mature miRNA and both sequencing and RT-PCR confirmed these results. Similarly, the recently identified miRCB22-np2 is downregulated in proliferating cells in drought conditions and slightly in expanding cells. Tissue specific expression of miRNAs under drought conditions is still a poorly understood process with varying patterns. These studies were carried out in drought stress by microarray analysis in *Brachypodium* a model monocot temperate grass related to wheat. The expression levels of known miRNAs were quantified by qRT-PCR after 4 and 8 hour stress treatment. In this study three previously unreported miRNAs were identified miR1450, miR406, and miR188. In response to drought stress miR1850, miR390, miR170, miR1450, and miR1881 were upregulated. In leaf tissue under both stress treatments, increased upregulation of miR1850 was observed and the expression of miR528 was downregulated after 8-hour stress. In roots varying expression patterns were observed for both drought treatments. Only after 4 hours miR1450 was induced whereas miR406 was suppressed. Upregulation only upon 8-h was seen for miR1881 and miR170, and in leaf tissue miR390 was also induced in this drought stress time span. In both stress conditions miR390 was responsive (Unver and Budak 2009). In a similar study 438 miRNAs in drought treated leaf and tissues were expressed from which seven were dehydration stress responsive including miR896, and miR1867. Other drought responsive miRNAs were miR406, miR528, miR390, miR170, miR1850, and miR896. These dehydration responsive *Brachypodium* miRNAs were also detected in wild emmer wheat and barley (Budak and Akpinar 2011). In a next generation sequencing data analysis miRNA156 and miRCB159b were found highly abundant. miRCB159b was the most highly expressed miRNA whose targets included MYB65 and MYB33 transcription factors and

potentially Histidinol-phosphate transaminase. Other highly expressed miRNAs in drought were miR160a, miR166c, miRCB167e, miR168, miR169c, miR171d, miR396e, miRCB88, miRCB141. Tissue specificity was found in miR156 and miR396 families (Bertolini et al. 2013b).

1.7 miR7757

miR7757 has been newly identified and characterized as having major roles in abiotic and biotic stress over several plant species. In a study on regulation of alkaloid biosynthesis in the opium poppy it was observed that miR7757 is also expressed as one of the conserved microRNAs found by deep sequencing (Boke et al. 2015). In a study on *Hordeum vulgare* the conserved miRNAs in the diploid check variety showed the highest expression of miR7757 in the diploid check, with decreasing expression in the diploid salt stressed, tetraploid check and the least expression in the tetraploid stress variety. Differential expression of miRNAs in the diploid and tetraploid varieties under salt stress showed that the expression of miR7757 was detected but did not change under the diploid stress variety as compared to the diploid check variety and was not detected in the tetraploid stress variety versus the tetraploid check (Liu and Sun 2017).

miR7757 has recently been studied in wheat. In a study involving the young spikes of common wheat *Triticum aestivum* under cold treatment the miR7757 was found to be cold responsive. Target prediction showed that miR7757 the Leucine-rich Repeat Receptor-like protein kinase family (LRR) also involved in disease resistance was targeted (Song et al. 2017). The microRNAs involved in embryonic development in the immature and mature embryonic calli in *Triticum aestivum* were studied. Deep sequencing of sRNAs of these embryo calli from *Triticum aestivum* showed that miR7757 family was one of the most abundantly expressed. miR7757 had the highest expression values for the non-differentially expressed and upregulated known miRNAs after 3 days of culture. A significant fold change was observed after 6 days in the mature versus immature embryo.

1.8 microRNA Overexpression and Studies

In analytical methods used for downstream miRNA analysis, the microRNA activity is modulated by controlling miRNA expression. A sequence containing pre-miRNA is driven by the 35S promoter resulting in miRNA overexpression (Chen et al. 2010). Overexpression studies have

revealed numerous roles of miRNAs in regulating stress response tolerance. e.g. miR172 when overexpressed in *Arabidopsis* has been shown to influence early flowering and floral organ identity (Aukerman 2003). Furthermore, in another study it was seen that the overexpression of miR159a has been shown to postpone

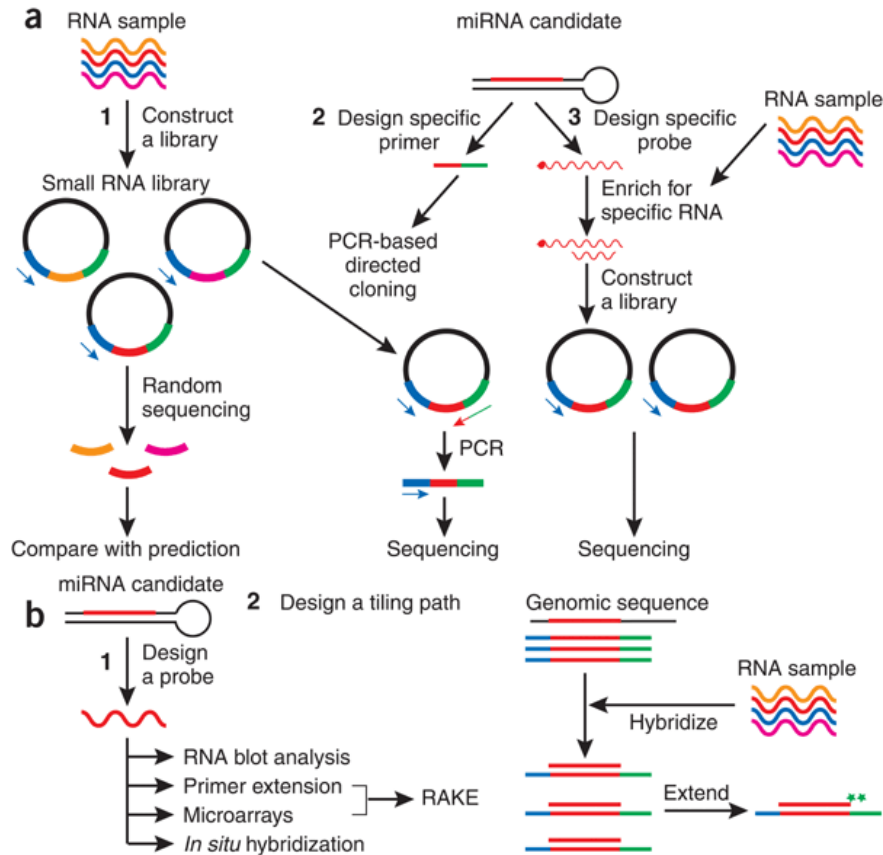


Figure 2.3 miRNA overexpression overview as depicted in Approaches to microRNA discovery, Nature Genetics (Berezikov, Cuppen, and Plasterk 2006)

floral development resulting in smaller leaves than the wildtype plants (Achard et al. 2004). Similarly in transgenic tobacco in vascular development the overexpression of miR166 resulted in the *men1* phenotype, a gain of function mutant of MIR166a (Kim et al. 2005). In nutrient stress miR399 was found to be upregulated, whereas its target gene E2, a ubiquitin-conjugating enzyme was downregulated in phosphorus deficiency, whereas the overexpression of miR399 in *Arabidopsis* suppressed the accumulation of the E2 transcript (Chiou, Aung, and Lin 2006). Furthermore the role of miR399 in enhancing phosphorus uptake was confirmed by the overexpression of miR399 resulting in the increase in phosphorus accumulation (Fujii et al. 2005).

1.9 Overexpression in Drought Studies

Drought stress is one of the most abiotic stress factors affecting crop yield drastically worldwide. Various miRNAs have been identified and characterized under drought stress in numerous plant species. The role of miRNAs in drought stress is therefore of consequence in understanding plant stress tolerance. Many studies overexpressing miRNAs, their target genes and transcription factors have been undertaken e.g. in drought stress the overexpression of miR169 resulted in increased water loss and thus more sensitivity to drought (Li et al. 2008). In wheat and *Arabidopsis* the target gene of miR408, was found to be the plantacyanin TaCLP1. This gene was overexpressed in *Schizosaccharomyces pombe* which showed increases resistance to high salinity, Cu²⁺ stress and stripe rust (Feng et al. 2013). In rice a drought-hypersensitive mutant phenotype dsm2 was created through T-DNA insertion in the putative gene for b-carotene hydroxylase- a gene for zeaxanthin biosynthesis, a precursor of ABA. The overexpression of DSM2 lead to high drought and oxidative stress resistance by increase in the xanthophylls, upregulation of stress related ABA genes and non-photochemical quenching (Du et al. 2010). In another study for increased drought tolerance in *Arabidopsis thaliana* the overexpression of RING H2 E3 ligase RHA2a- a positive regulator for ABA signalling showed ABA hypersensitivity resulting in physiological adaptations (reduced water loss, greater stomatal closure) for increased drought tolerance (H. Li et al. 2011). Similarly, in other studies in drought tolerance, homologous U-box E3 ubiquitin ligases AtPUB18 and AtPUB19 were shown to be involved in negative regulation of abscisic acid through overexpression tests. This resulted in higher stomatal closure and water stress responses. Their ABA-dependent and ABA independent roles both were elucidated by overexpression studies in different mutant phenotypes. (Seo et al. 2012). In AtTRE1 overexpressing mutant lines lower trehalose levels showed better recovery after drought stress and increased water retaining capacity.(Van Houtte et al. 2013). The overexpression of *MYB15*, a promoter of the *MYB* gene encoding transcription factor R2R3 MYB encoding gene was previously shown using the floral dip method, to confer improved drought and salt tolerance through increased sensitivity to abscisic acid in *Arabidopsis thaliana*. (Ding et al. 2009). More specifically related to miRNA studies, a miRNA target gene *gma-MIR394a* was overexpressed in *Arabidopsis* which reduced the transcript level of the miR394 complementary site target. (Ni et al. 2012).

2 Materials and Methods

2.1 Production of Immature Embryos from Bd21-3 Wildtype and miR7757 T-DNA Mutant Plants

The tillers from 10 week old Bd21-3 plants were collected when the immature seeds were swollen but still green. The immature seeds with soft endosperm were selected, the lemma was removed sterilized and rinsed as previously described above in section 2.6.1 for mature seeds. The immature embryos up to and including 0.3mm in length were isolated from seeds using fine forceps and a stereomicroscope under sterile conditions in the laminar flow hood. 15 immature embryos were cultured per plate scutellum facing up onto MSB3 Cu0.6 solid medium plates for 3 weeks at 25°C in the dark. The shoots were excised with surgical scissors under sterile conditions during the first 3 days of culture. At week 3 the compact embryonic callus with a creamy colour and pearly surface was fragmented into 3 pieces and transferred onto fresh MSB3 + Cu0.6 solid medium (16 calli per plate) and grown for another 2 weeks at 25°C in the dark. All non-CEC tissue was discarded. At week 5 the CEC with a creamy colour and pearly appearance was split into further 4-6 pieces and transferred onto fresh MSB3 + Cu0.6 solid medium (16 calli per plate) and grown for another week at 25°C in the dark. At week 6 this step was repeated for one last time and 50-100 CEC pieces were placed on fresh MSB3+Cu0.6 solid medium before inoculation with *Agrobacterium*.

2.2 RNA Isolation, DNase Treatment and Gel Electrophoresis

RNA isolation was done according to the protocol given by Life Technologies Ambion RNA Trizol Reagent manual. 0.3g of root tissue, and separately 60µg of leaf tissue was each homogenized in 1.7ml of Trizol (1700µl+500µl). 1ml of this mixture was transferred to a 2ml tube and kept on ice. 400µl chloroform was subsequently added and shaken by hand (vigorously invert for 15 secs) then incubated at room temperature for 7 minutes. The tubes were then centrifuged for 15 minutes at 11400 rpm at 4°C and the supernatant transferred to a new tube. 500µl of isopropanol was added and incubated at room temperature for 10 minutes. The tubes were then centrifuged for 10 minutes at 11400 rpm at 4°C. The pellet was washed with 1ml 75% DEPC treated ethanol. Centrifugation was done for 5 minutes at 9000 rpm at 4°C. The pellet was dried

for 10 minutes. To dissolve the pellet 30-50 μ l RNase free water was added and the RNA pellet was kept at 55°C for 1 hour. Nanodrop measurement was done to check the RNA yield. After obtaining the desired 20 μ g to 50 μ g of RNA, DNase treatment was proceeded. For DNase treatment the RNA was suspended in the DNase treatment solution which contained 5 μ l of 10xbuffer, 20 μ l of RNA, 0.5 μ l of RNase out (40 μ l/ μ l), 2 μ l of DNase I, 12.5 μ l of distilled H₂O (to complete the volume up to 50 μ l with water). After mixing everything, the tubes were placed in waterbath at 37°C. 2.5 μ l of EDTA-DEPC (50mM) was added. The tubes were placed in 80°C heat block for 10 minutes then immediately put on ice. 50 μ l plus 2.5 μ l of EDTA-DEPC made a total volume of 52.5 μ l to which 1/10 of total volume of NaOAC was added in this case 5.25 μ l. 2Volumes of total EtOH was added in this case 105.5 μ l. It was held in -80°C for 30-40minutes. It was then centrifuged at 13000rpm for 15 minutes at 4°C and then the supernatant was discarded. 1ml of 70% EtOH was add and centrifuged again at 1300rpm for 5 minutes. The supernatant was discarded, and tubes left to dry for 5 minutes. The RNA was dissolved in 10-20 μ l DEPC water and placed at 55°C for 10 minutes. The concentration of RNA was rechecked on the nanodrop and a gel was run to check the integrity of the RNA. For running the gel 2 μ l of samples was taken and 8 μ l of DEPC water was added and heated at 65°C for 10minutes. The tubes were then cooled on ice for 2 minutes, then and 2 μ l (6X) loading dye was added making the total volume 12 μ l which was loaded onto the gel.

2.3 Native Page Gel Electrophoresis

After DNA treatment to have a clear image of the RNA purity native PAGE was performed by making 6% PAGE gels. 3ml of acrylamide, 3ml of 5X TBE, 7ml of water, 20 μ l TEMED, and 200 μ l of APS was added. (TBE formula was 10X TBE buffer made by adding 108g Tris Base, 55g Boric Acid, 40ml 0.5M EDTA (pH 8.0) Autoclave). 5 μ l of all RNA samples were loaded from the DNase treated stock RNA solutions.

2.4 cDNA Synthesis by Reverse Transcription

For qRT-PCR the protocols from Bertolini et al 2013 and Varkonyi-Gasic et al 2007 were followed. Stem loop primers for reverse transcription were designed according to Varkonyi-Gasic et al 2007. cDNA synthesis was done by adding 1 μ l RNA (100ng/ μ l), and 1 μ l of 1 μ M stem loop

RT primer to 9µl DEPC treated water. After a 5 minute incubation at 70°C, the samples were chilled on ice for 2 minutes. In a PCR tube 4µl of 5X reaction buffer, 2µl of 10mM dNTPs, and 0.5µl of 40U/µl Ribolock RNase inhibitor was added and the volume was made upto 19µl with the addition of DEPC treated water and put for incubation for 37°C for 5 minutes. After incubation 1µl of 200U ThermoScientific RevertAid Reverse Transcriptase enzyme was added and reverse transcription reaction was started for 30 minutes at 16°C, 30 seconds at 30°C for 60 cycles, 30 seconds at 42°C, 1 second for 50°C and 10 minutes at 70°C. Reaction resulted in 5ng/µl cDNA.

2.5 Semiquantitative and Quantitative qRT-PCR for miR7757 Expression Level Analysis

End point PCR was subsequently performed. In a microcentrifuge tube 15.4µl nuclease free water, 2µl of 10X PCR buffer, 0.4 µl of 10mM dNTP mix, 0.4 µl of 10µM forward primer and 0.4 µl of 10µM reverse primer and 0.4µl Taq Polymerase mix. Then 1µl of RT product was added to this mixture. The endpoint reaction was placed in a preheated 94°C thermal cycler and the endpoint PCR reaction was set as 94°C for 2 minutes, 20, 30, 40 cycles at 94°C for 15 seconds and 1 minute at 60°C. The reaction products were analysed by gel electrophoresis on a 4% agarose gel in 1X TBE. Normal leaf sample was taken as a reference point and the change in expression in drought leaf, normal root and drought root was analysed relative to the normal leaf expression.

The expression levels of miR7757 were measured by semiquantitative and quantitative RT-PCR. Forward primers were designed and universal reverse primers selected according to the protocol of Varkonyi-Gasic et al 2007. qRT PCR was performed with PerfectaSYBR® Green PCR mix. Each reaction volume was 20µl with 3 replicates. One reaction contained 1.5ng cDNA, 0.4 µl of 10µM forward primer, 0.4 µl of 10µM universal reverse primer and 10 µl of 2X Quanta SYBR Green SuperMix. Control samples included no reverse transcriptase (no-rt) and no RNA (no-RNA). The qPCR real time reaction was set as 95°C for 2 minutes, 40 cycles for 5 seconds at 95°C, annealing at 60°C for 15 seconds, 70°C for 15 seconds, 95°C for 1 minute and finally 1 minute at 55°C. MiR7757 was tested in normal leaf (NL), drought leaf (DL), normal root (NR) and drought root (DR) condition samples. The samples were run on the BioRad CFX96 Real Time System (BioRad). Fourteen different miRNAs were tested and 5.8s ribosomal RNA was used as the internal standard (Shi and Chiang, 2005; Xue et al., 2009). The reverse primer used is the Universal Primer provided with the kit, while forward primers each correspond to the entire sequence of the miRNAs tested; all primers used are listed Appendix D. Reaction efficiencies of RT-qPCR assays

for each individual miRNA/primer were determined using a fourfold dilution series of leaf cDNA and generating a standard curve plotting the cDNA concentration versus the corresponding Ct (Threshold cycle). Efficiency was calculated from the slope of the standard curve, using the BioRad CFX Manager Software. Relative quantification of each miRNA tested was calculated from Ct value, using the $2^{-\Delta\Delta Ct}$ method, directly with the BioRad CFX Manager Software (Bertolini et al. 2013b)

2.6 Bioinformatic Analysis of T-DNA Insertion Sites with *Brachypodium* miRNA Database

The complete list of T-DNA lines indexed by their flanking sequence tags was downloaded from the online Joint Genome Institute T-DNA *Brachypodium* resource website (<https://jgi.doe.gov/our-science/science-programs/plant-genomics/brachypodium/brachypodium-t-dna-collection/>). The table of mutants in the WRRRC *Brachypodium distachyon* T-DNA insertional mutant population version 09/10/13 was used. The insertion sites for all the mutants was selected. The summary of the complete list of *Brachypodium distachyon* microRNAs submitted to the miRbase version 20 was selected (http://www.mirbase.org/cgi-bin/mirna_summary.pl?org=bdi). By an in-house MATLAB code, the insertion sites of the T-DNA mutants were compared with the *Brachypodium* miRNAs start and end sites, and the miRNAs in which the T-DNA insertion site hit were selected.

2.6.1 Selection of miRNA Hits

5 miRNAs were found to contain the insertion sites of the T-DNA mutants. These miRNAs were selected and blasted on the T-DNA blast provided on the Joint Genome Institute T-DNA *Brachypodium* resource website.

2.7 T-DNA Genotyping with Multiplexed and Non-multiplexed Screening

To confirm the bioinformatic results of the MATLAB code and T-DNA blast search an experimental verification was performed. The T-DNA insertion mutants for *Brachypodium distachyon* (pre-ordered from the USDA-ARS-WRRC T-DNA collection) were planted in the green house (16 h light, 24°C /8h dark, 18°C) as described above. We used the T-DNA genotyping protocol provided by Vogel lab on the T-DNA collection website (<http://1ofdmq2n8tc36m6i46scovo2e-wpengine.netdna-ssl.com/wp-content/uploads/2015/05/T-DNA-genotyping.pdf>) with pre-designed T-DNA left border primer T3 and primer R9. According to their instructions pre-miRNA Gene Specific Primers (GSP) 1000bp apart, 500 bases on either side of the putative insertion site for pre-bdi-miR390a, pre-bdi-miR5049, pre-bdi-miR7716, pre-bdi-miR7757, and pre-bdi-miR169d were designed.

2.7.1 DNA Isolation from *Brachypodium* Mutant Lines

DNA from the plants after 5 weeks of growth in the greenhouse were taken, from which DNA was isolated (Bragg et al. 2012) and amplified by PCR for T-DNA selection. 2 young leaves, 3 inches in length, chopped into small lengths were put in liquid nitrogen. Steel beads were added to the tubes and the plants were keep it in -80°C and then transferred to liquid nitrogen for handling. Directly after freezing the tissue was ground at 30 cycles per minute for 1 minute. This step was repeated for 5 times. Before opening the tubes, the tubes were centrifuged at 4000rpm for 20 minutes at 4°C. 800µl of extraction buffer 1 was added to the ground tissue and incubated for half an hour-1 hour at 65°C with intermittent mixing every 5-10 minutes. Then the tubes were transferred to ice for 15 minutes before centrifuging at 4000 rpm for 5 minutes at 4°C. Afterwards 400µl of 6M ammonium acetate was added and the tubes were inverted several times then put on ice for 15 minutes. Then centrifuged at 4000 rpm for 15 min at 4°C. 900µl of the supernatant was then transferred to another tube containing 540µl isopropanol. The tubes were then placed on -20°C for half an hour to precipitate out the DNA, then the tubes were centrifuges at 4000 rpm for 30min at 4°C. The supernatant was decanted, tube was air dried for a while. Next the pellets were washed with 1ml of ethanol and centrifuged at 4000rpm for 20min at 4°C. Pellets were dried in the hood overnight and resuspended in 125ul TE buffer. To dissolve the DNA the samples were placed at 4°C overnight.

2.7.2 Amplification of T-DNA Sequence by Multiplex PCR

A three-primer multiplex PCR given by the Vogel T-DNA Genotyping Protocol was used to screen for mutants in the selected miRNA lines. In this PCR 3 different reactions were setup. First reaction had gene specific forward (GSP Fwd) and gene specific reverse primers (GSP Rev) primers. Reaction 2 had the GSP Fwd + GSP Rev + T-DNA LB, in which both the T3 Left Border primer and separately the R9 Left border primer were used in two separate reactions. Reaction 3 comprised only of the T-DNA LB in which both the T3 Left Border primer and separately the R9 Left border primer were used in two separate reactions. A single reaction mixture for a 50ul reaction contained 18.75 µl of PCR Grade water for 3 primer reaction (GSP Fwd + GSP Rev + T-DNA LB) 20.25 µl for 2 primer reaction (GSP Fwd/GSP Rev + T-DNA LB), 21.75 µl for 1 primer reaction (only T-DNA left border primer, either T3 or R9), 0.25µl of 5U/µl KAPA polymerase, 5µl of 10X buffer A, 5µl of 10mM dNTPs, 4µl of 25mM MgCl₂, 1.5µl of 10mM Forward Primer, 1.5µl of 10mM Reverse Primer, 1.5 µl of 10mM T-DNA Primer and 12.5µl of the template DNA from 20ng/µl. The PCR program used was 30 cycles with initial denaturation at 95°C for 3mins, denaturation at 95°C for 30 seconds, annealing was at 59°C for 30 seconds, extension was at 72°C for 1min/kb and final extension was at 72°C for 1min/kb.

2.8 Amplification of T-DNA Sequence by Non-Multiplexed PCR

To confirm the T-DNA orientation of the PCR product from the mutliplex PCR a non-multiplexed PCR was performed. 4 reactions were set up for the gene specific primers with the left border T-DNA primers. Reaction 1 contained the GSP Fwd + R9 T-DNA LB primers. reaction 2 had GSP Rev + R9 T-DNA LB, reaction 3 had GSP Fwd + T3 T-DNA LB, and reaction 4 had GSP Rev + T3 T-DNA LB. PCR conditions for a single 50µl reaction were 0.25µl Taq Pol, 5 µl Taq Pol PCR buffer, 5µl of 2mM dNTPs, 4 µl of 25mM MgCl₂, 1.5µl of forward primer, 1.5µl of reverse primer, 1.5µl of T-DNA primer (T3/R9), 12.5 µl of 20ng/µl template DNA and 18.75 µl water. The PCR program was the same as for the multiplex PCR.

2.9 Gel Electrophoresis and Gel Extraction

1% Agarose gel, 1g in 100ml TBE Buffer (0.5X) was prepared. The gel running time was 60 min at 100 volts. BIORON 1 kb DNA Ladder 250 µg, with no stain Cat.-No. 305025 was used as a ladder. Gel extraction of the T3tDNA+Reverse primer and T3tDNA+R+F primer products was performed with the QIAquick gel extraction kit as per the manual's instructions. It was checked on the nanodrop for DNA concentration and on agarose gel for DNA integrity.

2.10 PCR Product Purification and Sequencing

For PCR product purification the QIAGEN QIAquick PCR Purification Kit (Catalog No. 28104) was used. Ethanol was added to the Buffer PE before use. 1:250 volume of pH indicator 1 was added to Buffer PB. 5 volumes of Buffer PB to 1 volume of the PCR reaction was added and mixed. 10ul of 3M sodium acetate pH 5.0 was added and mixed making the colour of the mixture yellow. A QIAquick column was placed in the provided 2ml collection tube and the DNA applied to the QIAquick column to bind the DNA. The flowthrough was discarded and the QIAquick column was placed back in the same tube. For washing 0.75ml of Buffer PE was added to the QIAquick column and centrifuged for 30-60 seconds. The flowthrough was discarded and the QIAquick column was placed back in the same tube and centrifuged once more in the 2ml collection tube for 1 minute to remove the residual wash buffer. The QIAquick column was then placed in a clean 1.5 ml microcentrifuge and 50ul of Buffer EB was added to the center of the QIAquick membrane and the column was let to stand for 1 minute and centrifuged for 1 minute. The purified samples were sent for sequencing to Ref Gen Biotechnologies, Ankara. SeqTrace Program was used to analyze the sequenced products.

2.11 Target Analysis of miR7757

miR7757 *in silico* target prediction was performed. The *Brachypodium* coding sequence was downloaded from the plant genome database (<http://www.plantgdb.org/XGDB/phplib/download.php?GDB=Bd>). The coding sequence file chosen was Bdistachyon_192_cds.fa.bz2. The online program used for microRNA target prediction psRNATarget was used (<http://plantgrn.noble.org/psRNATarget/analysis?function=3>). All 4 variants of miR7757 (5p.1, 5p.2, 3p.1, 3p.2) were taken from miRbase

(http://www.mirbase.org/cgi-bin/mirna_entry.pl?acc=MI0025377). The sequences of the variants are in Appendix G. These were submitted to psRNA target with the score cut off set at 2.5 (according to Bertolini et al 2013). Only bdi-miR7757-5p.1 gave hits, these hits were then blasted to the ncbi blastx Non Redundant Protein Sequences (nr) database to find putative target proteins (https://blast.ncbi.nlm.nih.gov/Blast.cgi?PROGRAM=blastx&PAGE_TYPE=BlastSearch). The result for each of the 8 target hits were analysed separately. Additionally, only the plant hits were taken. The data was sorted on the basis of query coverage, length, plant species and lowest e values. The putative targets from *Brachypodium distachyon* were selected separately from each of the 8 target hits (Table 3). Likewise blast highest score targets from *Brachypodium*-related plant species were analysed separately

2.12 Gateway BP-LR Cloning

2.12.1 Design of Gateway Cloning Primers for miR7757

For designing att primers we used the alternate transcript intron sequence to afterwards have subsequent GFP expression too. The pre-miR7757 sequence of *Brachypodium distachyon* Bd21 genotype was downloaded from the microRNA database miRbase (20th release, June 2013). The whole genome sequences of Bd21 genotype of *Brachypodium distachyon* and sequences upstream and downstream the Bd21 chromosome 2 genomic scaffold were downloaded from the Plant Genome Database (<http://www.plantgdb.org/BdGDB/>). miR7757 sense strand (miRBASE premiRNA sequence: Accession MI0025377 was used for primer design. The attachment primers were designed according to instructions from the Gateway Cloning Manual (ThermoScientific) checked for checked for 3' stability (2 G-C in the last 3bps; no more than 3 G-C in the last 3bps; Tm no more than 67°C; idt for hairpin/selfdimer/crossdimer - however dimer occurs.) The primers were selected 395 bp upstream of the start of the pre-miRNA sequence of miR7757. The created primers were blasted to the *Brachypodium* genome to confirm that the primers hit only one location in the whole genome.

2.12.2 Amplification of miR7757 Sequence from Wildtype *Brachypodium* with Attachment Sites

For the amplification of miRNA sequence with attachment overhangs the Taq polymerase PCR protocol was optimized for 10 μ l. For a single reaction 1 μ l of 10X PCR buffer, 0.8 μ l of MgCl₂, 0.2 μ l of 10mM dNTPs, 0.25 μ l of 10 μ M Forward Primer, 0.25 μ l of 10 μ M Reverse Primer, 0.03 μ l of Taq Polymerase, 2 μ l of 30ng/ μ l template DNA (final conc.) and 5.47 μ l nuclease free water was used for to make up the total volume reaction as 10 μ l. The PCR Program for this was initialization at 95°C for 5 minutes, denaturation at 95°C for 1 minute, annealing at 52°C for 1 minute, extension at 72°C for 1 minute, then final extension at 72°C for 7 minutes. The final hold was at 4°C.

2.12.3 Gel Electrophoresis and Purification of att PCR Products

1.5% gel in 0.5X TBE was prepared and the gel ran for 30 minutes. The DNA ladder used was GeneRuler DNA ladder Mix (SM0331) The PCR product was amplified, purified and gel extracted with QIAGEN gel extraction kit and sent for sequencing to RefGen Ankara

2.12.4 Preparation of Competent Cells

Tu et al 2005 improved protocol for followed without any alterations and slight upscaling. A 25 μ l fresh overnight culture of OmniMax cells (Thermo Scientific) and DH5 α (without F' episome) each was added to 100 μ l of LB broth each. This culture was incubated for 1hr at 37°C. It was transferred to a mixer shaker at 200rpm at 37°C for 2-3 hours until the OD was 0.2-0.4. The 100 μ l cells were transferred to 50 μ l falcon tubes and left on ice for 10 minutes, centrifuged at 4500 rpm at 4°C for 5 minutes. The supernatant was discarded, and cells resuspended in half volume 25 μ l of sterile cold TB (PIPES, MnCl₂, CaCl₂, KCl solution) and incubated on ice for 25 minutes. After centrifugation as above the cell pellet was resuspended in 5 ml (one tenth) volume to create the final cell suspension. 200 μ l of competent cells were transferred into microcentrifuge tubes and immediately put into liquid nitrogen. To check whether the cells were competent the bacterial transformation of the competent cells was done according to the protocol provided by Tu et al. LB agar plates and LB agar plates with ampicillin to a final concentration of 100 μ g/ml were prepared. These were preheated to 37°C for an hour. In 200 μ l of competent 1 μ g/ μ l plasmid DNA 2 μ l was added and 2 μ l of DMSO was also added. The reaction was incubated on ice for 30 minutes, then given a heat shock for 90 seconds at 42°C, and immediately put on ice for 2 minutes. Afterwards 400 μ l of liquid SOC medium was added and tubes incubated at 37°C for 2 hours in an incubator

shaker for 1 hour. The tubes were centrifuged briefly and 50µl each was taken from the bottom of the tubes and spread onto the LB plates and the LP plate with ampicillin. The plates were incubated overnight for 16 hours overnight at 37°C.

2.12.5 BP Reaction

BP cloning was performed according to the Gateway Cloning Systems Protocol (Catalog no 12535 – 029) at 25°C and given 10 hours of incubation. Competent OmniMax *E. coli* cells were transformed for the positive sample and competent DH5α *E. coli* cells for the negative, positive and pUC19 cells. The following components were added to the sample, positive and negative respectively. 5µl of att-PCR product, 1µl of pDONR vector (150ng/µl), and 2µl of TE buffer was added to the sample. To the positive control 1µl of pDONR, 2µl of pEXP7-tet positive control (50ng/µl) and 5 µl TE buffer pH 8.0 was added. In the negative control 5µl of att-PCR product, 1µl of pDONR vector (150ng/µl) and 4µl of TE buffer were added each to 1.5ml centrifuge tubes at room temperature and mix. The Gateway® BP Clonase II enzyme was taken from -20°C and thawed for 2min on ice, vortexed briefly twice and 2µl of it was added to the sample and positive control vials. The reactions were incubated for 10 hours. 1µl of proteinase K solution was added to all reactions and incubated for 10 minutes at 37°C. Next the competent cells were transformed.

2.12.5.1 DH5α chemical transformation protocol

1 vial of DH5α chemically competent cells was thawed on ice for each transformation. 1µl of BP recombination reaction was transferred into each vial of competent cells and mixed gently without pipetting. 10pg (1µl) of pUC19 control DNA was added into a separate vial of competent cells and gently mixed. The vials were incubated on ice for 30 minutes. A 30 seconds heat shock at 42°C was given to the cells without shaking, then placed on ice for 2 minutes. 250µl of SOC medium was added to each vial capped tightly and incubated on a horizontal shaker 225 rpm at 37°C for 1 hour. Before plating the transformation, mixture was diluted 1:10 into LB Medium. 20µl and 100µl of each transformation mixture was spread on a prewarmed selective plate and incubated overnight at 37°C.

2.12.5.2 M13 primers colony PCR

Colony PCR was performed in order to confirm the insertion of att:MIR7757. 4µl of water was taken, a tip of colony cells was added, (then inoculated LB broth for subsequent plasmid isolation).

2 µl of the colony mixture was added to the PCR reaction. The Taq Polymerase Colony PCR Protocol was optimized for 15µl reaction. 1.5µl of 10X PCR buffer, 1.2µl of MgCl₂, 0.3µl of 10mM dNTPs were added, 0.4µl of 10µM Forward Primer and Reverse Primer each, 0.05µl of Taq Polymerase and 11.87µl of nuclease free water was added to make the total reaction volume 15µl. To lyse the bacterial colony a pre-incubation was performed at 95°C for 10 minutes, the cells were kept at 10°C for 10 minutes. The PCR cycle initialization was at 95°C for 5 minutes, denaturation was at 95°C for 30s, annealing 50°C for 30s, extension was at 72°C for 1min and then the final extension was at 72°C for 10 minutes. The final hold was at 4°C. The number of cycles was 35.

2.12.5.3 miR gene specific colony PCR

Protocol used for MIR gene specific colony PCR was Taq Polymerase protocol optimized for a 50µl single reaction. 5µl of 10X PCR buffer, 4µl of MgCl₂ and 1µl of 10mM dNTPs, 1µl of 10µM forward primer and reverse primer each was used. 0.5µl of Taq Polymerase, 5µl of 50ng/µl DNA (final concentration), 32.5µl of nuclease free water was added to make the total volume reaction 50µl. The PCR Program for this was initialization at 95°C for 3 minutes, denaturation at 95°C for 30s, annealing at 52°C for 30s and extension at 72°C for 1 minute. Then final extension was at 72°C for 10 minutes with final hold at 4°C

2.12.5.4 Plasmid DNA isolation from transformed *Escherichia coli* cells.

Plasmid isolation was performed with samples 2, 4, 6, 7 with the Roche HighPure Plasmid Isolation kit with freshly added RNase A. The protocol followed was as per the user's instructions. The binding buffer was placed on ice. 2ml of bacterial cells were pelleted from 2 ml (O.D A₆₀₀ per ml) of *E. coli* culture. The supernatant was discarded and 250µl of suspension buffer + freshly added RNase was added to the tube containing the bacterial pellet and resuspended well. 250µl of lysis buffer was added and mixed gently by inverting 3-6 times. The tubes were incubated for 5 minutes at room temperature. The lysed solution was treated with 350µl of chilled binding buffer and gently inverted 3-6 times and incubated. It was incubated on ice for 5 minutes until it became a cloudy and flocculent precipitate. The tubes were then centrifuged for 10 minutes at 13000g, then the supernatant was out into a High Pure Filter tube inserted into a collection tube and centrifuged for 1 minute at 13000g. The flow through was discarded and 700µl of wash buffer was

added to the upper reservoir of the filter tube. The tube was centrifuged for 1min, the supernatant discarded, the empty tube recentrifuged for one minute again and the collection tube was discarded. The filter tube was then inserted into a clean sterile 1.5ml microcentrifuge tube. 100µl of elution buffer was added to the upper reservoir of the collection tube and the tube assembly was centrifuged for 1 minute at full speed. The DNA was directly stored at -20°C.

2.12.5.5 Transformation of Plasmids from LR reaction into *Escherichia coli*

LR cloning was performed according to the Gateway Cloning Systems Protocol (Catalog no 12535 – 029) and competent DH5α *E. coli* cells were transformed all reactions. The following components were added to the sample, positive and negative respectively. 5µl of entry clone (50-150ng/reaction), 1µl of destination vector (150ng/µl) and 2µl of TE buffer, pH 8.0 was added to the sample vial. 5µl of entry clone (50-150ng/reaction), 1µl of destination vector (150ng/µl) and 4 µl of TE buffer pH 8.0. In the positive control there is 1µl of destination vector and 2µl of pENTR™-gus (50ng/µl) and 5µl of TE buffer. The Gateway® LR Clonase® II enzyme mix was thawed on ice for 2 minutes and briefly vortexed for 2 seconds twice. 2µl of Gateway® LR Clonase® II enzyme mix was added to the sample and positive vials and mixed well by vortexing for 2 seconds twice. The reactions were incubated for 10 hours at 25°C. 1µl of proteinase K solution was added to each reaction and incubated for 10 minutes at 37°C. The DH5α competent *E. coli* cells were transformed the same way as in the BP reaction protocol by the transformation Protocol described in 2.2.12.5.1 Plasmid Isolation was also the same as above mentioned. The purified DNA was sent for sequencing.

2.13 SEM analysis of leaf blades

7cm leaf blades from mature plants of T-DNA mutant jj15278 and wildtype Bd21 plants were taken. The leaves were placed on glass slides and cut to 5cm long and covered with glass cover and left to dry for 3 days. After air drying 1cm pieces were cut with surgical razor and mounted on SEM sample holder. To avoid surface charging, the specimens were carbon coated and then mounted into the SEM chamber for visualization. The morphology of the leaf blades was examined by secondary electron imaging in a scanning electron microscope (JEOL, JSM-6010LV) using an accelerating voltage of 3KV.

2.14 *Agrobacterium tumefaciens* Transformation into *Brachypodium* Compact Embryonic Callus

2.14.1 Transformation of Destination Clones into *Agrobacterium tumefaciens* cells

According to the sequencing results obtained. 4 distinct clones were chosen to transform the AGL1 strain of *Agrobacterium tumefaciens*. According to the protocol for transformation (Wise, Liu et al 2006) 100µl of competent AGL1 strain of *Agrobacterium tumefaciens* cell stocks stored at -80°C were thawed on ice and 1µg of destination clone was added to each tube, covered with aluminum foil and incubated in liquid nitrogen for 5 minutes, then at 37°C in water bath to provide heat shock. Cells were transferred to 10ml tubes and 2ml LB medium was added and incubated with shaking 140rpm at 28°C for 3 hours. Then the cells were centrifuged for 5 minutes at 4000rpm and the pellet was resuspended in 500µl LB medium. 20µl and 100µl of resuspended cells were plated on 200µg/ml carbenicillin and 100ug/ml kanamycin agar plates. Finally, the petri plates were incubated at 28°C for 15 hours.

2.14.2 Plasmid DNA Isolation from *Agrobacterium tumefaciens* Cells

The same plasmid isolation protocol was used as in part 1.1.4.6.4 except that a 10ml starting culture was used in place of a 4 ml starting culture. The isolated *Agrobacterium* plasmids were sent for sequencing.

2.14.3 Preparation of *Agrobacterium tumefaciens* Infection Inoculum

5µl of *Agrobacterium* (AGL1 strain) carrying the vector was inoculated into a 1ml of LB+ S50 liquid medium. It was left to grow overnight in an incubator-shaker at 28°C and 200 rpm. 200µl of this overnight culture was plated onto solid MGL+S50+AS30 media using a sterile spreader. The plates were cultured upside down for 2 days at 28°C in the dark (Alves et al. 2009).

2.14.4 Transformation of *Brachypodium* by Callous Embryonic Culture

From the cultures plate half of the *Agrobacterium* layer was scraped from the surface. The end of the spreader covered with *Agrobacterium* was broken into a 50ml disposable sterile tube containing 10 ml of MSB+AS45 liquid medium and strongly shook by hand to resuspend the

Agrobacterium. The suspension was put for 45minutes at 220rpm in a 28°C incubator to ensure dispersion of *Agrobacterium*. The optical density of the cell suspension was measured at 600nm and diluted to OD 1 with MSB+AS45. The CEC plates were flooded with 13ml of *Agrobacterium* culture and inoculated for 5 minutes at room temperature in a laminar flow hood. The bacterial suspension was pipetted out completely from the CEC plates and each callus was handpicked directly into a dry sterile filter paper in an empty petri dish. The CECs were left uncovered under the laminar flow for 7 minutes for desiccation treatment. Next these CECs were cocultured on MSB3+AS60 medium plates for 2days at 25°C in the dark to produce 50-100 calli per plate.

2.14.5 Selection of Transformed Calli with GFP and PPT

The cocultured CECs were transferred onto MSB3 +Cu0.6+H4O+T225 solid medium (20 calli per plate). Culture for 3 weeks at 25°C in the dark. Three weeks after transformation the CEC growing on phosphinothricin were screened for the presence of small bright GFP sectors using a fluorescent microscope. Each fluorescent sector was dissected with fine forceps and cultured as independent transgenic lines onto MSB3+CuO.6+H30 +T225 solid medium for another 3 weeks at 25°C in the dark.

2.15 Regeneration of Transgenic MIR7757 Overexpressing Plants

Six weeks after transformation, regeneration of calli was done by screening calli for green fluorescence with a UV fluorescent microscope. The phosphinothricin-resistant and GFP-positive calli were transferred onto the MSR26+H20+T225 regeneration medium (12 calli per plate) for 2-3 weeks at 25°C under 16hr photoperiod. After 8-9 weeks of transformation, the shoots were transferred to tubes containing MSR63+Ch7+T112 germination medium and cultured for 2-3 at 25°C under 16hr photoperiod. At 10-11 weeks after transformation the plantlets in the tubes were confirmed to be GFP positive in the roots of the plantlets before transferring to CER.

For miR7716 the BLAST hit for query= bdi-**MIR7716**MI0025327*358 was:

```
>gnl|bFST|IL000007324 WRRRC Bd21-3 FST: Intergenic
  Length = 1201
  Score = 710 bits (358), Expect = 0.0
  Identities = 358/358 (100%)
  Strand = Plus / Minus
```

For miR169d the BLAST hit for Query= bdi-**MIR169d**MI0018079*187 was:

```
>gnl|bFST|IL000007756 WRRRC Bd21-3 FST: intergenic
  Length = 1201
  Score = 371 bits (187), Expect = e-103
  Identities = 187/187 (100%)
  Strand = Plus / Plus
```

3.2. Multiplex and Nonmultiplex Screening of T-DNA Mutants

With the T-DNA genotyping protocol provided by the *Brachypodium* T-DNA Collection - DOE Joint Genome Institute, the blast results were verified with a 3-primer multiplex PCR system.

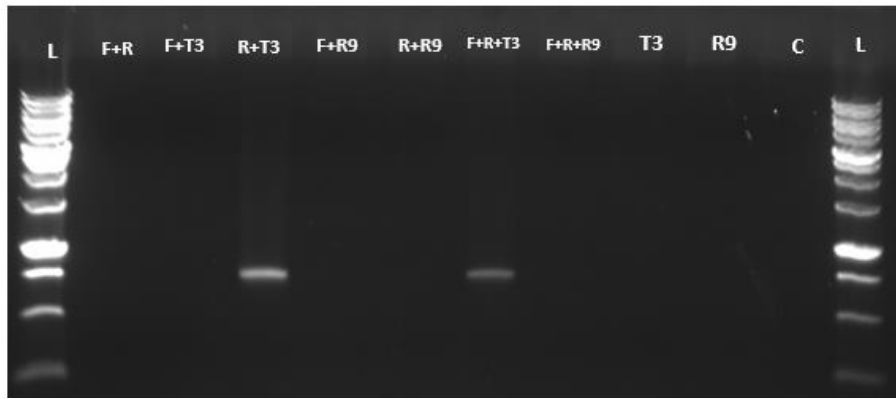


Figure 2.4 miR7757 screening by T-DNA genotyping.1, 6ul Ladder,2, 3,4,5,6 F+R, F+T3tDNA, R+T3tDNA, F+R9tDNA, R+R9tDNA, 7,8,9,10, F+R+T3tDNA, F+R+R9tDNA, T3 TDNA, R9 TDNA, 11 Ladder, 12, 13 Controls

The gel showed that the band generated by forward, reverse MIRNA primers and T-DNA T3 primer showed a band around 750bp lower than what would be expected for the MIRNA forward and reverse primers as 1138bp. It was evident that the band had been generated by the combination of the T-DNA primer with either of the premiRNA specific forward or reverse primers. Following the presence of desired band in the multiplex PCR, next to check for the orientation of insertion a 2 primer PCR was performed. Both the non-multiplexed PCR performed alongside the multiplexed

PCR for 3, 2, and 1 primer (Figure 2.4), bands were obtained in R+T3tDNA and F+R+T3tDNA. The TDNA primer gave a lower band at 750bp with the reverse primer. The band also appeared in F+R+T3tDNA since it also contained the reverse and T-DNA primer and came at the same 750bp. This result confirmed the blast search performed earlier.

3.3 Gel Extraction of T-DNA Genotyping for Selection of T-DNA Mutants

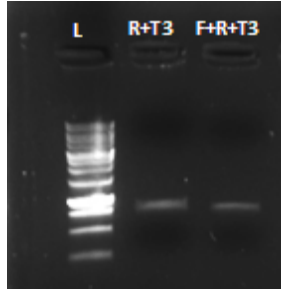


Figure 2.5 Gel extracted PCR products of amplified T-DNA regions

Gel extraction of the T3tDNA+Reverse primer and T3tDNA+R+F primer products was performed with the QIAquick gel extraction kit as per the manual's instructions. It was checked on the nanodrop for DNA concentration and on agarose gel for DNA integrity (Figure 2.5).

3.4 Sequencing Results

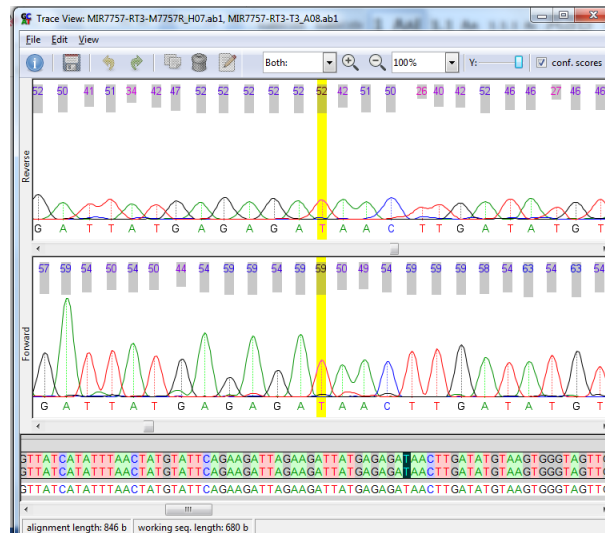


Figure 2.6 Sequencing results from SeqTrace showing alignments of the T-DNA amplified PCR product with the wildtype MIR7757 gene

Gel extracted T-DNA products were purified and sent for sequencing to RefGen (Ankara) for sequencing. SeqTrace Program was used to analyze the sequenced products. After checking the alignment of the entire working sequence with the wildtype miR7757 gene and the mutation location of JJ15278 on Phytozome (<https://phytozome.jgi.doe.gov/jbrowse/index.html>) the strands aligned, and the mutation confirmed. The genotyping protocol provided by the WRRRC suggested the product to be around 700 bp and from the results a working sequence of 680bp was obtained which is as follows:

```

>consensus: MIR7757-RT3-M7757R_H07.ab1, MIR7757-RT3-T3_A08.ab1
TCCGNTCNCANTCCACACAACATNCGAGCCGGAAGCATAAAGTGTAAGCCTGGGGTNGCCTAATGAG
TGA GCTTACTTGTAGATTATGCCAAACCATGATCTATAAGTCAAGTCTCTTTACTAATAGTTTTGATCCAC
CTTCTCATCTTTAGTGTAGTTATCATATTTAACTATGTATTCAGAAGATTAGAAGATTATGAGAGATAACT
TGATATGTAAGTGGGTAGTTGAATGTTTTGTTTATCATGAAAACAAGAAATTAGCCTACGTGAGCTCGGA
GAGAGTAACTCAATGAGCACATAAATAGAAGCATGATTCAACCAATAGACACCGATGACGATGGTGAAG
GCAAGGAAATGTATTATTGTATACGTGTGTGTGCATGATATTATGGTTGATCCCATATGTTCCCTTGCCAAC
CGAAGACAAGCTTGCGACGAGATTGCATGGTTTGAGCAAACATCATCATCAAGCAAGATCCAAGATTATT
CATCTGAAAAGAGTACGGCGGATATGGCCACCATCAGGATTCCAGAAGCGGGGTATCTGGGACCTATTG
TTGACCAAGTATACAGCTTGGTTCATGCAAGCTTTCAGGTTCTATGTGGAATGGATTTTATTGGTCTCACT
NNCATTATCCCAACCAAGANGGTCAAGACTGANCAAGANTCAAGAN

```

Figure 2.7 Working sequence generated from sequencing results of T-DNA insertion in MIR7757. The light blue highlight sequence corresponds to the BLAST alignment of this working sequence to the *Brachypodium distachyon* nucleotide sequence (Figure 2.8)

The consensus sequence obtained from SeqTrace was used for nucleotide BLAST against the *Brachypodium distachyon* (taxid:15368) nucleotide database as the search set. 99% identity was observed against miR7757 with a coverage of only 43% clearly pointing towards a missing part of the MIR7757 gene and a possible insertion (Figure 2.7)

To confirm that the insertion is present with the amplified miR7757 region the T-DNA working sequence was visualized in Phytozome which displays the T-DNA insertion sites of *Brachypodium distachyon*. After blasting the working sequence to the *Brachypodium* genome, the subject sequence appeared right at the T-DNA insertion in the miR7757 gene shown with the green arrow (Figure 2.8).

Job title: consensus: MIR7757-RT3-M7757R_H07.ab1, MIR7757-RT3-T3_A08

Brachypodium distachyon microRNA MIR7757 (MIR7757), microRNA
 Sequence ID: [NR_127046.1](#) Length: 598 Number of Matches: 1

Range 1: 301 to 598 [GenBank](#) [Graphics](#) ▼ Next Match ▲ Previous

Score	Expect	Identities	Gaps	Strand
534 bits(289)	9e-151	295/298(99%)	0/298(0%)	Plus/Plus
Query 73	GCTTACTTGTAGATTATGCCAAACCATGATCTATAAGTCAAGTCTCTTTTACTAATAGTT	132		
Sbjct 301	GCTTACTTGTAGATTATGCCAAACCATGATCTATAAGTCAAGTCTCTTTTACTAATAGTT	360		
Query 133	TTGATCCACCTTCTCATCTTTAGTGTAGTTATCATATTTAACTATGTATTCAGAAGATT	192		
Sbjct 361	TTGATCCACCTTCTCATCTTTAGTGTAGTTATCATATTTAACTATGTATTCAGAAGATT	420		
Query 193	AGAAGATTATGAGAGATAAAGTATGTAAGTGGGTAGTTGAATGTTTGGTTTATCATG	252		
Sbjct 421	AGAAGATTATGAGAGATAAAGTATGTAAGTGGGTAGTTGAATGTTTGGTTTATCATG	480		
Query 253	AAAACAAGAAATTAGCCTACGTGAGCTCGGAGAGAGTAACTCAATGAGCACATAAATAGA	312		
Sbjct 481	AAAACAAGAAATTAGCCTACGTGAGCTCGGAGAGAGTAACTCAATGAGCACATAAATAGA	540		
Query 313	AGCATGATTCAACCAATAGACACCGATGACGATGGTGAAGGCAAGGAAATGTATTATT	370		
Sbjct 541	AGCATGATTCAACCAATAGACACCGATGACGACTGTGAAGGCAAGGAAATGTATTATT	598		

Figure 2.8 Nucleotide BLAST results of the T-DNA working sequence with pre-miRNA sequence showing only 598 nucleotides

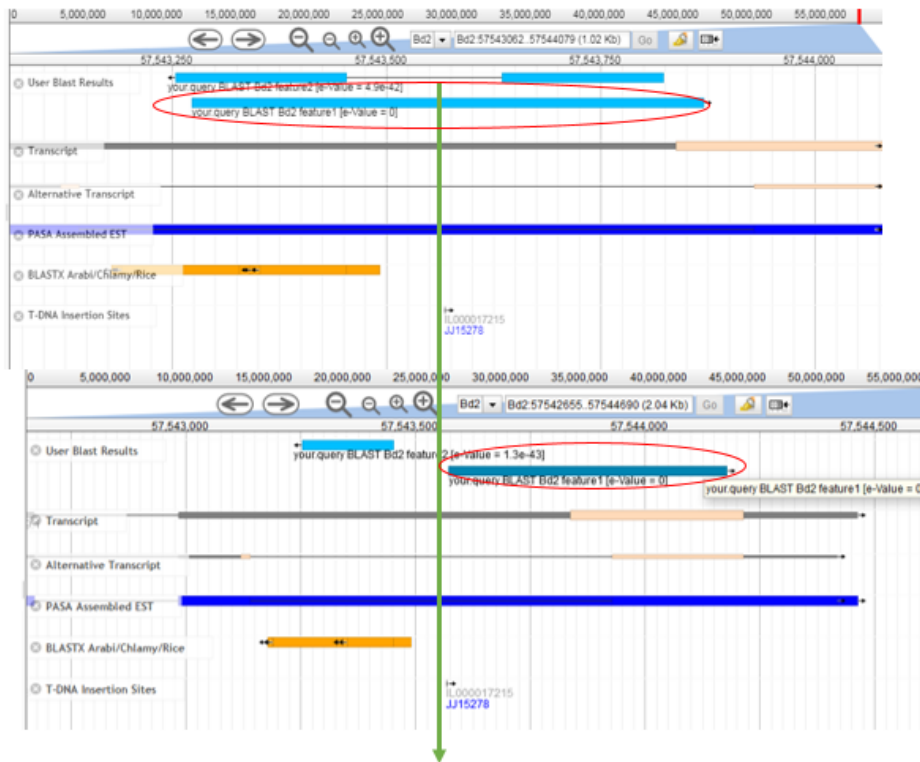


Figure 2.9 Alignment of the T-DNA+miR7757 PCR product with wildtype MIR7757 gene. The entire MIR7757 gene can be seen in light blue on both sides of the green arrow. The amplified region is shown in medium blue corresponds to the T-DNA insertion given below it JJ15278.

3.5 Target Analysis of the Selected Screened miR7757

The highest score for the predicted genes for each target hit from psRNA target are listed in Table 2. 8 target hits were obtained all of which showed miRNA inhibition by cleavage. Only bdi-miR7757-5p.1 gave hits, these hits were then blasted to the ncbi blastx Non Redundant Protein Sequences (nr) database to find putative target proteins (https://blast.ncbi.nlm.nih.gov/Blast.cgi?PROGRAM=blastx&PAGE_TYPE=BlastSearch). The result for each of the 8 target hits were analysed separately. Additionally, only the plant hits were taken. The data was sorted based on query coverage, length, plant species and lowest e values. The putative targets from *Brachypodium distachyon* were selected separately from each of the 8 target hits (Table 3). Likewise blast highest score targets from *Brachypodium*-related plant species were analysed separately (Table 2), here highest hits were from *Aegilops tauschii* subsp. *tauschii* and other hits were of *Triticum urartu* and *Oryza sativa Japonica* group. Table 4 depicts the target genes only for *Brachypodium distachyon* and the targets were all disease resistance genes expect for one transposon Tf2-1 polyprotein. This shows the involvement of miR7757 in biotic stress.

3.6 Gel Electrophoresis of Wildtype miR7757 with Attachment att Sites for Sequencing

For designing att primers we used the alternate transcript intron sequence to have subsequent GFP expression. These are listed in the appendix. The MIR7757 gene transcript was amplified with the att sites as per the Thermo Scientific Gateway Cloning Protocol.

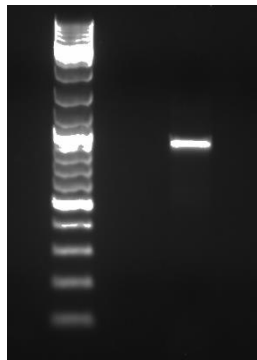


Figure 2.10 The amplified att:MIR7757 PCR product at 850bp.

Comparing the results with the ladder the band obtained was in between 800-900 basepairs. These results are in line with the calculated PCR product size including the att primers which was 872

basepairs. The PCR product was amplified, purified and gel extracted with QIAGEN gel extraction kit and sent for sequencing to RefGen Ankara. Sequencing results show the amplification of the desired region with the att overhangs. The sequencing results were compared with *Brachypodium distachyon* (taxid:15368) by nucleotide BLAST option of NCBI. Identity percentage with raw sequence: MIR7757-ATTF_D03 and raw sequence (reverse complemented): MIR7757-ATTR_E03 was found to be 99% (Figure 2.11 and 2.12)

Job title: raw sequence: MIR7757-ATTF_D03

Brachypodium distachyon microRNA MIR7757 (MIR7757), microRNA
 Sequence ID: [NR_127046.1](#) Length: 598 Number of Matches: 1

Range 1: 1 to 598 [GenBank](#) [Graphics](#) ▼ Next Match ▲ Previous

Score	Expect	Identities	Gaps	Strand
1075 bits(582)	0.0	593/598(99%)	1/598(0%)	Plus/Plus
Query 118	TGGATCATGCTTCTATTATAAGCTCATTGAAGTAACTCTCTCCGAGCTCAAATAGGCCA	177		
Sbjct 1	TGGATCATGCTTCTATTATAAGCTCATTGAAGTAACTCTCTCCGAGCTCAAATAGGCCA	60		
Query 178	ATTTTTGTGGTGTGATACACAAAACCTTCAGCTACCCACTTCCATATCAAATCATCTC	237		
Sbjct 61	ATTTTTGTGGTGTGATACACAAAACCTTCAGCTACCCACTTCCATATCAAATCATCTC	120		
Query 238	TCTTGGTTTTCTTGCTTTTGGAAATATACTTTGATATGATAAAAAGATGAGAAGGTAGAT	297		
Sbjct 121	TCTTGGTTTTCTTGCTTTTGGAAATATACTTTGATATGATAAAAAGATGAGAAGGTAGAT	180		
Query 298	CCTAGCTAGAACAACATCATATTAGGCTTTAGTCTCAAGTAAAGTCCGGGTAGGCTAGAG	357		
Sbjct 181	CCTAGCTAGAACAACATCATATTAGGCTTTAGTCTCAAGTAAAGTCCGGGTAGGCTAGAG	240		
Query 358	ATGAAATCCAATAGGAGCTTAACGTTGTTTCAGGTAGTGTACAACTTGTAGTAAAAGAT	417		
Sbjct 241	ATGAAATCCAATAGGAGCTTAACGTTGTTTCAGGTAGTGTACAACTTGTAGTAAAAGAT	300		
Query 418	GCTTACTTGTAGATTATGCCAAACCATGATCTATAAGTCAAGTCTCTTTTACTAATAGTT	477		
Sbjct 301	GCTTACTTGTAGATTATGCCAAACCATGATCTATAAGTCAAGTCTCTTTTACTAATAGTT	360		
Query 478	TTGATCCACCTTCTCATCTTTAGTGTAGTTATCATATTTAACTATGTATTGAGAAGATT	537		
Sbjct 361	TTGATCCACCTTCTCATCTTTAGTGTAGTTATCATATTTAACTATGTATTGAGAAGATT	420		
Query 538	AGAAGATTATGAGAGATAACTTGATATGTAAGTGGGTAGTTGAATGTTTTGTTTATCATG	597		
Sbjct 421	AGAAGATTATGAGAGATAACTTGATATGTAAGTGGGTAGTTGAATGTTTTGTTTATCATG	480		
Query 598	AAAACAAGAAATTAGCCTACGTGAGCTCGGAGAGAGTAACTCAATGAGCACATAAATAGA	657		
Sbjct 481	AAAACAAGAAATTAGCCTACGTGAGCTCGGAGAGAGTAACTCAATGAGCACATAAATAGA	540		
Query 658	AGCATGATTC-ACCAATAGACACCGATGACGATGGTGAAGGCAAGGAAATGTATTATT	714		
Sbjct 541	AGCATGATTC-ACCAATAGACACCGATGACGACTGTGAAGGCAAGGAAATGTATTATT	598		

Figure 2.11 Percentage identity and sequence alignment of miR7757 sequence with overhangs. This shows the working sequence generated from the att forward primer

Job title: raw sequence (reverse complemented): MIR7757-ATTR_E03

Brachypodium distachyon microRNA MIR7757 (MIR7757), microRNA

Sequence ID: [NR_127046.1](#) Length: 598 Number of Matches: 1

Range 1: 1 to 598 [GenBank](#) [Graphics](#) ▼ Next Match ▲ Previous Match

Score	Expect	Identities	Gaps	Strand
1083 bits(586)	0.0	594/598(99%)	0/598(0%)	Plus/Plus
Query 163	TGGATCATGCTTCTATTTATAAGCTCATTGAAGTAACTCTCTCCGAGCTCAAATAGGCCA	222		
Sbjct 1	TGGATCATGCTTCTATTTATAAGCTCATTGAAGTAACTCTCTCCGAGCTCAAATAGGCCA	60		
Query 223	ATTTTTGTTTGTGTGATACACAAAACCTTCAGCTACCCACTTCCATATCAAATCATCTC	282		
Sbjct 61	ATTTTTGTTTGTGTGATACACAAAACCTTCAGCTACCCACTTCCATATCAAATCATCTC	120		
Query 283	TCTTGGITTTCTTGICTTTTGGAAATATACTTTGATATGATAAAAAGATGAGAAGGTAGAT	342		
Sbjct 121	TCTTGGITTTCTTGICTTTTGGAAATATACTTTGATATGATAAAAAGATGAGAAGGTAGAT	180		
Query 343	CCTAGCTAGAACAACATCATATTAGGTCTTTAGTCTCAAGTAAGTCCGGGTAGGCTAGAG	402		
Sbjct 181	CCTAGCTAGAACAACATCATATTAAGTCTTTAGTCTCAAGTAAGTCCGGGTAGGCTAGAG	240		
Query 403	ATGAAATCCAATAGGAGCTTAACGTTGTTTCAGGTAGTGTACAACCTGTTAGTAAAAGAT	462		
Sbjct 241	ATGAAATCCAATAGGAGCTTAACGTTGTTTCAGGTAGTGTACAACCTGTTAGTAAAAGAT	300		
Query 463	GCTTACTTGTAGATTATGCCAAACCATGATCTATAAGTCAAGTCTCTTTACTAATAGTT	522		
Sbjct 301	GCTTACTTGTAGATTATGCCAAACCATGATCTATAAGTCAAGTCTCTTTACTAATAGTT	360		
Query 523	TTGATCCACCTTCTCATCTTTAGTGTAGTTATCATATTTAACTATGTATTCAGAAGATT	582		
Sbjct 361	TTGATCCACCTTCTCATCTTTAGTGTAGTTATCATATTTAACTATGTATTCAGAAGATT	420		
Query 583	AGAAGATTATGAGAGATAACTTGATATGTAAGTGGGTAGTTGAATGTTTGTATTATCATG	642		
Sbjct 421	AGAAGATTATGAGAGATAACTTGATATGTAAGTGGGTAGTTGAATGTTTGTATTATCATG	480		
Query 643	AAAACAAGAAATTAGCCTACGTGAGCTCGGAGAGAGTAACTCAATGAGCACATAAATAGA	702		
Sbjct 481	AAAACAAGAAATTAGCCTACGTGAGCCCGGAGAGAGTAACTCAATGAGCACATAAATAGA	540		
Query 703	AGCATGATTCAACCAATAGACACCGATGACGATGGTGAAGGCAAGGAAATGTATTATT	760		
Sbjct 541	AGCATGATTCAACCAATAGACACCGATGACGACTGTGAAGGCAAGGAAATGTATTATT	598		

Figure 2.12 Working sequence generated from the att reverse primer aligned to the *Brachypodium distachyon* nucleotide database shows alignment and 99% identity to miR7757

3.7 Transformation of BP Cloning Products into Competent Cells

BP cloning was performed according to the Gateway Protocol at 25°C and given 10 hours of incubation. Competent DH5α cells were transformed for the test sample, negative, positive and pUC19 cells. For tetracycline and kanamycin supplemented LB agar plates, positive samples showed the appearance of colonies. The negative sample showed no growth on both kanamycin and tetracycline. The test sample reaction containing our att:MIR7757 and pDONR vector gave

the correct result with a few transformed colonies on the kanamycin plate and no growth on the tetracycline plate (Figure 2.13).

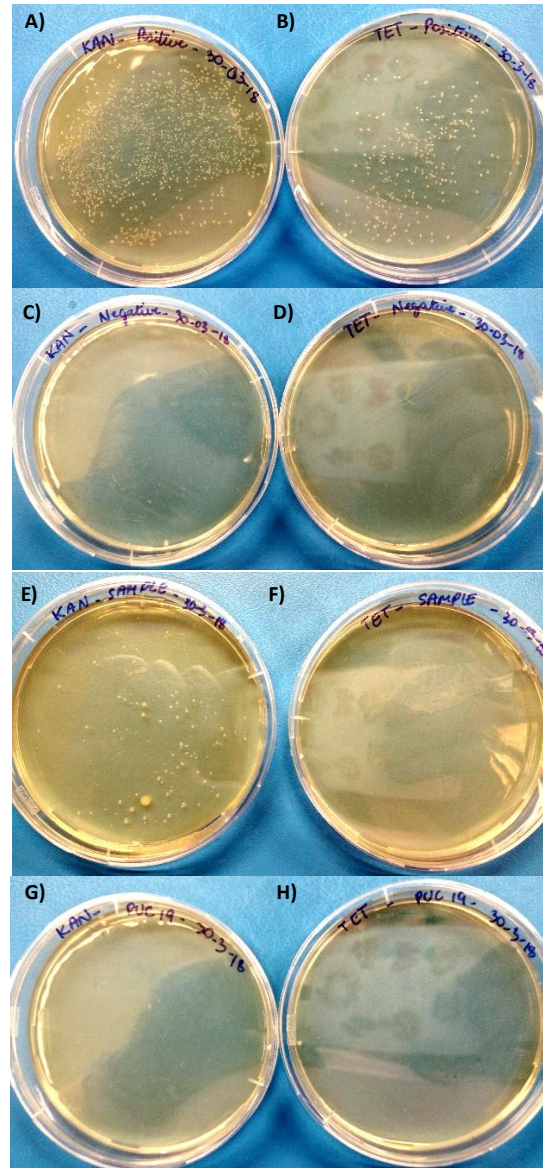


Figure 2.13 Transformation of BP reaction att:MIR7757 into pDONR and transformants on selective media containing antibiotics tetracycline and kanamycin. A) and B) shows the positive control pEXP7-tet vector growth on both the kanamycin and tetracycline plates. C) and D) shows no growth on the negative plates as was expected. E) and F) shows the att:MIR7757 gene inserted into the pDONR221 vector and growth on the kanamycin and tetracycline plates respectively. G) and H) shows no growth of cell transformed with pUC19 which harbours resistance gene to ampicillin.

3.7.1 Colony PCR of BP Reaction Transformants

Calculation of the basepairs from page 20 of the Gateway Cloning manual according to the PCR M13 binding sites the product should fit at 1100 bp. Colony PCR with the plasmid specific primers M13 primers show that the bands appear to be at the correct size (Figure 2.14).

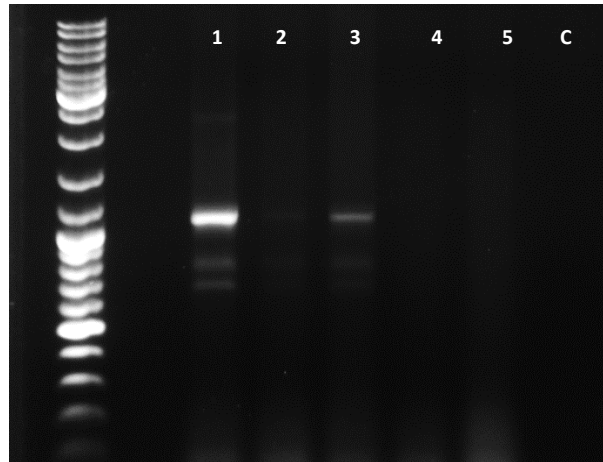


Figure 2.14 Colony PCR amplification of att:MIR7757 transformant colonies with M13 primers. 1,2,3,4,5 represent bacterial colonies. Colonies 1,3 and weakly colony 2 showed positive bands at 1100bp

For further verification miR7757 specific primers were used in colony PCR. miRNA primers yielded a band at 395bp which was the expected size (Figure 2.15).

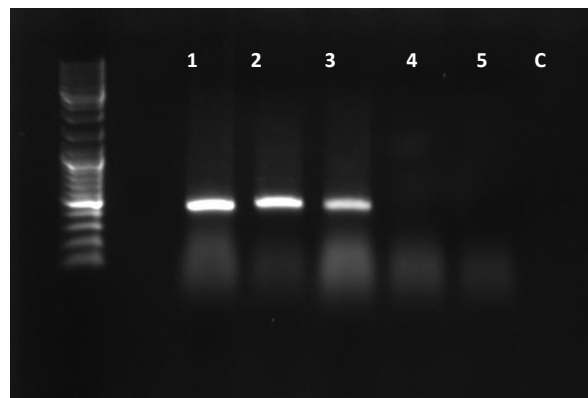


Figure 2.15 Colony PCR amplification of att:MIR7757 transformant colonies with MIR7757 forward and reverse primers. Colonies 1, 2, and 3 showed positive bands.

3.8 Transformation of LR Reaction Products into Competent Cells

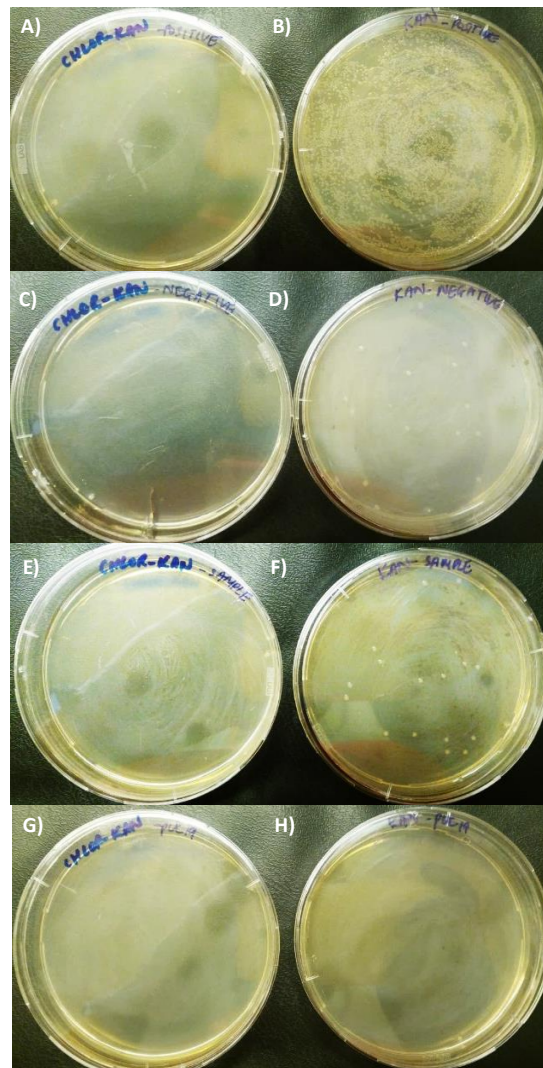


Figure 2.16 LR reaction and the transformants plated on the selective antibiotic plates containing kanamycin, and chloramphenicol and kanamycin. A) shows the positive sample, B) shows the negative samples, c) shows the sample. A, C, E, G depict the LB media plated supplemented with chloramphenicol and kanamycin. B, D, F, H show the LB media having only kanamycin.

LR reaction was performed and the reactions were transformed into competent DH5 α cells as in BP transformation. The LR cloning reaction of pDONR:MIR7757 into pEarleyGate103 was verified by plating the transformants on chloramphenicol+ kanamycin and kanamycin plates. The transformation results are shown in Figure 2.16. The reaction was successful and the transformants appeared on expected selection media.

3.8.1 Colony PCR of LR Reaction Transformants

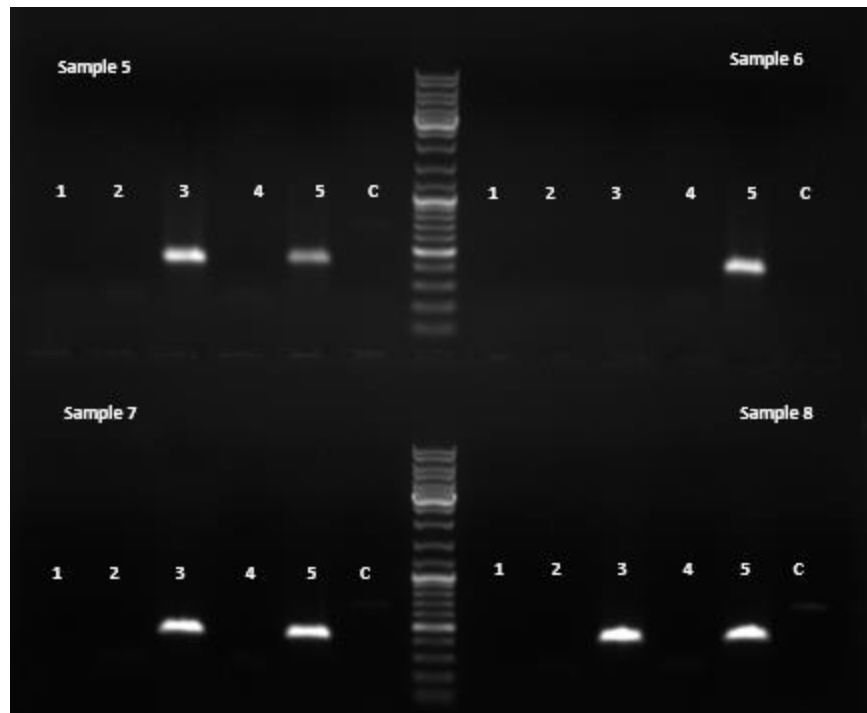


Figure 2.17 Colony PCR of LR reaction transformant colonies 5,6,7 and 8 with miR specific primers and CaMV promoter primers. 1 CamV F+ miR R, 2 CamV F + miR F, 3 miR F+ R, 4 CamV F+R, 5 CamV R+miR R, 6 CamV R+miR F

Colony PCR was performed with miR specific primers with CaMV promoter Primers. Both sets of primers were used alone and in combination. The miRNA forward and reverse primers used in combination with the CaMV promoter forward and reverse primers generated the required PCR product as seen in Figure 2.17. The sample shows the PCR with plasmid isolated from colonies 5, 6, 7 and 8 obtained from the LR cloning. The samples were 1. CaMV F+ miRRev, 2. CaMVF+ miRF, 3. miRF+miRRev, 4. CaMVF+CaMVR, 5. CaMVR+miRRev, 6. CaMVR+miRF (Figure 2.17)

3.9 Transformation of LR Reaction Products into *Agrobacterium tumefaciens* cells

The LR reaction product plasmid pEarleyGate103withstop+pre-miRNA7757 (35S::MIR7757) was transformed into *Agrobacterium*. 200 µl of the transformed cells was fully spread on selective LB media containing carbenicillin, kanamycin and both carbenicillin and kanamycin.

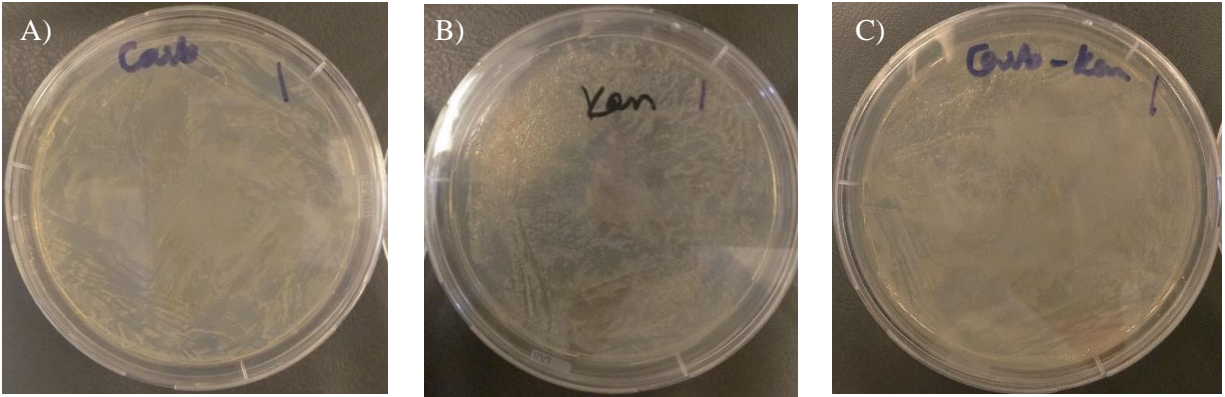


Figure 2.18 *Agrobacterium* transformed with LR reaction product and spread on plates for use for transformation. A) shows the growth of *Agrobacterium* on carbenicillin, B) shows growth on kanamycin and C) shows growth on both carbenicillin and kanamycin.

Untransformed *Agrobacterium* was resistant only to carbenicillin whereas LR reaction transformed *Agrobacterium* harbouring 35S::MIR7757 was resistant to kanamycin and carbenicillin both. Growth was observed on all selective media (Figure 2.18). The resistance to carbenicillin was due to the AGL1 strain of *Agrobacterium* and the resistance to kanamycin was due to harbouring the pEarleyGate 103 plasmid.

3.10 *Brachypodium* Wildtype and T-DNA Mutant Growth and Phenotype

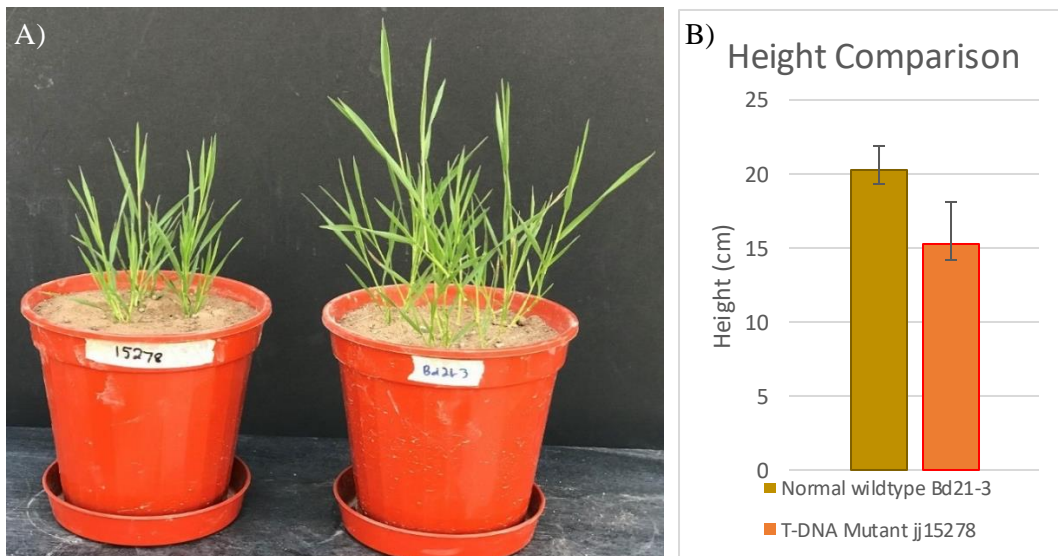


Figure 2.19 Comparison of plant height between mutant line JJ15278 and wildtype Bd21-3. A) depicts the direct observation of stunted growth as compared to the control. B) shows the average growth of wildtype and mutant plants.

Similar to the phenotypic analyses in Hsia et al 2017 phenotypic analysis of the mutant and normal plants was performed for plant height and leaf cuticles. Average height of 10 week old mature plants was measured and it was confirmed that the height of the mutant plants was significantly shorter than the wildtype plants (Figure 2.19).

3.10.1 Microscopic Analysis of Mutant and Wildtype Leaf Blades

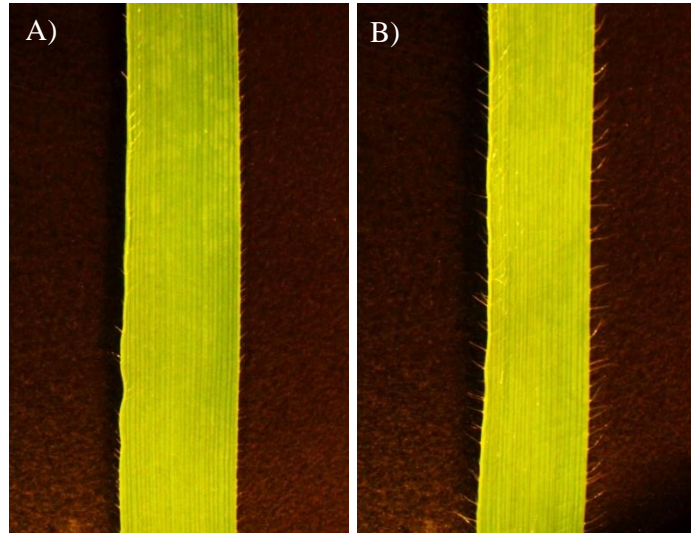


Figure 2.20 Light microscopic analysis of hair cuticle density of mutant A) and wildtype B) *Brachypodium distachyon*. Light microscopic analysis revealed that the mutant displayed lesser leaf hair density as compared to the wildtype (Figure 2.20)

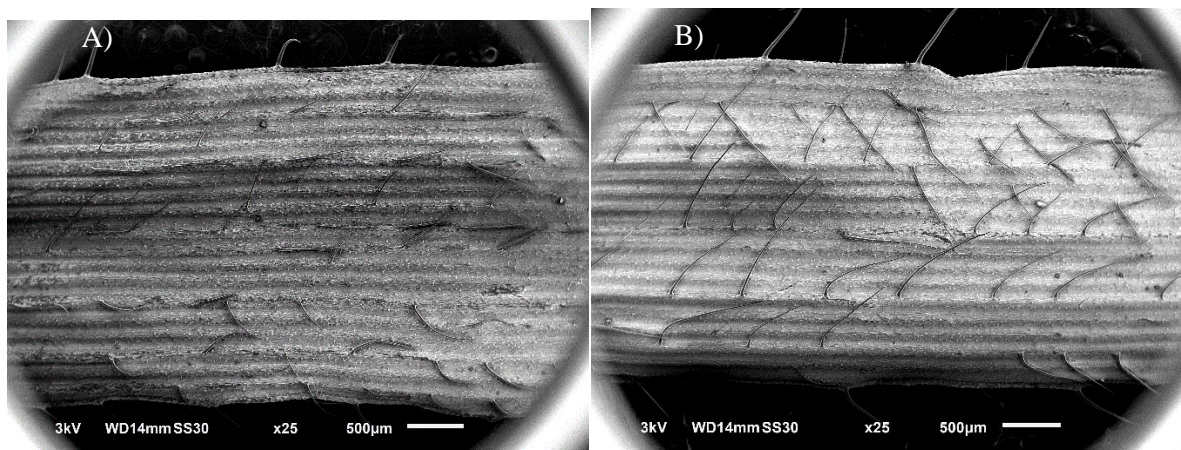


Figure 4.21 Scanning electron micrographs of mutant A) and normal B) *Brachypodium distachyon* mature leaf blades. The miR7757 T-DNA mutant shows lesser hair cuticles as compared to the normal.

Electron micrographs of 7cm air dried leaf blades from mature plants of T-DNA mutant jj15278 and wildtype Bd21-3 plants confirmed the light microscopic analysis. Fewer hair cuticles were observed in the mutant as compared to the wildtype (Figure 2.21).

3.11 RNA Gel of Leaf and Root Samples and Semiquantitative qPCR

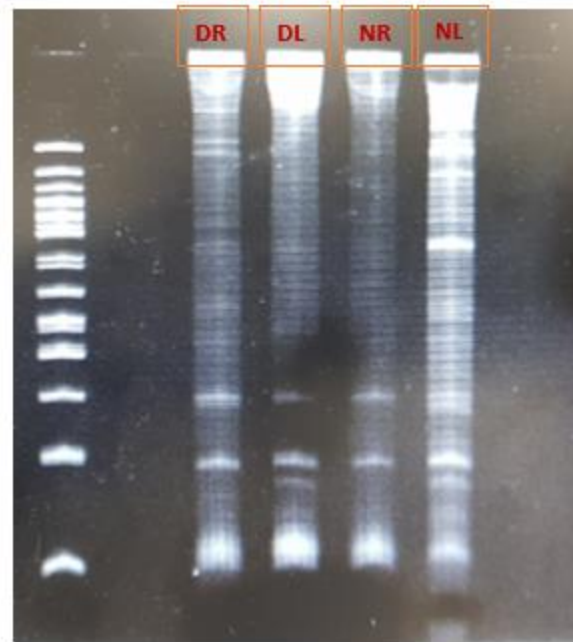


Figure 2.22 Native page gel of RNA samples from drought root, drought leaf, normal root and normal leaf of Bd21 wildtype. Lane 1 50bp Ladder NEB, Lane 2 Drought Root, Lane 3 Drought Leaf, Lane 4 Normal Root, Lane 5 Normal Leaf. The ladder used was 50 bp DNA Ladder (NEB #B7025), Size range was 50 bp - 1350 bp

RNA isolated from drought stressed and normal leaves and roots ran on native PAGE gel clearly confirmed the integrity and purity of the RNA. Tight RNA bands after DNase treatment for both the roots and the shoots were observed which enabled the RNA samples to be used for downstream qPCR reaction. Subsequent semi-quantitative PCR of drought associated miR7757 showed its expression in all samples from the gel (Figure 2.19). Verification of the involvement of miR7757 in *Brachypodium distachyon* under drought stress was done by analyzing the expression levels in drought leaves and roots and normal leaves and roots. The normal leaf expression levels were taken as control and other expression levels were calculated relative to it. The expression analysis showed that there was no significant in the expression of miR7757 between the normal leaf and drought leaf conditions.

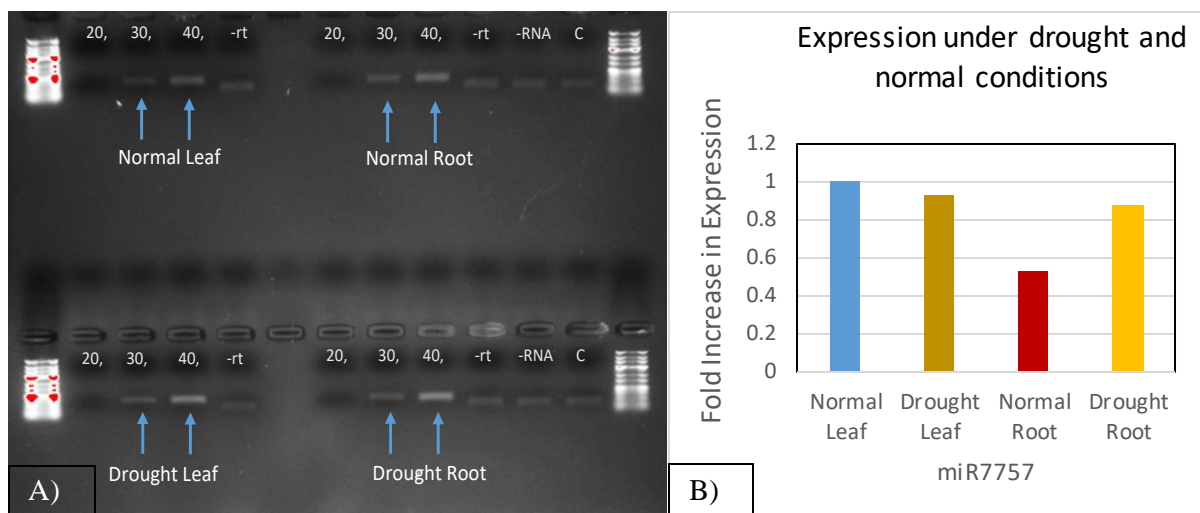


Figure 2.23 qRT-PCR of miR7757 of normal and drought stressed leaves and roots of wildtype *Brachypodium*. A) shows semi quantitative PCR gel from endpoint reaction. A) Expression of miR7757 is observed in all samples with 30 and 40 cycles of reaction. The order of the top gel is ladder, NL20, NL30, NL40, no-rtNL, empty, NR20, NR30, NR40, no-rtNR, no-RNA, Control, ladder. Bottom gel order is ladder, DL20, DL30, DL40, no-rtDL, empty, DR20, DR30, DR40, no-rtDR, no-RNA, Control, Ladder. B) Expression profile of miR7757 in leaf and roots in stressed and control samples.

However, there was a significant increase in the miR7757 expression levels in the root after drought stress as compared to the normal root (Figure 2.23 B)). Despite having faint bands in the control samples it is evident that they are lower than the miRNA expression in the 30 cycle and 40 cycle bands. The gel shows endpoint PCR results after 20, 30 and 40 cycles. Primers were used as 5 μ M each to avoid primer contamination. -rt depicts sample without stem loop primer. The expression profile shows that the roots showed difference in expression level under drought stress. A 0.4 fold increase was observed in miR7757 expression in the drought stressed root as compared to the normal watered root.

3.12 Growth Stages of *Brachypodium* Plants used in Transformation Studies

3.12.1 Compact Embryonic Callus Generation

Brachypodium green immature seedlings were grown as described in the Section 2. The immature embryo was grown on callus induction media MSB3+ CuO.6 as described by Alves et al 2009. The CEC (compact embryonic callus) was obtained from the immature calli. The calli were compact, creamy and pearly and grew well on the callus induction media (Figure 2.24). Supplementation with copper sulphate augmented the growth of the calli. Growth of creamy and

pearly compact embryonic calli was also observed from both mutant and normal wildtype at 6 weeks of growth. These were immediately split into 4-6 calli each (Figure 2.25 C and D).

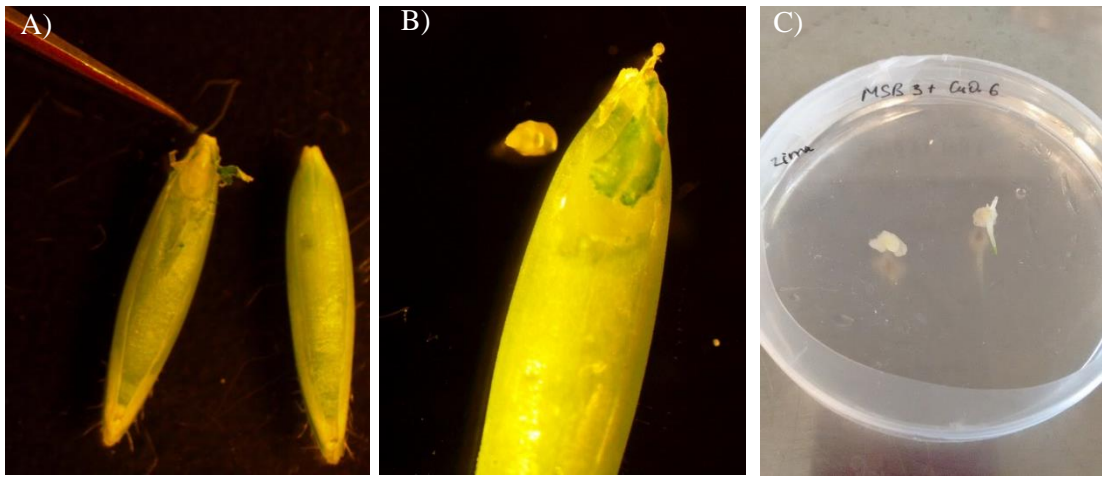


Figure 2.24 Swollen but green immature seed used for immature embryo dissection. A) and the dissection of the embryo B) as seen under the stereomicroscope. C) shows the early formation of callus with shoots after 3 days of culture.

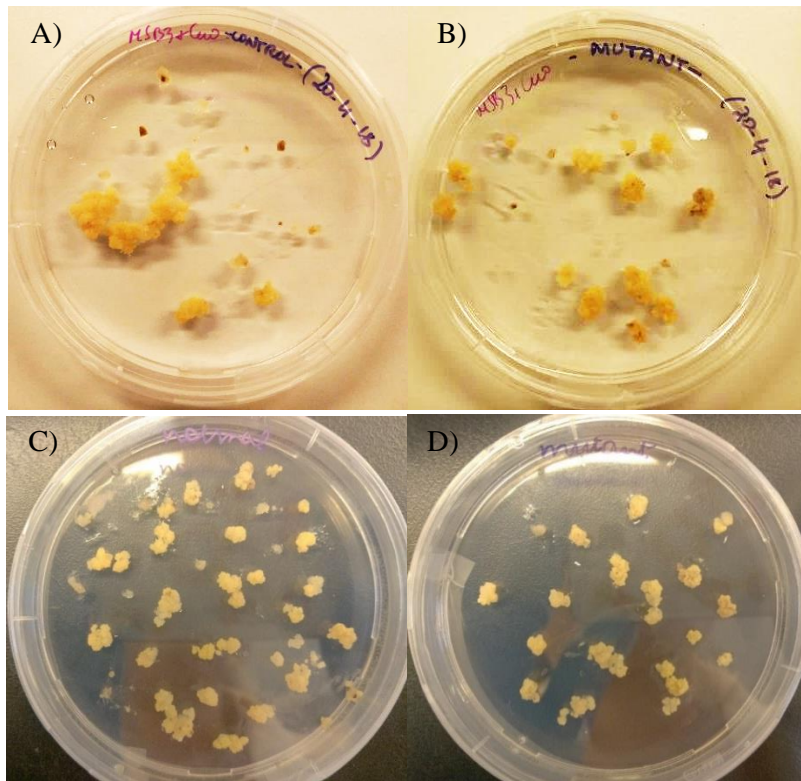


Figure 2.25. 6 weeks growth of the immature embryo into the opaque callus ready for splitting A) and B), Figure 2.21 The split calli at 6 weeks right before transformation by flooding with *Agrobacterium* C) and D).

3.12.2 *Agrobacterium tumefaciens* Infection of *Brachypodium* Immature Embryo

The fresh *Agrobacterium* cultures were transferred to the MSB+AS45 media. Half a plate of *Agrobacterium* was sufficient for 3 CEC plates similar to the protocol of Alves. Et al 2009.

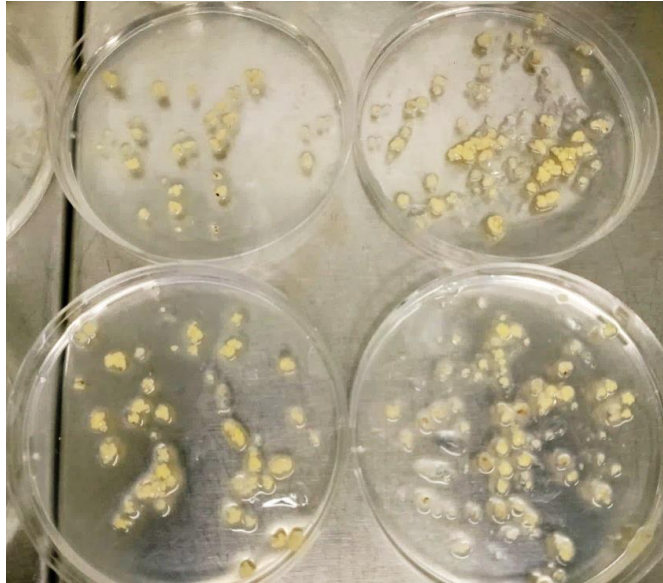


Figure 2.26 Flooding of the 6 week calli with *Agrobacterium* culture.

This way 24 plates were flood from *Agrobacterium* suspension from 6 plates. 12 plates were for mutants and 12 plates were for wildtype calli. The calli were placed on empty sterile petri plates to be flooded with *Agrobacterium* suspension (Figure 2.26). The time for incubation in *Agrobacterium* was 15 minutes for each culture plate since time was spent in handling all 24 plates and this proved to be beneficial in transformation.

3.12.3 Co-cultivation of Infected Embryonic Callus Culture

Initial incubation for 2 days on MSB3+AS60 media showed overgrowth of *Agrobacterium* on the compact embryonic calli (Figure 2.27). They were immediately transferred to selective media containing phosphinothricin to promote the growth of transformed calli. They were left in the dark and observed after 3 weeks to show growth of calli in creamy colour and also browning calli which were not transformed (Figure 2.24)

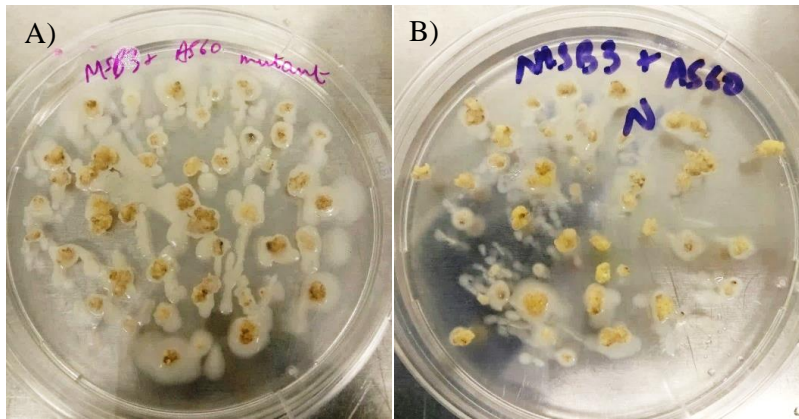


Figure 2.27 Initial incubation for 2 days on MSB3+AS60 media

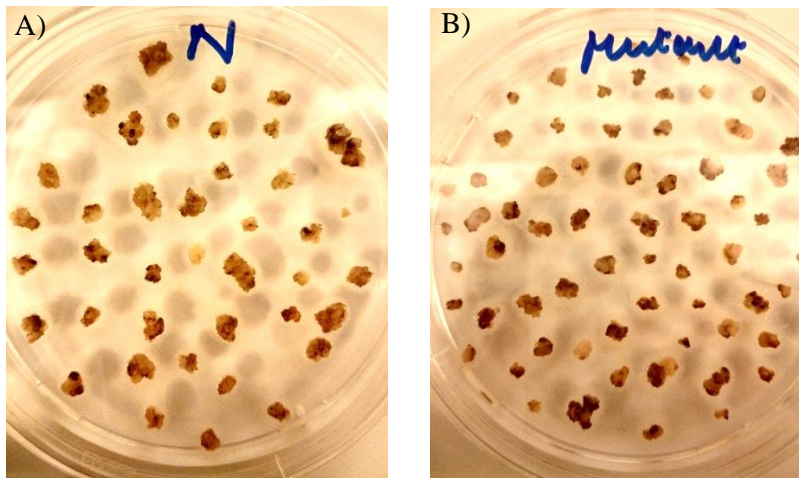


Figure 2.28 Growth on MSB+Cu0.6+H40+T225 showing growth of the calli after 3 weeks.

Figure 2.23 shows 3 weeks of growth of *Agrobacterim* transformed compact embryonic calli on MSB+Cu0.6+H40+T225. The darkened sectors dark brown/black in colour show necrotic tissue which did not transform and did not tolerate the herbicide phosphinothricin. Lighter calli display growth in the presence of selective agent. This type of calli grew larger and faster than other calli (Figure 2.29). Various calli also have light and dark sectors which show transformed and untransformed sectors (Figure 2.28). These were dissected out after observation of GFP sectors under the fluorescent microscope (Figure 2.30).

3.12.4 Screening of Transformed Calli with BASTA and GFP

After 6 weeks of growth on selection media containing timentin (320 mg/ml). Selected calli which grew under 5mg/L PPT (phosphinothricin) were subsequently verified for transformed sectors under GFP. Only the PPT resistant sectors which were fluorescing under UV were selected to be

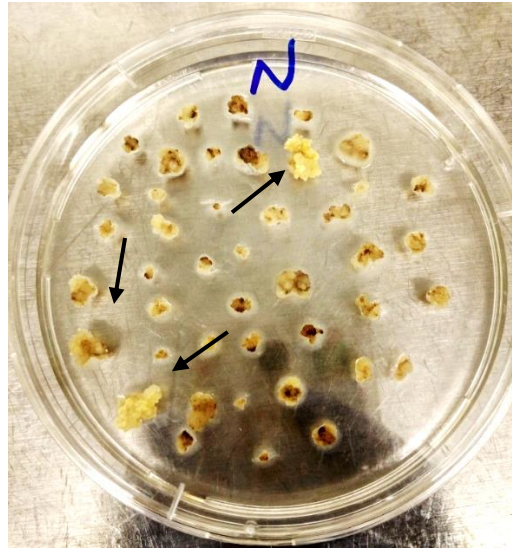


Figure 2.29 Selected calli which grew under PPI for 6 weeks and were subsequently analyzed under GFP.

grown in regeneration media. However, owing to the small size of the sectors some neighboring tissue was also transferred along to ensure that the calli can be able to regenerate. GFP fluorescence was analyzed under 5X lens in the Zeiss Axiovert A1 inverted microscope. The sectors which showed fluorescence were selected out as well as some neighbouring tissue to facilitate the growth of the transformed calli since at this stage the calli were small. This was performed according to Alves et al 2009.

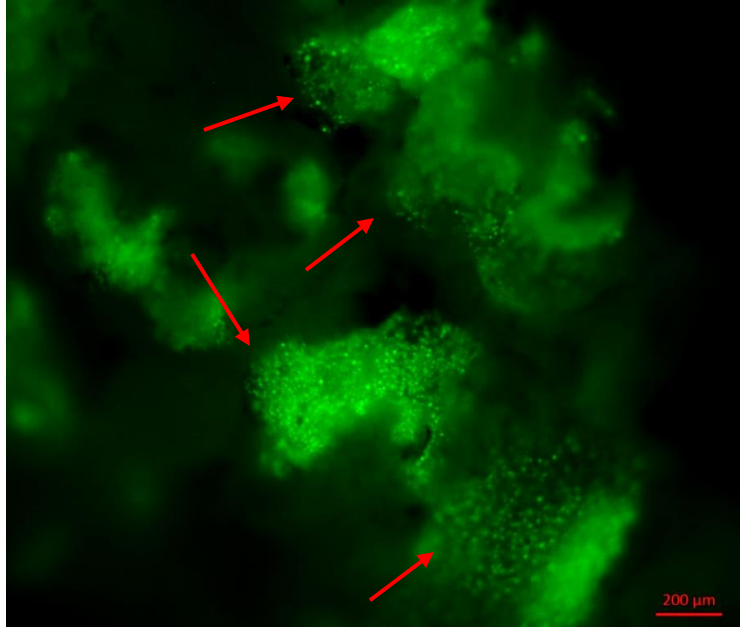


Figure 2.30 Transformed calli displaying clear GFP fluorescence

3.12.5 Regeneration of transgenic plants



Figure 2.31 Regeneration of the GFP calli on selective media to promote shoot growth

After selecting the desired GFP fluorescing sectors and the calli which grew well in phosphinothricin the transformed calli were taken along with some neighboring tissue and transferred to MSR26+H20+T225 regeneration medium. These were grown at 25°C at a 16 hour

photoperiod for 2-3 weeks. After the flooding of the calli the selection media and regeneration media was constantly supplemented with 5mg/L to ensure the correct selection of transformants. To prevent overgrowth of *Agrobacterium* on selection and regeneration plates the concentration of timentin (320 mg/ml) 700 μ L was increased to 1.4ml/L to ensure no overgrowth of *Agrobacterium* which was observed at various stages. This concentration resulted in better growth of the calli without bacterial culture hindering its growth and turning it brown (Figure 2.31).

4. Discussion

MiR7757 is a newly discovered and studied microRNA which is considered important in several abiotic stress conditions. Its role in abiotic stress has been documented including its role in water deficit in wheat plants. This study focused on the cloning and overexpression of this microRNA in *Brachypodium distachyon*. *Brachypodium* is a widely studied model plants for cereals and crop genetics, till yet the response of miR7757 in *Brachypodium* against drought had not been studied or reported.

Comparing both data from table 2 and 3 the highest score *in silico* identified gene targets of mi7757 from both *Brachypodium* and other monocots species were disease resistance genes which appeared most frequently. Thus, the most likely target of bdi-miR7757-5p.1 is the disease resistance family RGA and RPP in *Brachypodium distachyon*. Other putative targets are inositol monophosphatase 3, and transposon Tf2-1 polyprotein. A recent study in chickpea has indicated that the myo-inositol monophosphatase gene contributes to drought tolerance with a link between the repeat length variation in the 5'UTR of the gene and phytic acid content which is significant in development and stress tolerance (Joshi-Saha and Reddy 2015). The main targets hit by miR7757 were found to include the plant resistance genes R gene family including RPP and RGA genes and their proteins. The most frequently occurred target was disease resistance RPP13-like protein 3. miR7757 putatively inhibits gene expression of these genes by cleavage.

Agrobacterium tumefaciens transformation although highly popular and successful still has subtle intricacies which must be addressed. Loss of calli was regularly observed due to excessive growth of *Agrobacterium* after co-cultivation. Thus, the transfer of calli from co-cultivation to selection media involved increasing the volume of timentin (320mg/ml) from 700ul to 1.4ml in one litre. This ensured good growth of the calli without any overgrowth of *Agrobacterium* in the selection media. However, during the transfer of calli from selection media to regeneration media high contamination was observed both bacterial and fungal. Transfer thus involved a wash step of calli with sterile distilled water to remove *Agrobacterium* excessive growth from the surface of calli. The sterile water did control the excessive growth of *Agrobacterium* however to avoid bacterial and fungal contamination itraconazole and cefotaxime were supplemented to sterile water to prevent unwanted microbial growth.

In our study miR7757 was upregulated in drought stressed root. This could point towards the tissue specific expression of this microRNA to combat water deficit. Further studies on organ specific expression in developmental parts such as young leaves could prove vital to understanding its role in water deficit. Future studies pertaining to the role of microRNAs in stress tolerance are sure to utilize such multiple stress related microRNAs for producing stress tolerant varieties. In the future prospect of this study, the analysis of this miRNA could be maintained by carrying on the development of GFP fluorescing putatively transformed calli into plantlets and subsequently mature plants and analyzing their survival capacity of miR7757 overexpressed cultivars under conditions of drought and water deficit. Furthermore, since this miRNA was reported in several biotic and abiotic conditions these same overexpressing plants could also be utilized in other stress conditions and studied for disease resistance.

C. CONCLUSION TO THE THESIS

Brachypodium distachyon is a versatile and dynamic plant model which can be manipulated and studied in diverse biological setups. It has the highly flexible ability to be in controllable experimental setups and this amalgamation with its desirable genetic qualities and extensive genomic database gives it an edge in cereal and grass research. It provides a rapid platform for manipulation both genotypic and phenotypic. From this study a microfluidic platform can be created to analyze mechanical and physical dynamics of *Brachypodium* seed growth. This study can easily be adapted for further refined, comprehensive and in depth physical and physiological analyses under diverse stress conditions.

This approach can be further developed into novel monocot plant-on-a-chip microphysiological systems or root-chip models to provide a complete picture of cell-cell communication, stress response at the cellular level, and visualisation of other phenotypic changes. In addition, the reported methodology can be perfected to test different abiotic stress factors on a single device with the stress media (NaCl, PEG, nutrient deficient, hormone, growth factor, drug, and nanomaterials) poured into different channels of the same device and analyzed simultaneously for root dynamics (mechanical, physical and elastic properties) and adaptation period. These can then be further genetically analysed for gene expression levels in real time (Bennett and Hasty 2009; Busch et al. 2012), with drought related genes such as TdAtg8, DREB, WRKY and Lea (Kuzuoglu-Ozturk et al. 2012). Future chip platforms with high throughput capacities may reduce the labour, cost and troublesome in large-scale studies in the greenhouses and take the samples directly into microscopes for comprehensive analyses in microscale with high spatial resolution. With the optimization of such chip platforms a phenotyping array can be developed for *Brachypodium distachyon* which can be subsequently analyzed for genomics, transcriptomics and metabolomics. This novel platform can prove to be suitable for paralleling phenotypic and genotypic data one after the other from a single array.

In terms of genetic resource *Brachypodium* has well established itself as a bridge to explore the genetically complex *Triticeae* cereal clan. Our study displayed the ease of genetically manipulating *Brachypodium* for microRNA overexpression. *Brachypodium* T-DNA mutant collection is a geneticist treasure trove to explore abiotic and abiotic genes, and miRNAs and any sort of reverse genetics approach. This enables not only the understanding of the stress tolerance of

Brachypodium to drought and other stresses but also gives a view about tolerance in related species. Genes from other species can also be manipulated in *Brachypodium* since it has flexible genetic transformation and cloning. Not only its genetic flexibility but its short life cycle accelerates phenotypic and genotypic research and provide rapid results. All in all *Brachypodium* has been well selected as a versatile model for plant research whether it be morphological, physiological or genetic.

APPENDIX A

Molecular Biology Kits

Wizard® Genomic DNA Purification Kit	Promega	A1120
Gel Extraction Kit	QiagenQIAquick	28706
Gateway Cloning Systems	Invitrogen	12535-029
Plasmid DNA Isolation Kit	Thermo Scientific	K0502

APPENDIX B

Equipment

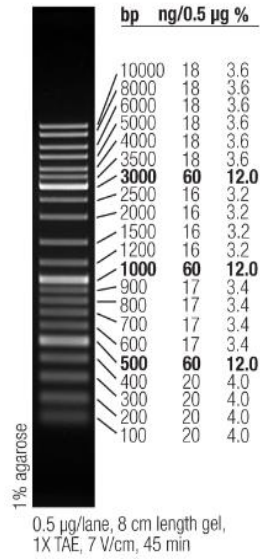
Autoclave:	Hirayama, Hiclave HV-110, JAPAN Nüve 0T 032, TÜRKİYE
Balance:	Sartorius, BP221S, GERMANY Schimadzu, Libror EB-3 200 HU, JAPAN
Centrifuge:	Microfuge 18 Centrifuge Beckman Coulter, USA Kendro Lab. Prod., Heraeus Multifuge 3S-R, GERMANY Kendro Lab. Prod., Sorvall RC5C Plus, USA Eppendorf, 5415D, GERMANY Eppendorf, 5415R, GERMANY
Deepfreeze:	-20 °C Bosch, TURKEY -80 °C Thermo electron corporation, USA
Distilled Water:	Millipore, Elix-S, FRANCE Millipore, MilliQ Academic, FRANCE
Electrophoresis:	Labnet Gel XL Ultra V-2, USA Biogen Inc., USA Biorad Inc., USA
Filter paper:	Whatman General Purpose Filtration Paper WHASE1141, Sigma, MO, USA
Gel Documentation:	Biorad Universal Hood II F1-F2 Fuses Type T2A, USA Biorad, UV-Transilluminator 2000, USA
Glassine crossing bags:	Focus Packaging & Design Ltd, North Lincolnshire, UK
Growth chamber:	Digitech DG12, Ankara, TURKEY
Heating block:	HDV Life Sciences, AUSTRIA Thermostat Bio TDB-100, LATVIA
Ice Machine:	Scotsman Inc., AF20, USA
Incubator:	Innova 4330, USA Mettler, Modell 300, GERMANY

	Memmert, Modell 600, GERMANY
Laminar Flow:	Holten LaminAir Model 1.8 82034000, DENMARK
	Heraeus, Modell HS 12, GERMANY
Magnetic Stirrer:	VELP Scientifica, ITALY
Microliter Pipette:	Gilson, Pipetman, FRANCE
	Eppendorf, GERMANY
Microwave Oven:	Bosch, TÜRKİYE
Nitrogen tanks:	Linde Industrial Gases, TURKEY
Oven:	Memmert D06062 Modell 600, GERMANY
pH Meter:	WTW, pH540, GLP MultiCal, GERMANY
Power Supply:	Biorad, PowerPac 300, USA
Real-Time PCR:	Roche LightCycler 480 Instrument II
Refrigerator:	+4 oC Bosh, TÜRKİYE
Shaker:	Forma Scientific, Orbital Shaker 4520, USA
	GFL, Shaker 3011, USA
	New Brunswick Sci., Innova™ 4330, USA
	New Brunswick Scientific Excells E24, USA
Spectrophotometer:	Amersham Biosciences Ultraspec 2100 pro, USA
	Nanodrop, ND-1000, USA
Sterilizer:	Steri 350, Simon Keller Ltd., SWITZERLAND
Thermocycler:	Eppendorf, Mastercycler Gradient, GERMANY
	Biorad Gradient Cycler DNA Engine, USA
Vortex Mixer:	VELP Scientifica 2X3, ITALY
Water bath:	Memmert, GERMANY

APPENDIX C

DNA Ladders

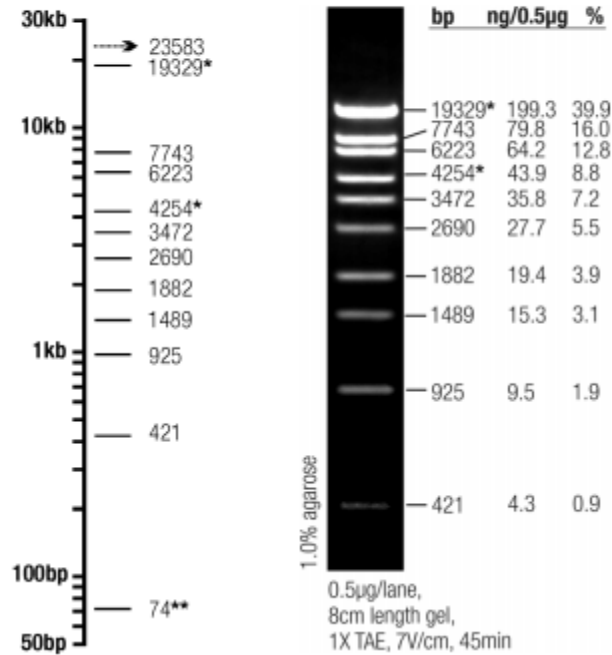
GeneRuler DNA Ladder Mix

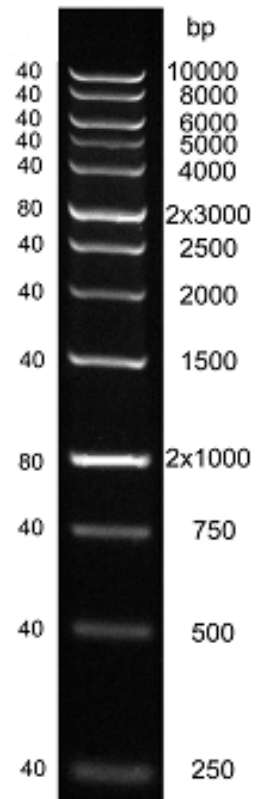


#SM0331

Lambda DNA/Eco130I (StyI) Marker, 16

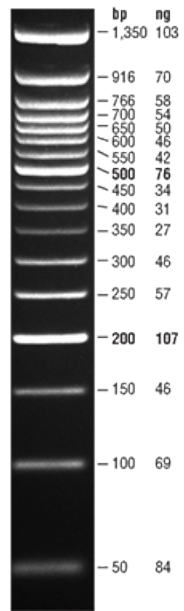
Fragment Sizes





Electrophoresis
conditions:
Gel: 1% agarose
Buffer: 0.5x TBE
Voltage: 10 V/cm

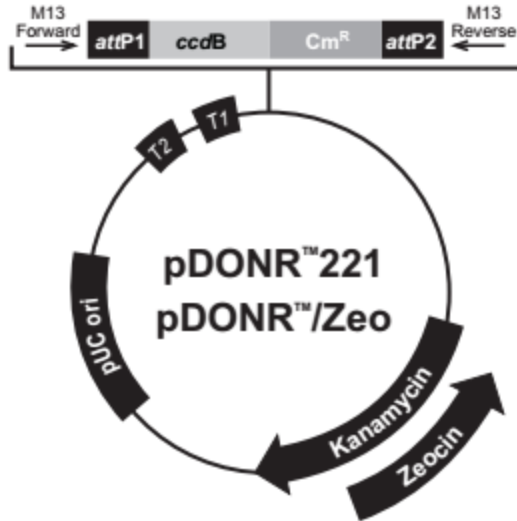
BIORON 1 kb DNA Ladder no stain
Cat.-No.: 305025 250 µg



50 bp DNA Ladder (NEB #B7025), Size range: 50 bp - 1350 bp

APPENDIX D

Vector map of pDONR 221



Comments for:

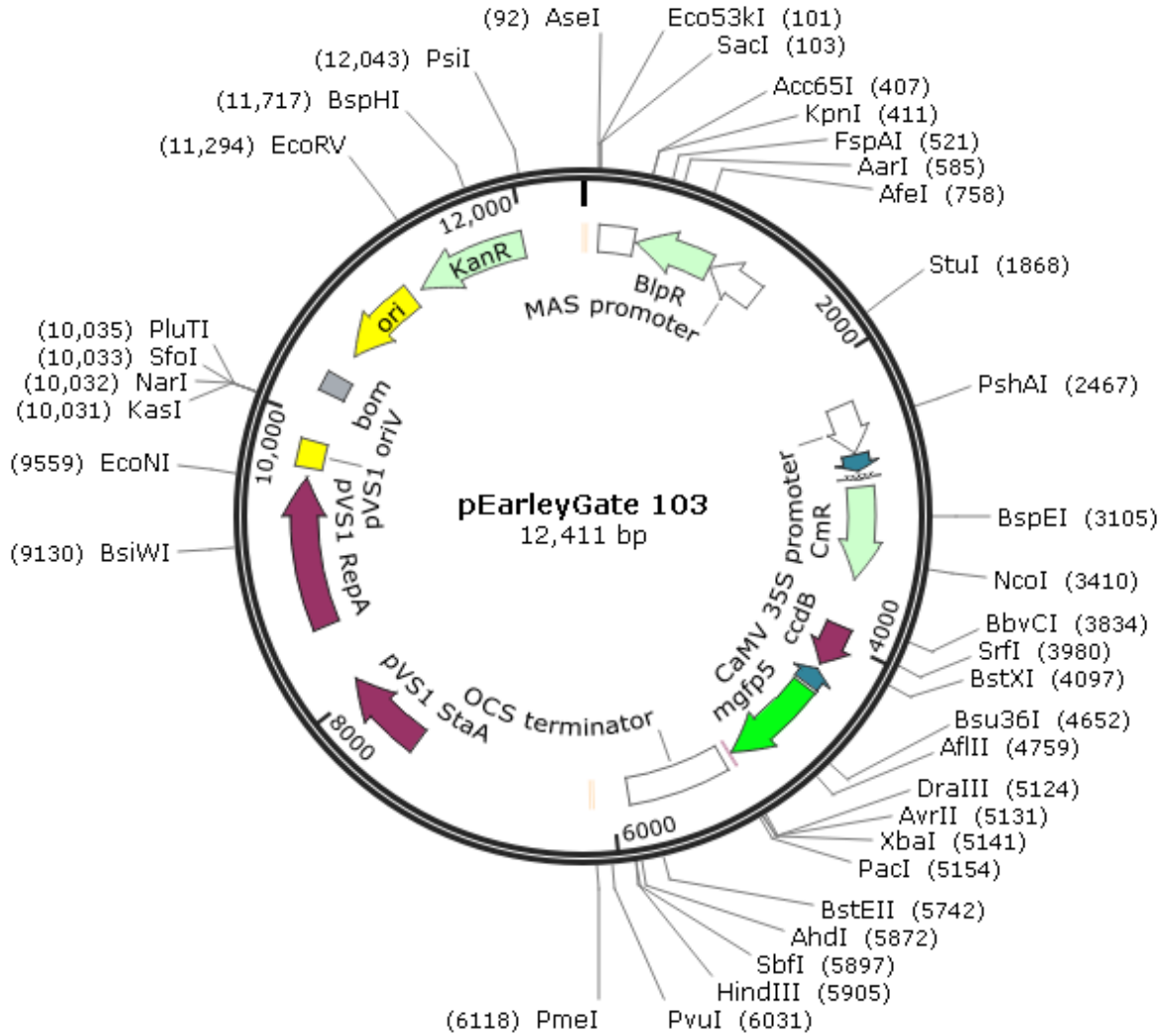
	pDONR™221 4761 nucleotides	pDONR™/Zeo 4291 nucleotides
<i>rrnB</i> T2 transcription termination sequence (c):	268-295	268-295
<i>rrnB</i> T1 transcription termination sequence (c):	427-470	427-470
M13 Forward (-20) priming site:	537-552	537-552
<i>attP1</i> :	570-801	570-801
<i>ccdB</i> gene (c):	1197-1502	1197-1502
Chloramphenicol resistance gene (c):	1825-2505	1847-2506
<i>attP2</i> (c):	2753-2984	2754-2985
M13 Reverse priming site:	3026-3042	3027-3043
Kanamycin resistance gene:	3155-3964	---
EM7 promoter (c):	---	3486-3552
Zeocin resistance gene (c):	---	3111-3485
pUC origin:	4085-4758	3615-4288

(c) = complementary strand

APPENDIX E

Vector map of pEarleyGate 103

Created with SnapGene®



APPENDIX F

TABLES

Table 1. Examples of microfluidic devices developed for plant biotechnology research

Species name	Seed Type	Organ studied	Device type	Physical Parameters	Reference
<i>Camellia japonica</i>	Dicot	Pollen tube	Lab-on-a-chip (LOC) technology	Influence of electric fields and conductivity	(Agudelo et al., 2014)
	Dicot, fungus	Pollen grains, root hairs or fungal spores	TipChip (serially arranged microchannels)	Experimentation and phenotyping of chemical gradients, microstructural features, integrated biosensors or directional triggers within the modular microchannels	(Agudelo et al., 2013)
	Dicot	Pollen grains	Microchannels and inlets/outlets	Protuberance growth of single plant cells in a micro- vitro environment	(Nezhad et al., 2014a)
	Dicot	Pollen grains	TipChip	penetrative forces generated in pollen tubes	(Nezhad et al., 2013a)
	Dicot	Pollen tube	Laminar flow based microfluidic device	Ca ²⁺ , pectin methyl esterase (PME) application for quantitative assessment of chemo attraction	(Nezhad et al., 2014b)
	Dicot	Pollen tube	Device with a knot shaped microchannels microfluidic	Trapping probability and uniformity of fluid flow conditions	(Ghanbari et al., 2014)
	Dicot	Pollen tube	Trapping microfluidic device	Primary and secondary peak frequencies in oscillatory growth dynamics	(Nezhad et al., 2013c)
	Dicot	Pollen tube	Bending-Lab-On-a-Chip (BLOC)	Flexural rigidity of the pollen tube and the Young's modulus of the cell wall	(Nezhad et al., 2013b)
	Dicot	Pollen grains	Microchannels and inlets/outlets	Protuberance growth of single plant cells in a micro- vitro environment	(Nezhad et al., 2014a)
	Dicot	Pollen grains	TipChip	Penetrative forces generated in pollen tubes	(Nezhad et al., 2013a)
	Dicot	Pollen tube	Laminar flow based microfluidic device	Ca ²⁺ , pectin methyl esterase (PME) application for quantitative assessment of chemo attraction	(Nezhad et al., 2014b)
	Dicot	Pollen tube	Device with a knot shaped microchannels microfluidic network	Trapping probability and uniformity of fluid flow conditions	(Ghanbari et al., 2014)

	Dicot	Pollen tube	Trapping microfluidic device	Primary and secondary peak frequencies in oscillatory growth dynamics	(Nezhad et al., 2013c)
<i>Arabidopsis thaliana</i>	Dicot	Plant body/Root	Microfluidic chip platform RootChip	Monitoring time-resolved growth and cytosolic sugar levels at subcellular resolution	(Grossmann et al., 2011)
	Dicot	Embryo	PDMS micropillar array	Live-Cell Imaging and Optical Manipulation	(Gooh et al., 2015)
	Dicot	Root/Plants	RootArray	Imaged by confocal microscopy	(Busch et al., 2012)
	Dicot	Root	RootChip16	Identification of defined [Ca ²⁺] _{cyt} oscillations, Förster resonance energy transfer (FRET)	(Keinath et al., 2015)
	Dicot	Plant body-pathogen interaction	Plant Chip : vertical and transparent microfluidic for high-throughput phenotyping	Quantitative monitoring of plant phenotypes	(Jiang et al., 2014)
	Dicot	Live Root	Plant on chip microfluidic platform	Stimuli and phyto hormones 2,4-dichlorophenoxyacetic acid (2,4-D), and its inhibitor N-1-naphthylphthalamic acid (NPA)	(Meier et al., 2010)
	Dicot	Pollen-ovule	Mimicry of in vivo micro-environment of ovule fertilization	Chemo attraction	(Yetisen et al., 2011)
<i>Torenia fournieri</i>	Dicot	Pollen tube, ovules	T-shaped microchannel device, microcage array	Pollen tube chemo attraction, long-term live imaging of ovules	(Arata and Higashiyama, 2014)
	Dicot	Pollen tubes	T-shaped channel	Quantitate the effect of chemo attractants on directional pollen tube growth, UV-irradiation	(Horade et al., 2013)
	Dicot	Pollen Tube	Crossroad device	Net guidance response ratio (GRR)	(Sato et al., 2015)
<i>Tobacco Nicotiana tabacum</i>	Dicot	Mesophyll Protoplast	Microcolumn array	Microscopic real-time optimization and dynamics of protoplast growth including size change, organelle motion, and cell mass formation	(Wu et al., 2011)
<i>Phalaenopsis</i>	Dicot	Protoplasts	Convex-concave sieving array	Real-time collection and lysis of <i>Phalaenopsis</i> protoplasts	(Hung and Chang, 2012)

APPENDIX G

Table 2 psRNATarget hits from the *Brachypodium* coding sequence for bdi-miR7757-5p.1

Target_Acc.	Expect	miRNA start	miRNA end	Target start	Target end	miRNA_aligned_fragment	Target_aligned_fragment
Bradi4g10050.1 PA Cid:21812309	1.5	1	21	1411	1431	CACAAAACCUUCAGCUACCCA	UGGGUUGUUGAAGGUUUUGUG
Bradi1g15350.1 PA Cid:21818854	2.0	1	21	679	699	CACAAAACCUUCAGCUACCCA	CAGGAAGCUGGGGGUUUUGUG
Bradi4g09587.3 PA Cid:21810371	2.5	1	21	1330	1350	CACAAAACCUUCAGCUACCCA	UGGGUAACCGAAGGUUUUGUG
Bradi4g09587.1 PA Cid:21810369	2.5	1	21	1330	1350	CACAAAACCUUCAGCUACCCA	UGGGUAACCGAAGGUUUUGUG
Bradi4g09587.2 PA Cid:21810370	2.5	1	21	1330	1350	CACAAAACCUUCAGCUACCCA	UGGGUAACCGAAGGUUUUGUG
Bradi2g39091.1 PA Cid:21809136	2.5	1	21	1360	1380	CACAAAACCUUCAGCUACCCA	UGGAUAGCUGAAGGCUUUGUG
Bradi4g10037.1 PA Cid:21812429	2.5	1	21	4030	4050	CACAAAACCUUCAGCUACCCA	UGGGUUGCUGAAGGUUUCGUG
Bradi1g54640.1 PA Cid:21818150	2.5	1	21	1304	1324	CACAAAACCUUCAGCUACCCA	AGGGCAACUGGAGGUUUUGUG

Table 3 Predicted target gene hits in relative monocot species

Target_Acc.	Description	Plant Species	Query cover	E value	Ident	Accession
Bradi4g10050.1 PA Cid:21812309	Putative disease resistance protein RGA3	<i>Triticum urartu</i>	93%	2.00E-152	54%	EMS49108.1
Bradi1g15350.1 PA Cid:21818854	inositol monophosphatase 3	<i>Aegilops tauschii</i> subsp. <i>tauschii</i>	99%	2.00E-177	94%	XP_020153324.1
Bradi4g09587.3 PA Cid:21810371	Disease resistance protein RPM1	<i>Triticum urartu</i>	98%	0	59%	EMS68463.1
Bradi4g09587.1 PA Cid:21810369	disease resistance protein RPP13-like	<i>Aegilops tauschii</i> subsp. <i>tauschii</i>	97%	0	50%	XP_020192033.1
Bradi4g09587.2 PA Cid:21810370	putative disease resistance RPP13-like protein 3	<i>Aegilops tauschii</i> subsp. <i>tauschii</i>	98%	0%	45%	XP_020159914.1
Bradi2g39091.1 PA Cid:21809136	putative disease resistance RPP13-like protein 3	<i>Aegilops tauschii</i> subsp. <i>tauschii</i>	97%	0	46%	XP_020162330.1
Bradi4g10037.1 PA Cid:21812429	putative disease resistance protein RGA4	<i>Aegilops tauschii</i> subsp. <i>tauschii</i>	97%	0	56%	XP_020153965.1
Bradi1g54640.1 PA Cid:21818150	retrotransposon protein, putative, unclassified	<i>Oryza sativa Japonica</i> Group	99%	0	51%	ABA94541.2

Table 4 Predicted target genes of miR7757 in *Brachypodium distachyon*

Target_Acc.	Description	Plant Species	Query cover	E value	Ident	Accession
Bradi4g10050.1 PA Cid:21812309	disease resistance protein RGA2-like	<i>Brachypodium distachyon</i>	92%	6.00E-156	56%	XP_010230450.1
Bradi1g15350.1 PA Cid:21818854	inositol monophosphatase 3	<i>Brachypodium distachyon</i>	99%	0	100%	XP_003562327.1
Bradi4g09587.3 PA Cid:21810371	putative disease resistance RPP13-like protein 3	<i>Brachypodium distachyon</i>	98%	0	100%	XP_003575644.1
Bradi4g09587.1 PA Cid:21810369	putative disease resistance RPP13-like protein 3	<i>Brachypodium distachyon</i>	98%	0	100%	XP_003575644.1
Bradi4g09587.2 PA Cid:21810370	putative disease resistance RPP13-like protein 3	<i>Brachypodium distachyon</i>	98%	0%	100%	XP_003575644.1
Bradi2g39091.1 PA Cid:21809136	disease resistance protein RPP13-like	<i>Brachypodium distachyon</i>	96%	0	100%	XP_014754595.1
Bradi4g10037.1 PA Cid:21812429	putative disease resistance protein RGA family	<i>Brachypodium distachyon</i>	97%	0	80%	XP_014758158.1
Bradi1g54640.1 PA Cid:21818150	transposon Tf2-1 polyprotein	<i>Brachypodium distachyon</i>	99%	0	45%	XP_014754072.1

APPENDIX H

Table 5 Comparison of average height between mutant and normal plants

	Normal wt Bd21-3	T-DNA Mutant jj15278	Difference
Average	20.289	15.226	5.063
Standard Deviation	1.593	2.944	1.658

Table 6 Sorted out *Brachypodium* T-DNA mutant lines having mutations in miRNAs.

ID	Strand	Start	End	Chrom.	Insertion site	FST name	T-DNA line
bdi-MIR390a	sense	2722067	2722275	Bd1	2722126	IL000004655	JJ13854, JJ3177, JJ12516, JJ2088, JJ5868
bdi-MIR5049	antisense	9873496	9873584	Bd1	9873538	JJ3284.0	JJ3284
bdi-MIR7716	antisense	7864984	7865341	Bd2	7864987	JJ54.1	JJ54
bdi-MIR7757	sense	57745334	57745931	Bd2	57745630	IL000017215	JJ15278
bdi-MIR169d	sense	26242409	26242595	Bd4	26242587	IL000007756	JJ5803, JJ5856, JJ5899, JJ5912, JJ5843, JJ5820

APPENDIX I

Sequence variants of miR7757 for target prediction.

miR7757 variants	Sequence
>bdi-miR7757-5p.1 MIMAT0030258	CACAAAACCUUCAGCUACCCA
>bdi-miR7757-5p.2 MIMAT0030259	CUUCCAUAUCAAAUCAUCUCU
>bdi-miR7757-3p.1 MIMAT0030261	GGUAGUUGAAUGUUUUGUUUA
>bdi-miR7757-3p.2 MIMAT0030260	AGAUAAUUGAUUAUGUAAGUG

Pre-miRNA sequence of MIR7757

>bdi-MIR7757MI0025377*598 premiRNA sequence 5' to 3'

UGGAUCAUGCUUCUAUUUAUAAGCUC AUUGAAGUAACUCUCUCCGAGCUCAAAU
 AGGCCAAUUUUUUGUUUGUGUGAUACACAAAACCUUCAGCUACCCACUCCAUAU
 CAAUCAUCUCUCUUGGUUUUCUUGUCUUUUGGAAAUAUACUUUGAUUAUGAUAA
 AAGAUGAGAAGGUAGA UCCUAGCUAGAACAACAUCAUAUUAAGUCUUUAGUCUC
 AAGUAAGUCCGGUAGGCUAGAGAUGAAAUCCAAUAGGAGCUUAACGUUGUUUC
 AGGUAGUGUACAACUUGUUAGUAAAAGAUGCUUACUUGUAGAUUAUGCCAAACC
 AUGAUCUAUAAGUCAAGUCUCUUUACUAAUAGUUUUGAUCCACCUUCUCAUCU
 UUAGUGUUAGUUAUCAUAUUUAACU AUGUAUUCAGAAGAUUAGAAGAUUAUGAG
 AGAUAAUUGAUUAUGUAAGUGGGUAGUUGAAUGUUUUGUUUAUCAUGAAAACAA
 GAAAUUAGCCUACGUGAGCCCGGAGAGAGUAACUCA AUGAGCACAUAAAUAGAA
 GCAUGAUUCAACCAAUAGACACCGAUGACGACUGUGAAGGC AAGGAAAUGUAUU
 AUU

T-DNA Primers provided by the DOE Joint Genome Institute (Vogel Lab)

Name	Sequence	G-C CONTENT	T _M
T3 T-DNA LB	AGCTGTTTCCTGTGTGAAATTG	41% G-C	63
R9 T-DNA LB	GATAAGCTGTCAACATGAGAATTG	37% G-C	64

Gene Specific Primers designed per instructions for T-DNA screening

Name	Forward Sequence	Reverse Sequence	Product Length
miR390a	GTGGTAGTGCACCTAGCTTTG	GCATGCTGACTCTGTTTTCT	1169bp
miR5049	CTTGCTTTCCTTGTGTGTGTA	CGTATCTCCCATACATTGCCC	1169bp
miR7716	GGGAGTAGTAGTGTGACTGC	TTAATGCGACTGCCAAGGC	1237bp
miR7757	CAGAGCAACAGCTGTATGGTC	TTCATGTCATCCAACGGCG	1138bp
miR169d	GCATTGTGATGTCCTGCGT	CCGGGTGTTTCGACATTG	1402bp

Primers used in gateway cloning

For 2 attB1-GFP	GGGG <u>ACA AGT TTG TAC AAA AAA GCA GGC T</u> ATGAAGGTGC GGTATTATTATTTA
Rev 2 attB2-GFP	GGGG <u>AC CAC TTT GTA CAA GAA AGC TGG GT</u> AAT CTT GTC ACA AGT TTG TCT T
miR7757gspF	AACCTTCAGCTACCCACTTCC
miR7757gspR	AGTTACTCTCTCCGGGCTCAC
M13 Forward	GTAAAACGACGGCCAG
M13 Reverse	CAGGAAACAGCTATGAC
CaMV35sF	GCTCCTACAAATGCCATCA
CaMV35sR	GATAGTGGGATTGTGCGTCA

D. References

- Achard, Patrick, Alan Herr, David C. Baulcombe, and Nicholas P. Harberd. 2004. "Modulation of Floral Development by a Gibberellin-Regulated MicroRNA." *Development (Cambridge, England)* 131(14):3357–65. Retrieved May 23, 2014 (<http://www.ncbi.nlm.nih.gov/pubmed/15226253>).
- Agudelo, Carlos G. et al. 2013. "TipChip: A Modular, MEMS-Based Platform for Experimentation and Phenotyping of Tip-Growing Cells." *The Plant Journal* 73(6):1057–68. Retrieved (<http://doi.wiley.com/10.1111/tpj.12093>).
- Agudelo, Carlos G., Muthukumaran Packirisamy, and Anja Geitmann. 2014. "Assessing the Influence of Electric Cues and Conductivity on Pollen Tube Growth via Lab-On-A-Chip Technology." *Biophysical Journal* 106(2):574a. Retrieved (<http://www.cell.com/article/S0006349513044445/fulltext>).
- Akmal, Mohammad and Tadashi Hirasawa. 2004. "Growth Responses of Seminal Roots of Wheat Seedlings to a Reduction in the Water Potential of Vermiculite." *Plant and Soil* 267(1–2):319–28. Retrieved January 31, 2017 (<http://link.springer.com/10.1007/s11104-005-0138-x>).
- Akpinar, B. Ani, Bihter Avsar, Stuart J. Lucas, and Hikmet Budak. 2012. "Plant Abiotic Stress Signaling." *Plant Signaling & Behavior* 7(11):1450–55.
- Akpinar, Bala Ani, Stuart J. Lucas, and Hikmet Budak. 2013. "Genomics Approaches for Crop Improvement against Abiotic Stress." *The Scientific World Journal* 2013:361921. Retrieved (<http://www.pubmedcentral.nih.gov/articlerender.fcgi?artid=3690750&tool=pmcentrez&rendertype=abstract>).
- Alves, Sílvia C. et al. 2009. "A Protocol for Agrobacterium-Mediated Transformation of Brachypodium Distachyon Community Standard Line Bd21." *Nature Protocols* 4(5):638–49. Retrieved (<http://www.nature.com/doi/10.1038/nprot.2009.30>).
- Anon. n.d. "Drought | Climate Education Modules for K-12." Retrieved (<http://www.nc-climate.ncsu.edu/edu/k12/drought>).
- Atkinson, Nicky J. and Peter E. Urwin. 2012. "The Interaction of Plant Biotic and Abiotic Stresses: From Genes to the Field." *Journal of experimental botany* 63:3523–43. Retrieved (<http://www.ncbi.nlm.nih.gov/pubmed/22467407>).
- Aukerman, M. J. 2003. "Regulation of Flowering Time and Floral Organ Identity by a MicroRNA and Its APETALA2-Like Target Genes." *THE PLANT CELL ONLINE* 15(11):2730–41. Retrieved June 20, 2014 (<http://www.plantcell.org/content/15/11/2730.short>).
- Axtell, Michael J., Jakub O. Westholm, and Eric C. Lai. 2011. "Vive La Différence: Biogenesis and Evolution of MicroRNAs in Plants and Animals." *Genome Biology* 12:221.
- Barrero, José M. et al. 2012. "Grain Dormancy and Light Quality Effects on Germination in the Model Grass Brachypodium Distachyon." *The New phytologist* 193(2):376–86. Retrieved June 28, 2017 (<http://doi.wiley.com/10.1111/j.1469-8137.2011.03938.x>).
- Barriopedro, David, Célia M. Gouveia, Ricardo M. Trigo, and Lin Wang. 2012. "The 2009/10 Drought in China: Possible Causes and Impacts on Vegetation." *Journal of Hydrometeorology* 13(4):1251–67. Retrieved January 15, 2014 (<http://journals.ametsoc.org/doi/abs/10.1175/JHM-D-11-074.1>).
- Bascom, Carlisle S., Shu-Zon Wu, Katherine Nelson, John Oakey, and Magdalena Bezanilla. 2016.

- “Long-Term Growth of Moss in Microfluidic Devices Enables Subcellular Studies in Development.” *Plant Physiology* 172(1):28–37.
- Bates, B., Z. W. Kundzewicz, S. Wu, and J. Palutikof. 2008. “Climate Change and Water.” Retrieved January 15, 2014 (<http://www.cabdirect.org/abstracts/20083307083.html;jsessionid=93FF98BBB19CE48363EE41E24AF12FD2>).
- Bennett, Matthew R. and Jeff Hasty. 2009. “Microfluidic Devices for Measuring Gene Network Dynamics in Single Cells.” *Nature reviews. Genetics* 10(9):628–38. Retrieved (<http://dx.doi.org/10.1038/nrg2625>).
- Berezikov, Eugene, Edwin Cuppen, and Ronald H. A. Plasterk. 2006. “Approaches to MicroRNA Discovery.” *Nature genetics* 38 Suppl(6s):S2-7. Retrieved (<http://www.nature.com/doi/finder/10.1038/ng1794>).
- Bertolini, Edoardo et al. 2013a. “Addressing the Role of MicroRNAs in Reprogramming Leaf Growth during Drought Stress in Brachypodium Distachyon.” *Molecular plant* 6(2):423–43. Retrieved December 20, 2013 (<http://www.pubmedcentral.nih.gov/articlerender.fcgi?artid=3603004&tool=pmcentrez&rendertype=abstract>).
- Bertolini, Edoardo et al. 2013b. “Addressing the Role of MicroRNAs in Reprogramming Leaf Growth during Drought Stress in Brachypodium Distachyon.” *Molecular Plant* 6(2):423–43. Retrieved December 20, 2013 (<http://mplant.oxfordjournals.org/content/6/2/423.short>).
- Bevan, Michael W., David F. Garvin, and John P. Vogel. 2010. “Brachypodium Distachyon Genomics for Sustainable Food and Fuel Production.” *Current Opinion in Biotechnology* 21(2):211–17. Retrieved January 29, 2017 (<http://linkinghub.elsevier.com/retrieve/pii/S0958166910000455>).
- Bhargava, Sujata and Kshitija Sawant. 2013. “Drought Stress Adaptation: Metabolic Adjustment and Regulation of Gene Expression” edited by R. Tuberosa. *Plant Breeding* 132(1):21–32. Retrieved January 11, 2014 (<http://doi.wiley.com/10.1111/pbr.12004>).
- Boke, Hatice et al. 2015. “Regulation of the Alkaloid Biosynthesis by MiRNA in Opium Poppy.” *Plant Biotechnology Journal* 13(3):409–20. Retrieved (<http://doi.wiley.com/10.1111/pbi.12346>).
- Bragg, Jennifer N. et al. 2012. “Generation and Characterization of the Western Regional Research Center Brachypodium T-DNA Insertional Mutant Collection” edited by S. P. Hazen. *PLoS ONE* 7(9):e41916. Retrieved July 25, 2014 (<http://www.pubmedcentral.nih.gov/articlerender.fcgi?artid=3444500&tool=pmcentrez&rendertype=abstract>).
- Brinker, Monika et al. 2010. “Linking the Salt Transcriptome with Physiological Responses of a Salt-Resistant Populus Species as a Strategy to Identify Genes Important for Stress Acclimation.” *Plant physiology* 154:1697–1709.
- Brkljacic, Jelena et al. 2011. “Brachypodium as a Model for the Grasses: Today and the Future.” *PLANT PHYSIOLOGY* 157(1):3–13. Retrieved (<http://www.plantphysiol.org/cgi/doi/10.1104/pp.111.179531>).
- Budak, Hikmet and Ani Akpınar. 2011. “Dehydration Stress-Responsive MiRNA in Brachypodium Distachyon : Evident by Genome-Wide Screening of MicroRNAs Expression.” *OMICS: A Journal of Integrative Biology* 15(11):791–99. Retrieved December 19, 2013 (<http://www.ncbi.nlm.nih.gov/pubmed/22122669>).

- Budak, Hikmet, Babar Hussain, Zaeema Khan, Neslihan Z. Ozturk, and Naimat Ullah. 2015. "From Genetics to Functional Genomics: Improvement in Drought Signaling and Tolerance in Wheat." *Frontiers in plant science* 6:1012.
- Busch, Wolfgang et al. 2012. "A Microfluidic Device and Computational Platform for High Throughput Live Imaging of Gene Expression." *Nature methods* 9(11):1101–6.
- Chen, Hao, Zhuofu Li, and Liming Xiong. 2012. "A Plant MicroRNA Regulates the Adaptation of Roots to Drought Stress." *FEBS letters* 586(12):1742–47. Retrieved January 12, 2014 (<http://www.ncbi.nlm.nih.gov/pubmed/22613571>).
- Chen, M., Yijun Meng, Chuanzao Mao, Dijun Chen, and Ping Wu. 2010. "Methodological Framework for Functional Characterization of Plant MicroRNAs." *Journal of Experimental Botany* 61(9):2271–80. Retrieved (<https://academic.oup.com/jxb/article-lookup/doi/10.1093/jxb/erq087>).
- Chen, Mingxun et al. 2012. "Seed Fatty Acid Reducer Acts Downstream of Gibberellin Signalling Pathway to Lower Seed Fatty Acid Storage in Arabidopsis." *Plant, Cell and Environment* 35(12):2155–69.
- Chiou, TJ, Kyaw Aung, and SI Lin. 2006. "Regulation of Phosphate Homeostasis by MicroRNA in Arabidopsis." *The Plant Cell* ... 18(February):412–21. Retrieved June 20, 2014 (<http://www.plantcell.org/content/18/2/412.short>).
- Colaiacono, Moreno et al. 2012. "On the Complexity of MiRNA-Mediated Regulation in Plants: Novel Insights into the Genomic Organization of Plant MiRNAs." *Biology direct* 7:15.
- Ding, Zhenhua et al. 2009. "Transgenic Expression of MYB15 Confers Enhanced Sensitivity to Abscisic Acid and Improved Drought Tolerance in Arabidopsis Thaliana." *Journal of Genetics and Genomics* 36(1):17–29. Retrieved December 21, 2013 (<http://www.sciencedirect.com/science/article/pii/S1673852709600035>).
- Du, Hao et al. 2010. "Characterization of the Beta-Carotene Hydroxylase Gene DSM2 Conferring Drought and Oxidative Stress Resistance by Increasing Xanthophylls and Abscisic Acid Synthesis in Rice." *Plant physiology* 154(3):1304–18. Retrieved December 21, 2013 (<http://www.plantphysiol.org/content/154/3/1304.short>).
- Dubrovsky, Joseph G. et al. 2006. "Neutral Red as a Probe for Confocal Laser Scanning Microscopy Studies of Plant Roots." *Annals of botany* 97(6):1127–38. Retrieved (<http://aob.oxfordjournals.org/cgi/content/full/97/6/1127%7B%25%7D5Cnpapers://89925b2b-2bb5-47ca-b5c6-edff5ec11ff7/Paper/p1862%7B%25%7D5Cnpapers://89925b2b-2bb5-47ca-b5c6-edff5ec11ff7/Paper/p2391>).
- Duque, Ana Sofia et al. n.d. "Abiotic Stress Responses in Plants : Unraveling the Complexity of Genes and Networks to Survive."
- Dutilleul, Christelle et al. 2003. "Leaf Mitochondria Modulate Whole Cell Redox Homeostasis, Set Antioxidant Capacity, and Determine Stress Resistance through Altered Signaling and Diurnal Regulation." *The Plant cell* 15:1212–26.
- Elitaş, Meltem, Meral Yüce, and Hikmet Budak. 2017. "Microfabricated Tools for Quantitative Plant Biology." *The Analyst* 142(6):835–48.
- Feng, Hao et al. 2013. "Target of Tae-MiR408, a Chemocyanin-like Protein Gene (TaCLP1), Plays Positive Roles in Wheat Response to High-Salinity, Heavy Cupric Stress and Stripe Rust." *Plant Molecular Biology* 83(4–5):433–43. Retrieved January 30, 2014 (<http://www.ncbi.nlm.nih.gov/pubmed/23864359>).

- Filiz, E. et al. 2009. "Molecular, Morphological, and Cytological Analysis of Diverse Brachypodium Distachyon Inbred Lines" edited by G. Scoles. *Genome* 52(10):876–90. Retrieved June 29, 2017 (<http://www.nrcresearchpress.com/doi/abs/10.1139/G09-062>).
- Fitzgerald, Timothy L. et al. 2015. "Brachypodium as an Emerging Model for Cereal–pathogen Interactions." *Annals of Botany* 115(5):717–31. Retrieved (<https://academic.oup.com/aob/article-lookup/doi/10.1093/aob/mcv010>).
- Frazier, Taylor P., Guiling Sun, Caitlin E. Burklew, and Baohong Zhang. 2011. "Salt and Drought Stresses Induce the Aberrant Expression of MicroRNA Genes in Tobacco." *Molecular biotechnology* 49(2):159–65.
- Fujii, Hiroaki, Tzyy-Jen Chiou, Shu-I. Lin, Kyaw Aung, and Jian-Kang Zhu. 2005. "A MiRNA Involved in Phosphate-Starvation Response in Arabidopsis." *Current biology: CB* 15(22):2038–43. Retrieved June 5, 2014 (<http://www.ncbi.nlm.nih.gov/pubmed/16303564>).
- Galkovskiy, Taras et al. 2012. "GiA Roots: Software for the High Throughput Analysis of Plant Root System Architecture." *BMC plant biology* 12(1):116. Retrieved (<http://bmcpantbiol.biomedcentral.com/articles/10.1186/1471-2229-12-116>).
- Ghanbari, Mahmood, Amir Sanati Nezhad, Carlos G. Agudelo, Muthukumaran Packirisamy, and Anja Geitmann. 2014. "Microfluidic Positioning of Pollen Grains in Lab-on-a-Chip for Single Cell Analysis." *Journal of Bioscience and Bioengineering* 117(4):504–11. Retrieved (<http://dx.doi.org/10.1016/j.jbiosc.2013.10.001>).
- Girin, Thomas et al. 2014. "Brachypodium: A Promising Hub between Model Species and Cereals." *Journal of Experimental Botany* 65(19):5683–96. Retrieved (<https://academic.oup.com/jxb/article-lookup/doi/10.1093/jxb/eru376>).
- Gooh, Keita et al. 2015. "Live-Cell Imaging and Optical Manipulation of Arabidopsis Early Embryogenesis." *Developmental Cell* 34(2):242–51. Retrieved (<http://linkinghub.elsevier.com/retrieve/pii/S1534580715003974>).
- Grossmann, Guido et al. 2011. "The RootChip: An Integrated Microfluidic Chip for Plant Science." *The Plant cell* 23(12):4234–40.
- Guillon, F. et al. 2012. "A Comprehensive Overview of Grain Development in Brachypodium Distachyon Variety Bd21." *Journal of experimental botany* 63(2):739–55. Retrieved June 28, 2017 (<http://www.ncbi.nlm.nih.gov/pubmed/22016425>).
- Guleria, Praveen, Monika Mahajan, Jyoti Bhardwaj, and Sudesh Kumar Yadav. 2011. "Plant Small RNAs: Biogenesis, Mode of Action and Their Roles in Abiotic Stresses." *Genomics, proteomics & bioinformatics* 9(6):183–99. Retrieved December 17, 2013 (<http://www.ncbi.nlm.nih.gov/pubmed/22289475>).
- Hong, Shin-Young, Pil Seo, Moon-Sik Yang, Fengning Xiang, and Chung-Mo Park. 2008. "Exploring Valid Reference Genes for Gene Expression Studies in Brachypodium Distachyon by Real-Time PCR." *BMC Plant Biology* 8(1):112. Retrieved (<http://www.ncbi.nlm.nih.gov/pubmed/18992143>).
- Van Houtte, Hilde et al. 2013. "Overexpression of the Trehalase Gene AtTRE1 Leads to Increased Drought Stress Tolerance in Arabidopsis and Is Involved in Abscisic Acid-Induced Stomatal Closure." *PLANT PHYSIOLOGY* 161(3):1158–71. Retrieved December 21, 2013 (<http://www.plantphysiol.org/content/161/3/1158.short>).
- Hsia, Mon Mandy et al. 2017. "Sequencing and Functional Validation of the JGI Brachypodium Distachyon T-DNA Collection." *The Plant Journal* 91(3):361–70. Retrieved

(<http://doi.wiley.com/10.1111/tpj.13582>).

- Hung, Min-Sheng and Jia-Hao Chang. 2012. "Developing Microfluidics for Rapid Protoplasts Collection and Lysis from Plant Leaf." *Proceedings of the Institution of Mechanical Engineers, Part N: Journal of Nanoengineering and Nanosystems* 226(1):15–22. Retrieved (<http://pin.sagepub.com/lookup/doi/10.1177/1740349912444511>).
- Iyer-Pascuzzi, A. S. et al. 2010. "Imaging and Analysis Platform for Automatic Phenotyping and Trait Ranking of Plant Root Systems." *PLANT PHYSIOLOGY* 152(3):1148–57.
- Ji, Hongtao et al. 2014. "PEG-Mediated Osmotic Stress Induces Premature Differentiation of the Root Apical Meristem and Outgrowth of Lateral Roots in Wheat." *Journal of Experimental Botany* 65(17):4863–72.
- Jia, Xiaoyun, WX Wang, L. Ren, and QJ Chen. 2009. "Differential and Dynamic Regulation of MiR398 in Response to ABA and Salt Stress in Populus Tremula and Arabidopsis Thaliana." *Plant molecular ...* 51–59. Retrieved December 20, 2013 (<http://link.springer.com/article/10.1007/s11103-009-9508-8>).
- Jiang, Huawei, Zhen Xu, Maneesha R. Aluru, and Liang Dong. 2014. "Plant Chip for High-Throughput Phenotyping of Arabidopsis." *Lab on a Chip* 14(7):1281. Retrieved (<http://xlink.rsc.org/?DOI=c3le51326b>).
- Jones-Rhoades, Matthew W. and David P. Bartel. 2004. "Computational Identification of Plant MicroRNAs and Their Targets, Including a Stress-Induced MiRNA." *Molecular cell* 14(6):787–99. Retrieved February 6, 2014 (<http://www.ncbi.nlm.nih.gov/pubmed/15200956>).
- KALEFETOĞLU, T. and Y. Ekmekci. 2010. "The Effects of Drought on Plants and Tolerance Mechanisms." *Gazi University Journal of Science* 18(4):723–40. Retrieved January 15, 2014 (<http://www.gujs.gazi.edu.tr/index.php/GUJS/article/viewArticle/466>).
- Kantar, M., SJ Lucas, and H. Budak. 2011. "Drought Stress: Molecular Genetics and Genomics Approaches." Pp. 445–93 in *Advances in botanical research*.
- Kantar, Melda, Stuart J. Lucas, and Hikmet Budak. 2011. "Chapter 13 - Drought Stress: Molecular Genetics and Genomics Approaches." Pp. 445–93 in *Advances in Botanical Research*, vol. Volume 57. Retrieved January 13, 2017 (https://www.google.com/books?hl=en&lr=&id=jwJ5OJVkAFYC&oi=fnd&pg=PA445&dq=Drought+stress+molecular+genetics+and+genomics+approaches.+Advances+in+botanical+research+57,+445-493&ots=Vey_imhZFP&sig=48D_AtKChvk9rF3BN25FkW5PrwI).
- Keinath, Nana et al. 2015. "Live Cell Imaging with R-GECO1 Sheds Light on Flg22- and Chitin-Induced Transient [Ca(2+)]Cyt Patterns in Arabidopsis." *Molecular plant* 1–13. Retrieved (<http://www.ncbi.nlm.nih.gov/pubmed/26002145>).
- Kellogg, Elizabeth A. 2015. "Brachypodium Distachyon as a Genetic Model System." *Annual Review of Genetics* 49(1):1–20. Retrieved (<http://www.annualreviews.org/doi/10.1146/annurev-genet-112414-055135>).
- Khan, MA, M. Iqbal, Moazzam Jameel, and Wajad Nazeer. 2011. "Potentials of Molecular Based Breeding to Enhance Drought Tolerance in Wheat (Triticum Aestivum L.)." *African Journal of ...* 10(55):11340–44. Retrieved January 15, 2014 ([http://scholar.google.com/scholar?hl=en&btnG=Search&q=intitle:Potentials+of+molecular+based+breeding+to+enhance+drought+tolerance+in+wheat+\(+Triticum+aestivum+L+.\)#0](http://scholar.google.com/scholar?hl=en&btnG=Search&q=intitle:Potentials+of+molecular+based+breeding+to+enhance+drought+tolerance+in+wheat+(+Triticum+aestivum+L+.)#0)).
- Khraiwesh, Basel, Jian-Kang Zhu, and Jianhua Zhu. 2012. "Role of MiRNAs and SiRNAs in Biotic and

- Abiotic Stress Responses of Plants.” *Biochimica et biophysica acta* 1819(2):137–48. Retrieved December 11, 2013 (<http://www.pubmedcentral.nih.gov/articlerender.fcgi?artid=3175014&tool=pmcentrez&rendertype=abstract>).
- Kim, Joonki et al. 2005. “MicroRNA-Directed Cleavage of ATHB15 mRNA Regulates Vascular Development in Arabidopsis Inflorescence Stems.” *The Plant Journal* 42(1):84–94. Retrieved June 4, 2014 (<http://www.pubmedcentral.nih.gov/articlerender.fcgi?artid=1382282&tool=pmcentrez&rendertype=abstract>).
- Ko, Jung-Moon, Jongil Ju, Sanghoon Lee, and Hyeon-Cheol Cha. 2006. “Tobacco Protoplast Culture in a Polydimethylsiloxane-Based Microfluidic Channel.” *Protoplasma* 227(2–4):237–40.
- Krysan, P. J. 1999. “T-DNA as an Insertional Mutagen in Arabidopsis.” *THE PLANT CELL ONLINE* 11(12):2283–90. Retrieved (<http://www.plantcell.org/cgi/doi/10.1105/tpc.11.12.2283>).
- Kumar, Ranjeet Ranjan et al. 2015. “Novel and Conserved Heat-Responsive MicroRNAs in Wheat (*Triticum Aestivum* L.).” *Functional and Integrative Genomics* 15(3):323–48.
- Kurtoglu, Kuaybe Yucebilgili, Melda Kantar, and Hikmet Budak. 2014. “New Wheat MicroRNA Using Whole-Genome Sequence.” *Functional & integrative genomics*. Retrieved January 26, 2014 (<http://www.ncbi.nlm.nih.gov/pubmed/24395439>).
- Kuzuoglu-Ozturk, Duygu et al. 2012. “Autophagy-Related Gene, TdAtg8, in Wild Emmer Wheat Plays a Role in Drought and Osmotic Stress Response.” *Planta* 236(4):1081–92.
- Lei, Rong, Wenjie Qiao, Fan Hu, Hongshan Jiang, and Shuifang Zhu. 2015. “A Simple and Effective Method to Encapsulate Tobacco Mesophyll Protoplasts to Maintain Cell Viability.” *MethodsX* 2(1):24–32.
- Li, Bosheng, Weilun Yin, and Xinli Xia. 2009. *Identification of MicroRNAs and Their Targets from Populus Euphratica*. Retrieved December 27, 2013 (<http://www.sciencedirect.com/science/article/pii/S0006291X09015460>).
- Li, H. et al. 2011. “The Arabidopsis RING Finger E3 Ligase RHA2b Acts Additively with RHA2a in Regulating Abscisic Acid Signaling and Drought Response.” *PLANT PHYSIOLOGY* 156(2):550–63. Retrieved December 21, 2013 (<http://www.plantphysiol.org/content/156/2/550.full>).
- Li, W. X. et al. 2008. “The Arabidopsis NFYA5 Transcription Factor Is Regulated Transcriptionally and Posttranscriptionally to Promote Drought Resistance.” *THE PLANT CELL ONLINE* 20(8):2238–51. Retrieved May 29, 2014 (<http://www.pubmedcentral.nih.gov/articlerender.fcgi?artid=2553615&tool=pmcentrez&rendertype=abstract>).
- Li, Yang, Chaoqun Li, Jie Xia, and Youxin Jin. 2011. “Domestication of Transposable Elements into MicroRNA Genes in Plants” edited by C. Schönbach. *PLoS ONE* 6(5):e19212. Retrieved (<http://dx.plos.org/10.1371/journal.pone.0019212>).
- Lipiec, J., C. Doussan, a. Nosalewicz, and K. Kondracka. 2013. “Effect of Drought and Heat Stresses on Plant Growth and Yield: A Review.” *International Agrophysics* 27(4):463–77. Retrieved December 18, 2013 (<http://www.degruyter.com/view/j/intag.2013.27.issue-4/intag-2013-0017/intag-2013-0017.xml>).
- Liu, Beibei and Genlou Sun. 2017. “MicroRNAs Contribute to Enhanced Salt Adaptation of the Autopolyploid *Hordeum Bulbosum* Compared with Its Diploid Ancestor.” *The Plant Journal*

- 91(1):57–69. Retrieved (<http://doi.wiley.com/10.1111/tpj.13546>).
- Liu, Qingpo. 2012. “Novel MiRNAs in the Control of Arsenite Levels in Rice.” *Functional & integrative genomics* 12(4):649–58.
- Massalha, Hassan, Elisa Korenblum, Sergey Malitsky, Orr H. Shapiro, and Asaph Aharoni. 2017. “Live Imaging of Root–bacteria Interactions in a Microfluidics Setup.” *Proceedings of the National Academy of Sciences* 114(17):4549–54.
- Meier, Matthias, Elena M. Lucchetta, and Rustem F. Ismagilov. 2010. “Chemical Stimulation of the Arabidopsis Thaliana Root Using Multi-Laminar Flow on a Microfluidic Chip.” *Lab on a Chip* 10(16):2147. Retrieved (<http://xlink.rsc.org/?DOI=c004629a>).
- Meng, Yijun and Chaogang Shao. 2012. “Large-Scale Identification of Mirtrons in Arabidopsis and Rice.” *PloS one* 7(2):e31163.
- Mittler, Ron. 2006. “Abiotic Stress, the Field Environment and Stress Combination.” *Trends in Plant Science* 11(1):15–19. Retrieved January 15, 2014 (<http://www.sciencedirect.com/science/article/pii/S1360138505002918>).
- Mittler, Ron and Eduardo Blumwald. 2010. “Genetic Engineering for Modern Agriculture: Challenges and Perspectives.” *Annual review of plant biology* 61:443–62. Retrieved January 14, 2014 (<http://www.annualreviews.org/doi/abs/10.1146/annurev-arplant-042809-112116?journalCode=arplant>).
- Morris, Erin R., David Chevalier, and John C. Walker. 2006. “DAWDLE, a Forkhead-Associated Domain Gene, Regulates Multiple Aspects of Plant Development.” *Plant physiology* 141(3):932–41.
- Nezhad, Amir Sanati, Muthukumaran Packirisamy, Rama Bhat, and Anja Geitmann. 2013. “In Vitro Study of Oscillatory Growth Dynamics of Camellia Pollen Tubes in Microfluidic Environment.” *IEEE transactions on bio-medical engineering* 60(11):3185–93. Retrieved (<http://www.ncbi.nlm.nih.gov/pubmed/23807421>).
- Ni, Zhiyong, Zheng Hu, Qiyan Jiang, and Hui Zhang. 2012. “Overexpression of Gma-MIR394a Confers Tolerance to Drought in Transgenic Arabidopsis Thaliana.” *Biochemical and Biophysical Research Communications* 427(2):330–35. Retrieved December 20, 2013 (<http://www.ncbi.nlm.nih.gov/pubmed/23000164>).
- Nishiyama, Rie et al. 2011. “Analysis of Cytokinin Mutants and Regulation of Cytokinin Metabolic Genes Reveals Important Regulatory Roles of Cytokinins in Drought, Salt and Abscisic Acid Responses, and Abscisic Acid Biosynthesis.” *The Plant cell* 23(6):2169–83. Retrieved December 21, 2013 (<http://www.plantcell.org/content/23/6/2169.short>).
- Nunes, C., S. S. Arajo, J. M. Silva, P. Fevereiro, and A. B. Silva. 2009. “Photosynthesis Light Curves: A Method for Screening Water Deficit Resistance in the Model Legume Medicago Truncatula.” *Annals of Applied Biology* 155:321–32. Retrieved (<http://blackwell-synergy.com/doi/abs/10.1111/j.1744-7348.2009.00341.x>).
- Oliveira, Evelyn Jardim et al. 2017. “Morpho-Histological, Histochemical, and Molecular Evidences Related to Cellular Reprogramming during Somatic Embryogenesis of the Model Grass Brachypodium Distachyon.” *Protoplasma*, March 13, 1–18. Retrieved June 28, 2017 (<http://link.springer.com/10.1007/s00709-017-1089-9>).
- Opanowicz, Magdalena, Philippe Vain, John Draper, David Parker, and John H. Doonan. 2008. “Brachypodium Distachyon: Making Hay with a Wild Grass.” *Trends in Plant Science* 13(4):172–77. Retrieved (<http://linkinghub.elsevier.com/retrieve/pii/S1360138508000800>).

- Paez-Garcia, Ana et al. 2015. "Root Traits and Phenotyping Strategies for Plant Improvement." *Plants* 4(2):334–55. Retrieved January 31, 2017 (<http://www.mdpi.com/2223-7747/4/2/334/>).
- Parashar, Archana and Santosh Pandey. 2011. "Plant-in-Chip: Microfluidic System for Studying Root Growth and Pathogenic Interactions in Arabidopsis." *Applied Physics Letters* 98(26):263703.
- Park, Mee Yeon, Gang Wu, Alfredo Gonzalez-Sulser, Hervé Vaucheret, and R. Scott Poethig. 2005. "Nuclear Processing and Export of MicroRNAs in Arabidopsis." *Proceedings of the National Academy of Sciences of the United States of America* 102(10):3691–96.
- Prelich, Gregory. 2012. "Gene Overexpression: Uses, Mechanisms, and Interpretation." *Genetics* 190(3):841–54. Retrieved (<http://www.genetics.org/cgi/doi/10.1534/genetics.111.136911>).
- Priest, Henry D. et al. 2014. "Analysis of Global Gene Expression in Brachypodium Distachyon Reveals Extensive Network Plasticity in Response to Abiotic Stress" edited by K. Wu. *PLoS ONE* 9(1):e87499. Retrieved January 30, 2017 (<http://dx.plos.org/10.1371/journal.pone.0087499>).
- Qiu, Qiang et al. 2011. "Genome-Scale Transcriptome Analysis of the Desert Poplar, *Populus euphratica*." *Tree physiology* 31:452–61.
- Rajagopalan, Ramya, Hervé Vaucheret, Jerry Trejo, and David P. Bartel. 2006. "A Diverse and Evolutionarily Fluid Set of MicroRNAs in Arabidopsis Thaliana." *Genes & development* 20(24):3407–25.
- Ramachandran, Vanitharani and Xuemei Chen. 2008. "Degradation of MicroRNAs by a Family of Exoribonucleases in Arabidopsis." *Science (New York, N.Y.)* 321(5895):1490–92.
- Ren, Guodong, Xuemei Chen, and Bin Yu. 2015. "Small RNAs Meet Their Targets: When Methylation Defends miRNAs from Uridylation." *RNA Biology* 11(9):1099–1104.
- Ren, Xiaozhi et al. 2010. "ABO3, a WRKY Transcription Factor, Mediates Plant Responses to Abscisic Acid and Drought Tolerance in Arabidopsis." *The Plant journal : for cell and molecular biology*. Retrieved December 21, 2013 (<http://www.pubmedcentral.nih.gov/articlerender.fcgi?artid=3117930&tool=pmcentrez&rendertype=abstract>).
- Rizhsky, L. 2004. "When Defense Pathways Collide. The Response of Arabidopsis to a Combination of Drought and Heat Stress." *PLANT PHYSIOLOGY* 134(4):1683–96. Retrieved January 15, 2014 (<http://www.plantphysiol.org/content/134/4/1683.full>).
- Rogers, Kestrel and Xuemei Chen. 2013. "Biogenesis, Turnover, and Mode of Action of Plant MicroRNAs." *The Plant cell* 25(7):2383–99.
- Rushton, Deena L. et al. 2012. "WRKY Transcription Factors: Key Components in Abscisic Acid Signalling." *Plant biotechnology journal* 10(1):2–11. Retrieved December 12, 2013 (<http://www.ncbi.nlm.nih.gov/pubmed/21696534>).
- Saad, Abu Sefyan I. et al. 2013. "A Rice Stress-Responsive NAC Gene Enhances Tolerance of Transgenic Wheat to Drought and Salt Stresses." *Plant Science* 203:33–40. Retrieved January 15, 2014 (<http://www.sciencedirect.com/science/article/pii/S0168945212002774>).
- Sanati Nezhad, A. 2014. "Microfluidic Platforms for Plant Cells Studies." *Lab on a Chip* 14(17):3262.
- Schiefelbein Lab. 2017. "Rapid Preparation of Transverse Sections of Plant Roots | Schiefelbein Lab." Retrieved April 1, 2017 (<http://sites.lsa.umich.edu/schiefelbein-lab/rapid-preparation-of-transverse-sections-of-plant-roots/>).

- Seo, Dong Hye et al. 2012. "Roles of Four Arabidopsis U-Box E3 Ubiquitin Ligases in Negative Regulation of Abscisic Acid-Mediated Drought Stress Responses." *PLANT PHYSIOLOGY* 160(1):556–68. Retrieved December 21, 2013 (<http://www.plantphysiol.org/content/160/1/556.short>).
- Seo, Pil Joon et al. 2009. "The MYB96 Transcription Factor Mediates Abscisic Acid Signaling during Drought Stress Response in Arabidopsis." *Plant physiology* 151(1):275–89. Retrieved December 21, 2013 (<http://www.plantphysiol.org/content/151/1/275.full>).
- Shah, Zahid Hussain, Muhammad Munir, Abdul Mujeeb Kazi, Tahir Mujtaba, and Zaheer Ahmed. 2009. "Molecular Markers Based Identification of Diversity for Drought Tolerance in Bread Wheat Varieties and Synthetic Hexaploids." *Current issues in molecular biology* 11(2):101–10. Retrieved (<http://www.ncbi.nlm.nih.gov/pubmed/19430030>).
- Song, Guoqi et al. 2017. "Response of MicroRNAs to Cold Treatment in the Young Spikes of Common Wheat." *BMC Genomics* 18(1):212. Retrieved (<http://bmcgenomics.biomedcentral.com/articles/10.1186/s12864-017-3556-2>).
- Sun, Guiling. 2012. "MicroRNAs and Their Diverse Functions in Plants." *Plant molecular biology* 80(1):17–36. Retrieved January 23, 2014 (<http://www.ncbi.nlm.nih.gov/pubmed/21874378>).
- Sunkar, Ramanjulu, Viswanathan Chinnusamy, and JK Zhu. 2007. "Small RNAs as Big Players in Plant Abiotic Stress Responses and Nutrient Deprivation." *Trends in plant science* 12(7). Retrieved December 20, 2013 (<http://www.sciencedirect.com/science/article/pii/S1360138507001276>).
- The Physical Science Basis: Working Group. 2007. *Climate Change 2007 - The Physical Science Basis: Working Group I Contribution to the Fourth Assessment Report of the IPCC*. Cambridge University Press. Retrieved January 15, 2014 (<http://books.google.com/books?hl=en&lr=&id=8-m8nXB8GB4C&pgis=1>).
- Unver, Turgay and Hikmet Budak. 2009. "Conserved MicroRNAs and Their Targets in Model Grass Species Brachypodium Distachyon." *Planta* 230(4):659–69. Retrieved January 12, 2017 (<http://link.springer.com/10.1007/s00425-009-0974-7>).
- Vain, Philippe. 2011. "Brachypodium as a Model System for Grass Research." *Journal of Cereal Science* 54(1):1–7. Retrieved (<http://dx.doi.org/10.1016/j.jcs.2011.04.002>).
- Verelst, Wim et al. 2013. "Molecular and Physiological Analysis of Growth-Limiting Drought Stress in Brachypodium Distachyon Leaves." *Molecular Plant* 6(2):311–22. Retrieved January 13, 2014 (<http://mplant.oxfordjournals.org/content/6/2/311.short>).
- Voinnet, Olivier. 2009. "Origin, Biogenesis, and Activity of Plant MicroRNAs." *Cell* 136(4):669–87. Retrieved (<http://linkinghub.elsevier.com/retrieve/pii/S0092867409001287>).
- Wasilewska, Aleksandra et al. 2008. "An Update on Abscisic Acid Signaling in Plants and More..." *Molecular plant* 1(2):198–217. Retrieved January 15, 2014 (<http://www.ncbi.nlm.nih.gov/pubmed/19825533>).
- Wilhite, Donald A. and Michael H. Glantz. 1985. "Understanding: The Drought Phenomenon: The Role of Definitions." *Water International* 10:111–20.
- Wu, Chaoyang and Jing M. Chen. 2013. *Diverse Responses of Vegetation Production to Interannual Summer Drought in North America*. Retrieved January 15, 2014 (<http://www.sciencedirect.com/science/article/pii/S030324341200164X>).
- Wu, Gang et al. 2009. "The Sequential Action of MiR156 and MiR172 Regulates Developmental Timing

- in Arabidopsis.” *Cell* 138(4):750–59. Retrieved May 28, 2014 (<http://www.sciencedirect.com/science/article/pii/S0092867409007788>).
- Wu, Heng et al. 2011. “Culture and Chemical-Induced Fusion of Tobacco Mesophyll Protoplasts in a Microfluidic Device.” *Microfluidics and Nanofluidics* 10(4):867–76. Retrieved (<http://link.springer.com/10.1007/s10404-010-0720-2>).
- Xie, Meng, Shuxin Zhang, and Bin Yu. 2015. “MicroRNA Biogenesis, Degradation and Activity in Plants.” *Cellular and Molecular Life Sciences* 72:87–99.
- YAZDANBAKSHI, NIMA, RONAN SULPICE, ALEXANDER GRAF, MARK STITT, and JOACHIM FISAHN. 2011. “Circadian Control of Root Elongation and C Partitioning in Arabidopsis Thaliana.” *Plant, Cell & Environment* 34(6):877–94. Retrieved (<http://doi.wiley.com/10.1111/j.1365-3040.2011.02286.x>).
- Yetisen, a K. et al. 2011. “A Microsystem-Based Assay for Studying Pollen Tube Guidance in Plant Reproduction.” *Journal of Micromechanics and Microengineering* 21(5):054018. Retrieved (<http://stacks.iop.org/0960-1317/21/i=5/a=054018?key=crossref.341c721d60e565829473e598f619053c>).
- Yu, Bin et al. 2005. “Methylation as a Crucial Step in Plant MicroRNA Biogenesis.” *Science (New York, N.Y.)* 307(5711):932–35.
- Yu, Bin et al. 2008. “The FHA Domain Proteins DAWDLE in Arabidopsis and SNIP1 in Humans Act in Small RNA Biogenesis.” *Proceedings of the National Academy of Sciences of the United States of America* 105(29):10073–78.
- Zhu, Cheng, Yanfei Ding, and Haili Liu. 2011. “MiR398 and Plant Stress Responses.” *Physiologia plantarum* 143(1):1–9. Retrieved December 20, 2013 (<http://www.ncbi.nlm.nih.gov/pubmed/21496029>).
- Zou, Jun-Jie et al. 2010. “Arabidopsis Calcium-Dependent Protein Kinase CPK10 Functions in Abscisic Acid- and Ca²⁺-Mediated Stomatal Regulation in Response to Drought Stress.” *Plant physiology* 154(3):1232–43. Retrieved December 21, 2013 (<http://www.plantphysiol.org/content/154/3/1232.short>).